

**Effect of Tank Cross-Section and Longitudinal Baffles on Transient Liquid Slosh in
Partly-Filled Road Tankers**

Abhijit Dasgupta

A Thesis

In

The Department

Of

Mechanical and Industrial Engineering

Presented in Partial Fulfillment of the Requirements
For the Degree of Master of Applied Science (Mechanical Engineering) at
Concordia University
Montreal, Quebec, Canada

August 2011

© Abhijit Dasgupta, 2011

CONCORDIA UNIVERSITY
SCHOOL OF GRADUATE STUDIES

This is to certify that the Thesis prepared,

By: **Abhijit DASGUPTA**

Entitled: **“Effect of Tank Cross-Section and Longitudinal Baffles on Transient Liquid Slosh in Partly-Filled Road Tankers”**

and submitted in partial fulfillment of the requirements for the Degree of

Master of Applied Science (Mechanical Engineering)

complies with the regulations of this University and meets the accepted standards with respect to originality and quality.

Signed by the final Examining Committee:

_____ Chair
Dr. A. Dolatabadi

_____ Examiner
Dr. S. Narayanswamy

_____ Examiner
Dr. L. Tirca (External)

_____ Supervisor
Dr. S. Rakheja

Approved by:

Dr. A. K. W. Ahmed, MASC Program Director
Department of Mechanical and Industrial Engineering

Dean Dr. Robin Drew
Faculty of Engineering & Computer Science

Date: _____

ABSTRACT

EFFECT OF TANK CROSS-SECTION AND LONGITUDINAL BAFFLES ON TRANSIENT LIQUID SLOSH IN PARTLY-FILLED ROAD TANKERS

Abhijit Dasgupta

Owing to high volume tank design and maneuver-induced liquid cargo motion, the partly-filled road tankers exhibit considerably lower stability and control limits compared to other commercial vehicles. The control limit of such vehicles are strongly related to the magnitudes of dynamic slosh forces and moments, which are governed by the tank cross-section, fill level and baffle design configuration apart from many vehicle related factors. Relatively higher overturning incidents of such vehicles suggest that roll stability is of primary concern, while the conventional transverse baffles yield negligible resistance to roll plane fluid slosh. This dissertation focuses on analyses of dynamic slosh characteristics in partly-filled industry prevalent tank cross-sections together with different transverse-longitudinal baffle configurations with an objective to reduce the magnitude of dynamic slosh in partly-filled tanks subject to idealized braking, turning, and combined braking and turning maneuver-induced excitations. Three-dimensional two-phase flow CFD models of three different cross-section tanks with and without baffles are formulated employing Navier-Stokes and continuity equations and solved using Fluent platform. The interface between the two fluid phases, namely air and liquid cargo, is tracked by applying volume of fluid technique and the fluid pressure at the boundaries is applied to determine the slosh forces. The dynamic fluid slosh with selected tanks is characterized by transient and steady-state cargo load shift, slosh forces and

moments under idealized maneuver-induced excitations, including the sprung mass roll motion. The tank cross-sections include the widely used circular as per the MC-407 design, a modified-oval as per MC-406 design and an elliptic cross-section. Three different transverse-longitudinal baffle arrangements are further proposed, and their relative anti slosh effectiveness are investigated under selected idealized excitations. The model validity is demonstrated by comparing the steady-state slosh responses with those derived from the widely-used kineto-static cargo shift model. Results suggest that wider cross-section designs, such as modified-oval and elliptic, yield considerably larger lateral load shift and thus overturning roll moment under partial fill conditions. These tanks would thus yield lower roll stability and poor braking performance, even though such designs offer lower mass center height. Furthermore, addition of full or partial longitudinal baffle helps limit the roll plane slosh considerably.

ACKNOWLEDGEMENT

The author is deeply indebted to his supervisor, Professor S. Rakheja, for his diligent guidance and support during the course of this work. This work would not have been possible without his incessant direction and inspiration.

The author is grateful to his colleagues, Dr. Anand Madakashira-Pranesh and Dr. Krishna Prasad Balike, for endless consultation and discussion related to the work.

Finally the author would like to acknowledge and appreciate his parents and sister for their continual support and motivation. The author specially thanks his sister in recognition to her financial support and encouragement during the course of this work.

Dedicated to my supervisor Dr. Subhash Rakheja

TABLE OF CONTENTS

LIST OF FIGURES	x
LIST OF TABLES	xv
NOMENCLATURE	xvi

CHAPTER 1 INTRODUCTION AND REVIEW OF THE RELEVANT LITRETURE

1.1 Introduction	1
1.2 Relevant Literature Review	3
1.2.1 Slosh analysis	4
1.2.2 Analysis methods	13
1.3 Scope and Objectives	17
1.4 Outline of the Thesis	18

CHAPTER 2 FORMULATION OF QUASI-STATIC ROLL PLANE AND DYNAMIC SLOSH MODELS OF PARTLY-FILLED TANKS

2.1 Introduction	20
2.2 Roll Plane Quasi-Static Model of Partly-Filled Tanks	21
2.2.1 Circular cross-section	24
2.2.2 Elliptic cross-section	27
2.2.3 Modified-oval cross-section	27
2.3 Dynamic Slosh Model of a Partly-Filled Tank	28
2.3.1 Method of analysis	32
2.4 Response Characteristics	33
2.4.1 Load shift	33
2.4.2 Forces and moments	33
2.5 Three-Dimensional Simulation Details	35
2.5.1 Tank geometry	35

2.5.2	Discretization and time step	35
2.5.3	Acceleration excitations	37
2.5.4	Fill volume	38
2.6	Summary	39

CHAPTER 3

ROLL PLANE FLUID SLOSH ANALYSIS IN CLEAN-BORE TANKS

3.1	Introduction	40
3.2	Measures of Dynamic Slosh in Roll Plane	41
3.2.1	Dynamic load shifts	41
3.2.2	Dynamic slosh forces and moments	43
3.2.3	Variation in roll mass moment of inertia	43
3.3	Model Validation	44
3.4	Effects of Tank Cross-Sections	47
3.4.1	Effect of tank cross-section on dynamic load shift	48
3.4.2	Effect of tank cross-section on dynamic slosh forces	53
3.4.3	Effect of tank cross-section on roll moment	55
3.4.4	Effect of tank cross-section on roll mass moment of inertia	58
3.5	Fundamental Slosh Frequency	60
3.6	Effect of Sprung Mass Roll Motion on Dynamic Slosh Measures	61
3.6.1	Effect of roll motion on dynamic load shift	62
3.6.2	Effect of sprung mass roll on dynamic slosh forces	63
3.6.3	Effect of sprung mass roll on roll moment	64
3.7	Summary	66

**CHAPTER 4
THREE-DIMENSIONAL FLUID SLOSH ANALYSIS IN BAFFLED
MODIFIED-OVAL TANK**

4.1	Introduction	68
4.2	Baffle Design Concepts for Modified-oval Tank	69
4.3	Responses to Lateral Acceleration	74
4.3.1	Dynamic load shift	74
4.3.2	Dynamic forces and moments	76
4.3.3	Fundamental slosh frequency	79
4.4	Response to Simultaneous Lateral and Longitudinal Accelerations	80
4.4.1	Dynamic load shift	80
4.4.2	Dynamic slosh forces	84
4.4.3	Dynamic slosh moments	85
4.5	Summary	89

**CHAPTER 5
CONCLUSIONS AND RECOMMENDATIONS**

5.1	Major Contributions of the Dissertation Research	91
5.2	Major Conclusions	92
5.3	Recommendations for Future Work	94
	REFERENCES	96

LIST OF FIGURES

Figure 1.1: The effects of roll angle and lateral acceleration excitation on free surface gradient and lateral load shift [5].	8
Figure 1.2: The optimal tank cross-section proposed by Kang [6].	10
Figure 1.3: Sectional view of a conventional baffled circular tank.	13
Figure 2.1: Translation of center of gravity of the liquid cargo under: (a) tank roll; and (b) lateral acceleration.	22
Figure 2.2: Tank cross-sections considered in the study: (a) Circular, MC-407; (b) Elliptic; and (c) Modified-oval, MC-406.	23
Figure 2.3: Liquid free surface intersections with the modified-oval cross-section tank.	29
Figure 2.4: Global (YZ) and body-fixed (Y'Z') axis systems considered for the modified-oval tank.	31
Figure 2.5: Position vector of an arbitrary wet boundary cell.	34
Figure 2.6: Clean-bore modified-oval tank geometry.	35
Figure 2.7: Two phase flow mesh in a partly-filled cylindrical tank.	36
Figure 2.8: Time-histories of ramp-step and exponentially decaying harmonic lateral acceleration excitations.	38
Figure 3.1: Comparison of lateral cg coordinates (Y_{cg}) of the liquid cargo in a circular tank subjected to roll motions.	45

Figure 3.2: Comparisons of mean dynamic and quasi-static lateral and vertical shifts in the cargo cg for a circular tank subjected to 7° roll and $0.4g$ lateral acceleration at various fill levels; (a) lateral; and (b) vertical.	46
Figure 3.3: Comparisons of mean dynamic and quasi-static lateral and vertical slosh forces for a circular tank subjected to 7° roll and $0.4g$ lateral acceleration at various fill levels; (a) lateral; and (b) vertical.	47
Figure 3.4: Time-histories of lateral load shift of the cargo within various tank cross-sections subjected to idealized path-change maneuver and 7° sprung mass roll (40% fill level).	49
Figure 3.5: Comparisons of peak values of transient lateral cg coordinate of the cargo within various tank cross-sections subjected to idealized path-change maneuver and 7° sprung mass roll.	49
Figure 3.6: Comparisons of variation in vertical cg coordinate within various tank cross-sections subjected to idealized path-change maneuver and 7° sprung mass roll	50
Figure 3.7: Comparisons of normalized lateral cg coordinates for various tank cross-sections subjected to steady-turning maneuver and 7° sprung mass roll.	51
Figure 3.8: Comparisons of variation in vertical cg coordinate within various tank cross-sections subjected to steady-turning maneuver and 7° sprung mass roll.	52
Figure 3.9: Comparisons of static cg height of liquid cargo of selected tank cross-sections for different fill levels.	52
Figure 3.10: Comparisons of peak transient lateral slosh force of the cargo subjected to idealized path-change maneuver and 7° sprung mass roll for different fill levels.	53
Figure 3.11: Comparisons of lateral slosh force amplification factor of the selected tank cross-sections with different fill levels subjected to steady-turning maneuver and 7° sprung mass roll.	54
Figure 3.12: Comparisons of peak roll moment caused by fluid slosh within partly-filled tanks subjected to idealized path-change maneuver and 7° sprung mass roll.	56
Figure 3.13: Time-histories roll moment caused by fluid slosh within 40% filled tanks subjected selected steady-turning maneuver and 7° sprung mass roll.	57

- Figure 3.14: Comparisons of variation in roll moment amplification factor for tanks of various cross-sections subjected to selected steady-turning maneuver and 7° sprung mass roll. 58
- Figure 3.15: Illustrates the variations in peak deviation of roll mass moment of inertia ($max I_X$) as a function of tank cross-section and fill level under idealized path-change maneuver and 7° sprung mass roll. 59
- Figure 3.16: Comparison of fundamental frequency of slosh as a function of fill level and tank cross section. 61
- Figure 3.17: Influence of tank roll motion on the steady-state lateral cg coordinates of liquid cargo within the partly-filled tanks subjected to 0.25g lateral: (a) Circular; (b) Elliptic and (c) Modified-oval. 63
- Figure 3.18: Comparisons of lateral force amplification factor due to cargo shift within partly-filled tank subjected to 0.25g lateral acceleration and sprung mass roll motion. 64
- Figure 3.19: Illustrates the variations in roll moment for partly-filled circular tank subjected to 0.4g lateral acceleration with and without roll under constant load at various fill levels. 65
- Figure 3.20: Time histories of roll moment caused by sloshing cargo within partly-filled modified-oval tank subjected to 0.25g lateral acceleration and sprung mass roll at 40% fill level. 66
- Figure 4.1: Schematics of different baffle arrangements considered in the present study. 71
- Figure 4.2: Illustrates three-dimensional sectional views of baffled tank configurations; (a) FT-FL; (b) FT-PL; and (c) PT-PL 73
- Figure 4.3: Comparisons of the time-histories of instantaneous lateral cg coordinates of fluid cargo within 40 and 60% filled modified-oval baffled tank configurations under 0.25g ramp-step lateral acceleration and 7° sprung mass roll motion: (a) 40% fill; and (b) 60% fill. 76
- Figure 4.4: Comparisons of slosh force amplification factors of different configurations under 0.25g lateral acceleration and 7° sprung mass roll motion: (a) lateral force amplification; and (b) vertical force amplification. 77

- Figure 4.5: The time-histories of roll moment responses of the configurations with 40% filled tanks under idealized constant lateral acceleration and 7° sprung mass roll motion. 78
- Figure 4.6: Comparisons of roll moment amplification factors (of tank configurations subject to 0.25g lateral acceleration and 7° sprung mass roll motion (40 and 60% fill conditions). 79
- Figure 4.7: Comparisons of roll plane fundamental slosh frequency for baffled tank configurations under idealized steady-turning and 7° sprung mass roll motion.80
- Figure 4.8: Comparisons of time-histories of lateral cg coordinate of the cargo in partly-filled tanks with different baffle subject to $a_x=0.6g$, $a_y=0.25g$ and $\theta = 7^\circ$; (a) 40%; and (b) 60% fill level. 82
- Figure 4.9: Shows the two phase flow view of 40% filled tank A under $a_x=0.6g$, $a_y=0.25g$ and $\theta = 7^\circ$ at $t=15s$ where blue and red colors represent fuel oil and air respectively; (a) Top view; (b) Side view. 82
- Figure 4.10: Comparisons of variation in instantaneous longitudinal cg coordinate of cargo in tanks with different baffle arrangements subject to $a_x=0.6g$, $a_y=0.25g$ and $\theta = 7^\circ$; (a) 40; and (b) 60% fill level. 83
- Figure 4.11: Comparisons of force amplification factors for all baffled tank configurations subject to $a_x=0.6g$, $a_y=0.25g$ and $\theta = 7^\circ$; (a) Lateral; and (b) Longitudinal. 85
- Figure 4.12: Comparisons of roll moment time-histories for all considered tank configurations subject to simultaneous acceleration and 7° sprung mass roll motion at 40% fill level. 86
- Figure 4.13: Comparisons of roll moment amplification factor under selected accelerations and 7° sprung mass roll motion. 87
- Figure 4.14: Comparisons of pitch moment time-histories for all considered tank configurations subjected to simultaneous acceleration and 7° sprung mass roll motion at 40% fill level. 88

Figure 4.15: Comparisons of pitch moment amplification factor for all considered tank configurations subjected to simultaneous acceleration and 7° sprung mass roll motion. 89

LIST OF TABLES

Table 2.1: Influence of mesh density on the resulting mean dynamic lateral force.	37
Table 3.1: Comparisons of peak vertical cg coordinate of deflected cargo within tanks various cross-sections and fill levels subjected to steady-turning maneuver and 7° sprung mass roll.	60
Table 4.1: Comparisons of overall computation time requirement for simulating a 40% filled modified-oval tank configuration subjected to 0.25g lateral acceleration with a time step of 0.25ms.	74

NOMENCLATURE

A	Conventional transverse baffled modified-oval tank.
FT-FL	Complete longitudinal-transverse baffled modified-oval tank.
FT-PL	Partial longitudinal and complete transverse baffled modified-oval tank.
PT-PL	Partial longitudinal-transverse baffled modified-oval tank.
A_c	Cell area.
A_w	Wetted area.
a_x, a_y, a_z	Longitudinal(x), lateral (y) and vertical (z) component of vehicle acceleration.
a, b	Semi-major (a) and semi-minor (b) axes of elliptic cross-section.
B, H	Height (2B) and width (2H) of modified-oval cross-section.
C	Cell.
c	Z-intercept of free surface.
CFD	Computational fluid dynamics.
CFR	Code of federal regulations.
c_0	Static Z-intercept of free surface.

c_{yn}, c_{zn}	Lateral and vertical coordinate of n^{th} arc center forming modified-oval cross-section.
ε	Difference in static and steady-state volume per unit length of tank.
F_x, F_y, F_z	Slosh forces along longitudinal, lateral and vertical axes.
$\bar{F}_x, \bar{F}_y, \bar{F}_z$	Mean slosh forces along longitudinal, lateral and vertical axes.
g	Acceleration due to gravity.
I_x	Mass moment of inertia about longitudinal axis.
i, j, k	Unit vectors along X, Y, Z directions.
K_q	Normalized response variable.
\vec{M}	Moment vector.
M_x, M_y	Roll and pitch moment about the origin 'O'.
\bar{M}_x, \bar{M}_y	Mean roll and pitch moment about the origin 'O'.
m	Mass of fluid.
P	Fluid pressure.
P_c	Pressure of cell 'C'.
q	Response variable.

\bar{q}	Mean response variable.
R_n	Radius of n^{th} arc forming modified-oval cross-section.
R	Radius of circular cross-section.
\vec{r}_c	Position vector of cell 'C' from origin 'O'.
RT	Reuleaux triangle cross-section.
s	Seconds.
SRT	Static rollover threshold
t	Time.
UDF	User defined function.
u, v, w	Fluid velocity components along X, Y, Z directions.
V	Fluid volume per unit length of the tank at steady-state condition.
V_0	Fluid volume per unit length of the tank at static condition.
VOF	Volume of fluid.
XYZ	Longitudinal, lateral and vertical axes of Cartesian global coordinate system.
$X'Y'Z'$	Longitudinal, lateral and vertical axes of Cartesian body-fixed coordinate system.

x_c, y_c, z_c	Instantaneous position coordinates of cell 'C' with respect to origin 'O'.
y, z	Lateral and vertical coordinate of liquid particle at the free surface.
y_{r0}, z_{r0}	Right intersection point of the liquid free surface with the tank periphery at static condition.
y_{l0}, z_{l0}	Left intersection point of the liquid free surface with the tank periphery at static condition.
y_r, z_r	Right intersection point of the liquid free surface with the tank periphery at steady-state condition.
y_l, z_l	Left intersection point of the liquid free surface with the tank periphery at steady-state condition.
Y_{cg}	Steady-state lateral coordinate of cargo center of gravity.
Y_{cg}, Z_{cg}	Lateral and vertical coordinates of the cargo center of gravity.
\bar{Y}_{cg}	Mean lateral coordinate of the cargo center of gravity.
Z_0	Static center of gravity height.
Δz	Max variation in vertical center of gravity coordinate.
θ	Sprung mass roll angle.
\emptyset	Free surface inclination to the horizontal.
ρ	Density of the fluid.

γ

Kinematic viscosity of the fluid.

ξ

Damping ratio of fluid.

CHAPTER 1

INTRODUCTION AND REVIEW OF THE RELEVANT LITRETURE

1.1 Introduction

It has been identified that maneuver-induced liquid cargo motion in a partly-filled tank vehicle poses a serious threat to the stability and controllability of the vehicle. High center of mass (cg) design of the saddle-mounted tank together with moments induced by cargo shift lead to relatively lower stability and control limits of such vehicles. Even a reasonable maneuver could yield vehicle instability and thus a road accident. Accidents involving such vehicles are generally associated with highly unreasonable risks to road safety, safety of road users and the environment, when flammable and hazardous cargoes are involved. Rollover, jackknifing and trailer swing are some of the instability modes that have been attributed to liquid cargo slosh within a tank vehicle [1, 2]. Amongst all these instability modes, rollover accidents have been reported most frequently, although the eventual rollover may be caused by an yaw instability. The rollover accidents account for nearly 67% of all the serious single vehicle crashes involving liquid cargo tank vehicles [3]. It has been further reported that the injuries and fatalities among the truck drivers attributed to rollover accidents are in the order of 45% and 52%, respectively [3]. In a study by Battelle, it has been shown that partial fill in a road tanker accounts for relatively greater rollover incidents [3].

While negotiating a turn, a path change maneuver or in soft shoulders, the vehicle sprung mass experiences roll motion as well as centrifugal acceleration. In case of a partly-filled tank vehicle, the centrifugal acceleration and roll motions yield cargo

shifting and thus additional destabilizing moments on the vehicle, this could lead to one or more of the instability modes mentioned above. The magnitude of cargo shift and thus the destabilizing moment strongly depends upon the tank capacity, fill volume, tank cross-section and effectiveness of anti slosh devices, if any, apart from the severity of the maneuver (steer angle, steer rate, speed and brake pressure). The tank cross-section in particular influences the fluid motion in the roll plane, while its effect in pitch plane under braking input is very small to negligible. Widely used anti slosh devices, the transverse baffles, on the other hand tend to suppress the fluid slosh in the pitch plane [7].

Owing to their lower stability limits [5] and potentially catastrophic consequences of accidents involving partly-filled tank vehicles, it has been widely recognized that their stability limits need to be preserved at least to those of conventional commercial vehicles. This dissertation research focuses on two different tank design factors in an attempt to reduce fluid slosh loads, namely, the tank cross-section and baffle designs. Although a few studies have investigated the effects of tank cross-section on the roll stability limits using simple quasi-static load shift analyses [5, 6], the effect on transient fluid slosh has not yet been reported. A number of studies have concluded that magnitude of transient slosh forces and moments are significantly greater than the corresponding steady-state forces and moments [7, 14]. The current designs of baffles are known to be effective in suppressing fluid slosh in the pitch plane, while their effect on the roll plane slosh suppression is very small [7].

This dissertation research investigates a few baffle designs in an attempt to limit fluid slosh in both roll and pitch planes, in addition to the tank cross-section effect on transient

slosh responses. In particular, the steady-state and transient fluid slosh characteristics are evaluated for three different cross-sections: (i) a circular cross-section, as per MC-407 design [5]; (ii) a modified-oval cross-section, as per MC-406 design [5]; and (iii) an elliptic cross-section tank that are employed in farm spraying vehicles. The analyses are performed for both clean-bore and baffled tank designs under lateral and longitudinal accelerations applied independently and simultaneously, which represent pure braking, pure turning, and combined braking and turning maneuvers of the vehicles. Three different lateral slosh suppressing baffle arrangements are proposed and discussed in terms of their anti slosh effectiveness under excitations representing turning, braking-in-a-turn and path change maneuvers. The analyses are performed using the FLUENT [35] computational fluid dynamic (CFD) software.

1.2 Relevant Literature Review

Sloshing of liquid within partly-filled tanks has been studied since early 1960's for different applications involving spacecrafts, liquid bulk transportation, off-shore structures and ships. Given the complexities associated with analytically solving Navier-Stokes and continuity equations together with equation of free surface and intricate tank geometry, liquid slosh has been investigated using different approaches, namely experimental, semi-analytical and numerical. Due to challenges associated with dynamic analysis of coupled tank vehicle and associated enormous computational needs, the majority of the reported studies on directional dynamic analyses of tank vehicles have employed kineto-static fluid slosh models. Such analyses could neither account for significantly higher magnitudes of transient slosh forces nor the effects of baffles [5].

Alternatively, analysis of transient slosh within the tank structure alone would allow a better understanding of slosh phenomenon within tanks of different cross-sections with different baffle arrangements. The reported relevant studies are reviewed and discussed in the following subsections so as to gain knowledge on the methods of analysis and define specific scope of the dissertation research

1.2.1 Slosh analysis

Movement of liquid cargo within a partly-filled moving tank is governed by a number of tank design and operating parameters such as tank geometry, tank capacity, fluid properties, fill volume and nature of excitation as determined by the vehicle configuration, speed and the maneuvers. A few studies have investigated the effects of some of these parameters on the steady-state slosh forces and moments on the braking and roll dynamic properties of the vehicles [5, 17]. These suggest that the variation in tank design factors, the fill volume and nature of excitations yield strong coupled effects on the slosh forces and moments. The effects of some of these factors on the transient fluid slosh forces and moments, however, have been investigated in a very few studies limited to the maneuver- and fill- related parameters only[10, 19]. The effects of these parameters, as reported in various studies are discussed below.

Fill volume

Road tankers, employed in general purpose liquid bulk transportation often operate with partly-filled tanks due to variation in the product mass density and the road laws limiting the axle loads. Such vehicles operating on their local delivery routes may also encounter partial-fill conditions. The fill volume directly relates to the fluid inertia, cg height and

the load shift potential and thus the associated forces and moments. Studies have established a strong dependence of the slosh characteristics on the fill volume [9, 10]. It is worthwhile to highlight that these reported interdependencies are invariably coupled to the tank cross-section considered in these studies. A higher fill volume would cause larger roll moment due to higher fluid inertia and higher cg. These studies have also shown that partly-filled wider cross-section tanks such as modified-oval and elliptic cause relatively higher steady-state cargo shift and thus larger roll moment but could yield lower cg height. A circular cross-section tank, on the other hand, would lead to higher cargo cg but relatively lower steady-state cargo shift [5]. A lower fill volume, on the other hand, would yield greater variation in transient roll and pitch moments due to increased shift in cg and greater fluid slosh [1]. The effect of fill volume on the steady-state load shift and static rollover threshold of the vehicle was investigated in a few earlier studies using kineto-static fluid slosh model [5, 17]. These studies could not account for the transient fluid slosh and the fluid motion in the baffled tanks. The effects of fill volume on the transient peak forces and moments and mass moments of inertia have been investigated for circular and reuleaux triangle (RT) cross-sections in two different studies [13, 19]. These studies have shown that the magnitudes of transient forces and moments could be twice those derived from kineto-static analysis. Furthermore, the slosh characteristics are strongly affected by the baffles, particularly in the pitch plane.

Apart from slosh forces and moments, the fill volume also affects the natural slosh frequencies. It has been suggested that the fundamental slosh frequency in the

vicinity of the typical steering frequency may cause resonant fluid oscillations and thus greater magnitudes of slosh forces and moments on the vehicle and greater stresses of the container [13, 22]. Abramson [9] and Budiansky [11] employed linear fluid slosh theory to determine the natural frequencies of sloshing for different tanks and open canals. The recently reported studies on tanks, employed in road vehicles, have emphasized on the fundamental slosh frequencies identified from the CFD analysis [7, 13] and a semi-empirical approach [43, 44]. These studies show that the fundamental slosh frequencies of a 50% filled tank are in the order of 0.6Hz and 0.3Hz in the roll and pitch planes, respectively. These tend to decrease with lower fill volume and may coincide with the steering frequency in an emergency type maneuver. The reported studies, irrespective of the methodologies used, show quite comparable values of fundamental slosh frequencies for different fill volumes.

Fluid properties

The kineto-static fluid slosh models, considered for analysis of directional control limits of partly filled tank vehicles, do not consider the effects of fluid properties [5, 17]. The effect of viscosity and density on the transient behavior has been investigated in only a few studies for a circular tank [13, 26]. Even-though fluid viscosity is expected to strongly influence slosh characteristics, the variation in viscosity of frequently transported fluids showed only meager affect on sloshing behavior. Further, the effect of viscosity on slosh damping and fundamental slosh frequency was observed to be negligible. However, fluid density plays a pivotal role in slosh characteristics because it has direct bearing on both the cargo inertia and fill level [13].

Maneuver-induced excitation

The magnitude of transient as well as steady-state slosh forces and moments arising in partly filled tank vehicles are mainly attributed to maneuver-induced excitations. Consequently severity of such maneuvers plays decisive role in tank vehicle stability and controllability. A number of studies have highlighted the influence of maneuver-induced excitation on various slosh measures such as load shift, magnitudes of slosh forces and moments, and variations in the roll and pitch mass moments of inertia [10, 12, 13, 14]. Greater rollover incidents of tank vehicles have attracted far more attention towards slosh analysis in the roll plane. The reported studies have demonstrated that the magnitude of roll moment attributed to slosh is proportional to the amplitude of lateral acceleration caused by the maneuver [13, 15]. The magnitude of roll moment is associated to the amplitude of lateral acceleration through the translation of center of mass (cg) of liquid cargo; a large liquid cargo cg translation yields a higher roll moment. The magnitude of translation of cg, on the other hand, is a function of free surface gradient, given by $\tan \phi = \frac{\theta - a_y}{(1 + a_y \cdot \theta)}$; where a_y is vehicle lateral acceleration in g, θ is the sprung mass roll angle in radians and ϕ is the free surface gradient. Further, due to smaller roll angle magnitude compared to that of lateral acceleration, contribution of roll angle on load shift and thus the roll moment is considered to be relatively small as compared to that due to lateral acceleration excitation. Figure 1.1 illustrates the effects of roll angle and lateral acceleration excitation on free surface gradient and lateral cg translation [5], assuming kineto-static fluid slosh [1].

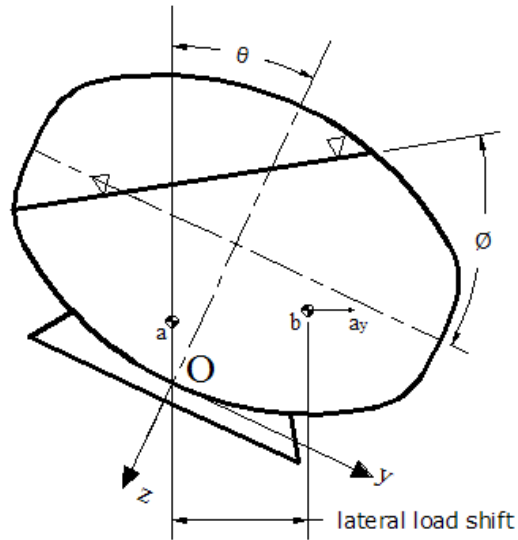


Figure 1.1: The effects of roll angle and lateral acceleration excitation on free surface gradient and lateral load shift [5]

Further, frequency of maneuver-induced excitations also plays a vital role in view of liquid cargo movement within the partly-filled tank vehicles. Although the frequency of steering maneuvers is typically well below 0.5Hz, the frequency of emergency evasive maneuver may approach the fundamental slosh frequency under low fill volumes. Recently, Yan [19] has experimentally shown that magnitude of lateral slosh force amplification factor and normalized roll moment could be as high as 4 and 7.5 times , respectively for a lateral harmonic excitation amplitude of 0.5m/s^2 with frequency close to the fundamental slosh frequency. Another study, based on CFD analysis of transient slosh within partly-filled tanks reported similar trends [13]. These studies invariably concluded that for continuous and single cycle harmonic excitations, the peak slosh forces and moments usually occur in the vicinity of the slosh natural frequency.

Tank geometry

The magnitude of fluid slosh is strongly influenced by the boundary constraints formed by the tank geometry. The presence of baffles or partitioning in a cargo tank constitutes additional boundaries and thus affects the fluid motion most significantly. The cross-section and length of the tank together with the shape and number of baffles affect the liquid slosh and thus the stability limit of the partly filled tank vehicles. Ranganathan [5] studied the effects of tank cross-section on stability of tank vehicles by integrating a two dimensional quasi-static slosh model of a clean-bore tank with a comprehensive roll plane model of an articulated vehicle. The study considered circular, elliptical and modified-oval cross-section tanks, and concluded that the rollover threshold of a partly-filled tank vehicle is strongly dependent on the tank cross-section, apart from the fill volume.

Kang [17] developed a three dimensional quasi-static fluid slosh model of a generic cross-section tank to evaluate the braking and roll dynamic responses of partly-filled articulated vehicles. The study, however, was limited to a single tank cross-section resembling a 'reuleaux triangle' (RT). The same kineto-static model was applied by Ziarani et al. [18] to derive an optimal tank cross-section for limiting the roll plane steady-state slosh. Both the studies proposed very similar optimal tank cross-sections that could yield minimum lateral load transfer and lower cg height. The cross-section was symmetric about the vertical centerline with a wider bottom and narrow top, as shown in the Figure 1.2, which revealed higher roll stability limit of tank vehicles compared to those with conventional circular and modified-oval tanks.

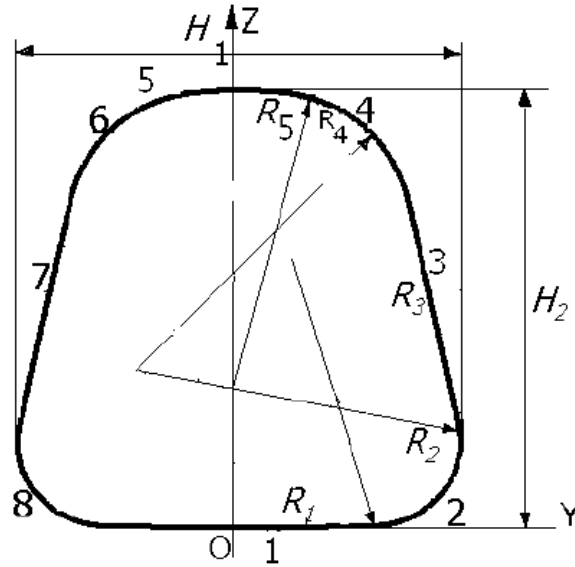


Figure 1.2: The optimal tank cross-section proposed by Kang [6].

The above studies employing the quasi-static fluid slosh model do not permit analysis of tank geometry effect on the transient slosh forces and moments, nor the effect of boundaries formed by the baffles. Two - and three-dimensional transient fluid slosh analyses have also been reported for circular [10, 48], rectangular [25, 46; 47] and RT [22] cross-section tanks, with and without baffles. The effect of tank cross-section on the transient fluid slosh and the corresponding rollover threshold of an articulated tank vehicle were investigated by Yan [19] considering the circular and RT tanks of identical cross-section area and length. The study showed that RT tank yields lower transient lateral load shift and higher rollover threshold compared to the circular tank under higher fill conditions, while it yields greater transient lateral load shift and yet higher rollover threshold compared to the circular tank at low fill conditions due to its wider bottom and narrow top sections. Even though, Yan [19] in his work has established that the optimal cross-section tank proposed by Knag [17] yields higher rollover threshold than the

circular cross-section tank, the analysis was based on the assumption that sustained peak transient forces and moments occur during a steady-turning maneuver.

Slosh suppression devices

Liquid cargo tanks are designed with either external ring stiffeners or internal transverse baffles to achieve enhanced integrity of the tank structure in accordance with current standards [42]. The internal baffles have proven to be highly efficient in suppressing the fore-aft motion of liquid cargo within the partly-filled tank. A few studies analytically, using a mechanical analogy modeled and or experimentally investigated the damping effectiveness of such slosh suppression devices [20, 21]. Anti slosh devices such as ring baffles, truncated perforated cones and flexible baffles, have been explored since early 1970's [20] by National Aeronautics and Space Administration (NASA) to mitigate propellant sloshing induced by the launch vehicle tank motion. Compartmenting of the launch vehicle tank was also employed in certain circumstances to shift the resonant frequency into a preferred frequency range. Optimum location of compartment walls within a partly-filled tank truck was investigated by Zhanqi et al. [32] to achieve improved braking performance, while the analysis employed kineto-static fluid motion. The reported study concluded that equal compartment lengths yield minimal longitudinal load shift under straight-line braking. Strandberg [21] experimentally evaluated the effectiveness of different longitudinal anti slosh baffle arrangements within scaled tanks, which were later emphasized by Ervin [38] and Winkler [30]. However owing to their excessive weight and difficulties associated with cleaning of the tanks in the general-

purpose liquid bulk transportation sector, such longitudinal baffle arrangements could not be considered practical.

A few recent studies have experimentally investigated the anti slosh effectiveness of different baffle designs within scaled tanks [14, 24, 45]. Yan [14] analyzed transient slosh in a partly-filled RT tank with and without transverse baffles, while Ibrahim [24] investigated anti slosh effectiveness of different longitudinal baffles with slots and orifices. For reasons of economy and complexities associated with experimental investigations, a few studies have employed CFD methods to analyze different baffle designs within partly-filled circular tank cross-sections [7, 8, 26]. Figure 1.3 illustrates the arrangement of widely employed conventional baffles within circular tanks. Even though most of these studies have focused on transverse baffles, Miralbes [8] recently studied the effects of horizontal split baffle configurations on roll dynamics of tank vehicles. However, due to inadequate baffle dimensioning and configurations, the study could not yield significant gain in terms of roll moment. All of these reported studies have invariably emphasized on the effectiveness of baffles in suppression of fluid slosh in the pitch plane and thus improving the dynamic behavior of the tank vehicles.

Perforated longitudinal baffle plates have shown significant benefits in suppressing fluid slosh in floating platforms [40, 41]. Strategically placed perforated longitudinal baffle plate arrangement was implemented for preventing mixing of gas, oil and water within the floating separator chamber, leading to considerable performance improvement for the separator. It has been suggested that similar performance

improvements could be achieved for tank vehicles through pragmatic longitudinal baffle arrangement and design. Given longitudinal baffle

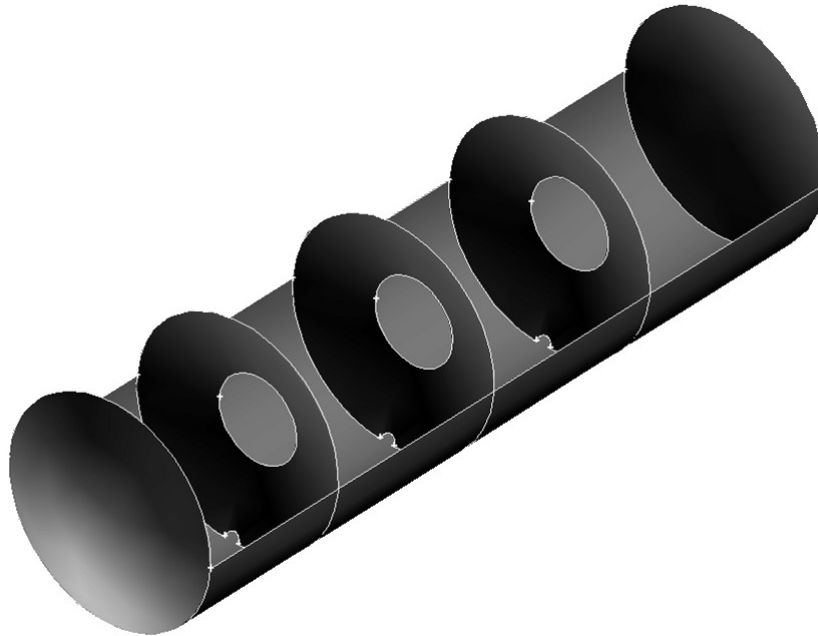


Figure 1.3: Sectional view of a conventional baffled circular tank

arrangements produce considerable improvement in roll stability limits, concerns regarding excessive weight and interference with cleaning could be addressed by introducing optimal perforations and baffles shapes.

1.2.2 Analysis methods

Earlier studies on slosh in partly-filled tanks were based on experimental investigations of scaled tanks or linear slosh theories. Strandberg [21] experimentally investigated liquid slosh within scaled circular, elliptic and rectangular tanks in-order to study lateral stability of tank vehicles. Although the contribution of sprung mass roll or the cargo shift was neglected, the study under different lateral accelerations provided significant insight in the field of lateral stability of tank vehicle. Abramson et al. [9] experimentally

investigated sloshing of liquid within scaled spherical and vertical cylinders with an objective to develop a better understanding of fluid sloshing within fuel tanks of in-flight rockets. Experimentally obtained slosh forces when compared with analytical values yielded reasonably good agreements considering the fact that analytical values were estimated from linear slosh theory. The differences between the two values were always less than 15%. Recently, Yan [22] conducted experiments on a scaled RT cross-section tank to analyze the effect of transverse baffles on slosh frequencies, forces and moments. The experimental study showed that transverse baffles have a significant contribution towards attenuation of pitch plane sloshing within partly-filled tanks. The longitudinal mode natural frequencies were noticeably higher compared to those of the un-baffled tank, while lateral mode natural frequencies were unaffected.

Owing to the challenges associated with integration of a comprehensive transient slosh model and a dynamic vehicle model for the analysis of tank vehicle stability, Rakheja et al. [1] developed a simple quasi-static slosh model capable of predicting steady-state slosh responses. Although this model was based on assumptions of inviscid fluid and gross movement of liquid bulk, the model provided good estimates of steady-state load shifts, forces and moments, and steady-state rollover threshold of the partly-filled vehicles. A number of studies have employed this kineto-static model of the partly-filled tanks for dynamic analysis of tank vehicles [1, 2, 5]. However, this model does not allow for analysis of dynamic slosh or analysis of baffle designs and configurations.

Following the work of Abramson [9] a number of researchers began modeling slosh either as a linear problem or developed analogous mechanical models for slosh analysis

[23, 24]. Salem et al. [23] studied rollover stability of a partly-filled elliptic tank vehicle using a pendulum model to simulate fluid sloshing. Although this study predicted considerably accurate values of rollover threshold, identification of parameters for the analogous slosh model was extremely challenging. Moreover slosh models based on pendulum analogy are limited to linear sloshing scenarios only. Most of these analytical and mechanical analogous slosh models were limited in their application since they could simulate only small amplitude sloshing.

One of the earliest studies which applied computational fluid dynamics (CFD) code based on finite difference method was by Popov et al. [25], to investigate fluid slosh within rectangular tanks. The model was subsequently applied to study roll dynamics of vehicles by Ranganathan et al. [5]. The study formulated a two-dimensional nonlinear dynamic slosh model to simulate liquid cargo motion within a clean-bore circular tank and coupled it with a comprehensive dynamic vehicle model to investigate roll dynamics of the tank vehicles. Popov et al. [25] developed the two-dimensional dynamic slosh model using finite difference methodology for circular and rectangular tank cross-sections with an objective of investigating the influence of various input parameters on dynamics of liquid slosh within a tank. The two-dimensional slosh model, however, could not analyze the responses to simultaneous lateral and longitudinal excitations and the coupling effects of fluid motion in roll and pitch planes. Both the studies have invariably highlighted the vulnerability of tank vehicle stability to transient slosh and the cross-section of the tank.

Bulk transportation industry has circumvented the transient slosh issue by placing lateral baffles within the tanks. Lateral baffles have proven to be most effective in suppressing longitudinal slosh motion but their contribution in the roll plane is insignificant. Shue et al. [26] developed an in-house CFD code to study the effect of baffle perforation under large amplitude slosh within a tank. The two-dimensional slosh analyses used in the above studies could not capture the motion of liquid cargo within the tanks employed in road transportation of liquid bulks nor the coupling between the lateral and longitudinal fluid motions.

With the advent of commercial CFD codes like FLUENT, FLOW3D and FLOTRAN, a number of three-dimensional liquid slosh models have been formulated and analyzed for cargo tanks [13, 27, 28]. These commercial CFD codes are able to comprehensively model liquid sloshing for different applications. Rhee [28] demonstrated the effectiveness of FLUENT in modeling both laminar and turbulent fluid flows, while Lee et al. [27] conducted a parametric sensitivity analysis of a LNG tank sloshing using FLOW3D. Modaressi et al. [13] investigated the transient slosh inside a partly-filled clean-bore circular tank using FLUENT. This study not only highlighted the transient effect of slosh, but also established the validity of FLUENT in modeling liquid cargo flows within tanks. These numerical studies on fluid slosh have generally focused on parametric sensitivity analysis while only a few have investigated the effects of baffle designs and configurations.

Fleissner et al. [29] proposed a completely new approach for investigating dynamic slosh motion within tank trucks. Fleissnar coupled a Lagrangian particle method

based tank model with a classical multi-body truck model and compared the tank truck responses for granular and fluid cargoes. The co-simulation was accomplished through linking Pasimodo, Lagrangian simulation platform for three-dimensional analysis of fluid models, with Simpack. Such an approach would be of great help for coupled tank vehicle studies. Yan et al. [14] studied the performance benefits of a multiple orifice transverse and partial baffle for the RT tank. Kandesamy et al. [7] investigated fluid slosh in a circular cross-section tank with different arrangements of full and partial baffles. These studies have concluded that oblique placement of baffles could help limit lateral slosh to an extent apart from the longitudinal slosh.

1.3 Scope and Objectives

From the review of literature, it is evident that the directional dynamics and stability limits of partly-filled tank vehicles have been widely investigated assuming quasi-static fluid slosh. The analysis of transient fluid slosh has been limited to either circular or reuleaux triangular or rectangular cross-section tanks, while only limited efforts have been made to assess anti slosh effectiveness of alternate baffles designs. Considering that the magnitudes of forces and moments induced by fluid slosh are strongly affected by the tank cross-section, and layout and design of baffles, this dissertation research focused on investigations of these design parameters.

Analyses of dynamic slosh within tanks of different cross-sections under a constant load condition would facilitate identification of a desirable tank cross-section that would help limit the magnitude of slosh forces in the roll plane. Alternate

arrangements and designs of baffles may be realized to limit fluid slosh not only in the pitch plane but also in the roll plane, so as to attain greater yaw as well as roll stability limits of tank vehicles. The primary objectives of the dissertation research are thus formulated as follows:

- Investigate transient fluid slosh within partly-filled clean-bore and baffled tanks of different cross-sections subjected to lateral and longitudinal accelerations and sprung mass roll excitations.
- Assess relative performance characteristics of selected tank cross-sections in terms of transient and steady-state slosh forces, moments, load shifts and mass-moments of inertia.
- Propose different design and arrangements of longitudinal and transverse baffles, and evaluate their effectiveness in lateral and longitudinal slosh suppression.

1.4 Outline of the Thesis

The quasi-static roll plane slosh models of different cross-section tanks are formulated in chapter 2, which would serve as the baseline models for validation of transient slosh models that are presented in chapter 3. The steady-state responses of the partly-filled tanks of circular, elliptic and modified-oval tanks, widespread in the industry, are evaluated and discussed to highlight the effects of tank cross-section, although the analyses are limited to clean-bore tanks alone.

At the onset of Chapter 3, measures of dynamic slosh in roll plane are discussed. The effects of tank geometry on the dynamic slosh measures are investigated and

discussed in terms of load shift, slosh forces and moments, and roll mass moment of inertia. Moreover, the effect of the tank cross-section on the fundamental slosh frequency under turning maneuver for different fill conditions is also estimated and discussed. Furthermore, the sprung-mass roll and its effects are quantified and presented in-view of fluid slosh.

Based on the analysis and discussions in chapter 3, the tank geometry most susceptible to roll plane instability is selected for subsequent analyses in chapter 4 involving baffles designs and three-dimensional slosh analysis. A number of different slosh suppressing baffle design configurations are conceived and three-dimensional CFD models are formulated. The effectiveness of the proposed baffle configurations are evaluated and discussed with respect to that of conventional tank baffle design under both lateral acceleration and simultaneous lateral and longitudinal acceleration conditions.

The major findings of the study are summarized in chapter 5 together with the thoughts on worthy further studies for deriving effective baffle designs.

CHAPTER 2

FORMULATION OF QUASI-STATIC ROLL PLANE AND DYNAMIC SLOSH MODELS OF PARTLY-FILLED TANKS

2.1 Introduction

It has been established, both experimentally [50] and analytically [31], that rollover acceleration limits of commercial vehicles are significantly lower than the passenger vehicles. The partly-filled tank vehicles exhibit even lower rollover limit due to the motion of liquid cargo within the partly-filled tank, which gives rise to an additional overturning moment [30]. General purpose tank vehicles employed for transportation of chemicals are often partly-filled due to regulations concerning limitations on axle loads, and variation in weight density of various products. The tank vehicle and cargo interactions have been investigated in a number of studies using different approaches. These studies have provided valuable insight on the steady-state, and transient forces and moments developed within the partly-filled tanks due to disturbances induced by steering and accelerating/braking maneuvers [1, 13, 52].

In view of the complexities associated with highly nonlinear dynamic slosh and directional dynamic vehicle models, the studies on coupled tank-vehicle dynamics have been mostly limited to quasi-static fluid slosh models of the cargo [1, 19, 51]. These studies have suggested significant influence of the tank cross-section on the steady-state dynamics, while the analyses have been limited only to clean-bore tanks. The assumption of quasi-static fluid motion could yield reasonably good prediction of the cargo shift and roll moment attributed to slosh in the roll plane, but would yield significant error for the pitch plane slosh within cargo tanks that are typically 7 to 13 m long. In this chapter, a

kineto-static roll plane model, described in [5, 13], is formulated to: (i) establish reference steady-state responses for verification of the dynamic slosh model presented later in the chapter; and (ii) enhance understanding of the effect of tank cross-section on the steady-state slosh responses.

2.2 Roll Plane Quasi-Static Model of Partly-Filled Tanks

During a steady turning maneuver, both the sprung and unsprung masses of a road vehicle experience roll and centrifugal (lateral) acceleration. In case of a partly-filled tank vehicle, the roll motion of the sprung mass cause motion of the free surface of liquid and as a result the center of gravity of the liquid cargo experiences a shift in the roll plane, as shown in Figure 2.1(a). The lateral acceleration experienced by the tank imposes an equal and opposite acceleration to the liquid cargo and hence causes further motion of the liquid free surface, thereby resulting in further shift in the position of center of gravity of the liquid bulk, as shown in Figure 2.1(b). This shift in the center of gravity of the liquid cargo induces an additional roll moment on the sprung mass and thereby reduces the overturning stability of the vehicle, and is a function of the fill level, tank cross-section and gradient of the free surface due to tank roll and lateral acceleration [2, 5].

Considering equilibrium of forces for an inviscid fluid element inside the partly-filled tank subjected to simultaneous roll motion and lateral acceleration, the free surface gradient could be derived from [5]:

$$\tan \phi = \frac{\theta - a_y}{(1 + a_y \cdot \theta)} \quad (2.1)$$

where a_y is vehicle lateral acceleration in g , θ is the sprung mass roll angle in radians and ϕ is the angle between free surface and horizontal axis of the tank. Neglecting roll motion of the tank, the free surface gradient could be directly related to the lateral acceleration, $\tan \phi \approx a_y$.

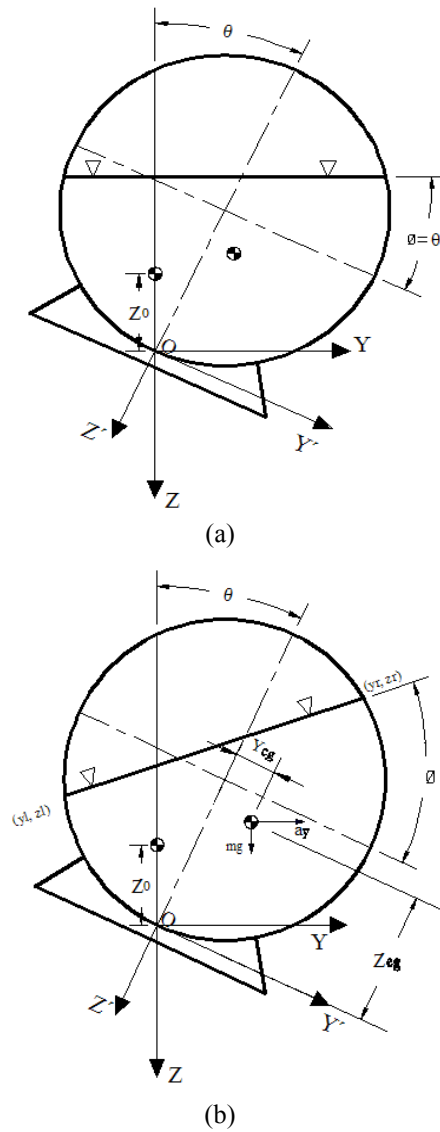


Figure 2.1: Translation of center of gravity of the liquid cargo under: (a) tank roll; and (b) lateral acceleration

For a given fill level, the translation of cg of liquid cargo strongly depends on the tank cross-section. Thus the rollover acceleration limits of a partly-filled tank vehicle are

highly influenced by the cross-section. The rollover acceleration limit, however, is further dependent upon the fill level and is coupled with the tank cross-section in a complex manner. Although various cross-section tanks have been designed for transportation of liquid cargo, circular and modified-oval cross-sections described in the current standards and denoted as MC-407 and MC-406 respectively, are widely used by the industry. Elliptic cross-section tanks are also employed in many applications such as farm spraying. Figure 2.2 illustrates the three tank cross-sections that are considered in this study to investigate the effects of tank cross-section on the steady-state and transient fluid slosh responses. The modified-oval cross-section is described by eight arcs; the upper and lower boundaries of radius R_1 , side walls of radius R_2 and blend arcs of radius R_3 . The dimensions of the selected cross-sections are chosen to yield nearly identical cross-sections area of 23.6 m^2 , which are summarized below:

Circular:	$R_1 = 1.015 \text{ m}$		
Elliptic:	$2a = 2.1 \text{ m};$	$2b = 2 \text{ m}$	
Modified-oval:	$R_1 = 1.78 \text{ m};$	$R_2 = 1.78 \text{ m};$	$R_3 = 0.39 \text{ m};$
	$2B = 1.65 \text{ m};$	$2H = 2.44 \text{ m}$	

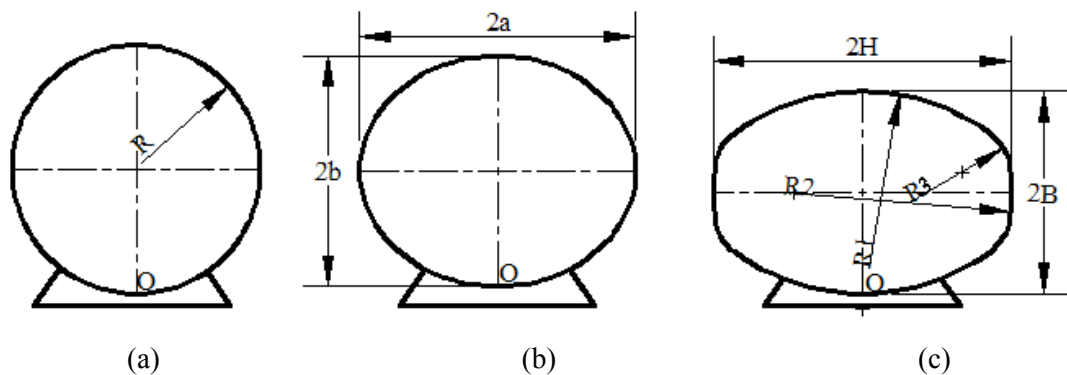


Figure 2.2: Tank cross-sections considered in the study: (a) Circular, MC-407; (b) Elliptic; and (c) Modified-oval, MC-406.

The overall width of the modified-oval tank (2H) is 2.44 m, while that of the elliptic tank is 2.1 m, which is closer to the circular tank diameter of 2.03 m. The overall height of the elliptic tank is 2 m, which is also comparable to that of the circular tank (2.03 m) but considerably higher than that of the modified-oval tank (2B=1.65 m). However, elliptic tanks manufactured under the existing regulation are wider than the older version used in the current study.

2.2.1 Circular cross-section

The quasi-static fluid slosh model of the circular cross-section tank is illustrated in Figure 2.1. The free surface gradient, defined in Eq. (2.1), can be applied to derive the steady-state load shift, and slosh forces and moments under roll motion of the tank and lateral acceleration. The model describes the steady-state free surface after the free surface oscillations have completely decayed. The equation of the free surface of the liquid cargo, subjected to roll motion and lateral acceleration in the steady condition could be written as [5]:

$$z = - \left\{ \frac{\theta - a_y}{(1 + a_y \cdot \theta)} \right\} y - c \quad (2.2)$$

where z and y are the vertical and lateral coordinates of the liquid particles at the free surface, respectively, $\frac{\theta - a_y}{(1 + a_y \cdot \theta)}$ is the free surface gradient and c is the free surface intercept with the Z -axis. The equation of free surface of the liquid cargo in the absence of roll motion and lateral acceleration is directly related to the fill height c_0 , measured from the bottom of the tank, 'O':

$$z = -c_0 \quad (2.3)$$

Furthermore, the equation of the circular tank periphery with respect to the body fixed coordinate system is expressed in terms of its radius R as:

$$y^2 + (z + R)^2 = R^2 \quad (2.4)$$

The intersection points of the initial free surface of liquid cargo on the tank periphery are estimated by simultaneously solving Eqns. (2.2) and (2.4) or Eqns. (2.3) and (2.4). The left and right intersection points (y_{l0}, z_{l0}) and (y_{r0}, z_{r0}) , are mirror reflection of each other due to the symmetry of circular tank. The fluid volume per unit length of the tank can be evaluated from area integral:

$$V_0 = 2 \int_0^{y_{r0}} \int_{f_1(y)}^{c_0} dz dy \quad (2.5)$$

where V_0 is the fluid volume per unit length of the tank in absence of roll motion and lateral acceleration, function $f_1(y)$ describes the tank geometry, and c_0 defines the domain of integration along the z -axis. The volume of fluid per unit length of the tank subjected to roll motion and lateral acceleration can be derived in a similar manner by considering coordinates of the intersection points of the deflected free surface (y_l, z_l) and (y_r, z_r) :

$$V = \int_{y_l}^{y_r} \int_{f_1(y)}^{f_2(y)} dz dy \quad (2.6)$$

where V is the fluid volume per unit length, $f_2(y)$ is the function of liquid cargo free surface derived from the Eqn. (2.3), and $f_1(y)$ defines the domain of integration along the z -axis. y_l and y_r are the y -coordinates of the left and right intersection points of the free surface with the tank periphery. Considering that the fluid volume per unit length remains

constant, $V=V_0$, the intercept c is subsequently computed by minimizing the volume error, $\varepsilon = |V_0 - V|$.

The coordinates of the left and right intersection points of the free surface (y_l, z_l) and (y_r, z_r), are derived from simultaneously solutions of Eqns. (2.2) and (2.4). The coordinates of the center of gravity (cg) of the deflected liquid cargo are then derived from the following moment integrals, which directly defines the steady-state load shift:

$$Z_{cg} = \frac{1}{V} \int_{y_l}^{y_r} \int_{f_1(y)}^{f_2(y)} z \, dz \, dy \quad (2.7)$$

$$Y_{cg} = \frac{1}{V} \int_{y_l}^{y_r} \int_{f_1(y)}^{f_2(y)} y \, dz \, dy \quad (2.8)$$

where (Y_{cg}, Z_{cg}) define the coordinates of the cargo cg with respect to the tank base, 'O'. The slosh forces and roll moment are subsequently derived from the mass of liquid cargo, acceleration excitation and the cg coordinates as:

$$F_y = ma_y ; \text{ and } F_z = ma_z \quad (2.9)$$

$$M_x = (ma_y \cos \theta)Z_{cg} - (ma_y \sin \theta)Y_{cg} + (ma_z \cos \theta)Y_{cg} + (ma_z \sin \theta)Z_{cg} \quad (2.10)$$

where a_z is the acceleration due to gravity, m is the mass of the liquid cargo, F_y and F_z are the steady-state lateral and vertical forces, respectively, and M_x is the steady-state roll moment about the tank base 'O'. This roll moment is an additional overturning moment imposed on a partly filled tank vehicle, which is not observed in conventional rigid cargo vehicles.

2.2.2 Elliptic cross-section

An elliptic cross-section tank is realized by the equation of an ellipse in the coordinate frame fixed to the tank base 'O', as shown in Figure 2.2, such that:

$$\frac{y^2}{a^2} + \frac{(z+b)^2}{b^2} = 1 \quad (2.11)$$

where a and b are the semi-major and semi-minor axes of the ellipse, as shown in the Fig. 2.2. A similar methodology has been applied to derive the coordinates of the liquid cargo cg when the tank is subjected to roll motion and a lateral acceleration. The intersection points of the free surface and the elliptical tank cross-section, in the absence roll and lateral acceleration, are estimated by simultaneously solving Eqns. (2.3) and (2.11). Whereas the intersection points of the deflected free surface and the elliptical tank cross-section, are derived from simultaneous solutions of Eqns. (2.2) and (2.11). The initial volume V_0 and the deflected cargo volume V per unit length of the tank are computed through solutions of integral (2.5) and (2.6), respectively. The error, ε , between V and V_0 is then minimized to derive the deflected free surface intercept c with the Z -axis. The coordinates of the liquid cargo cg within the elliptic tank subjected to roll motion and lateral acceleration are subsequently derived by solving moment integrals, Eqns. (2.7) and (2.8). Eqns. (2.9) and (2.10) are used to obtain the magnitudes of steady-state slosh forces and moment.

2.2.3 Modified-oval cross-section

Figure 2.2 shows the cross-section of a modified-oval tank enclosed by circular arcs of radii, R_1 , R_2 and R_3 . The tank circumference is obtained as a combination of 8 circular

arcs with origin located at ‘O’, as shown in Figure 2.2 (c) [33]. A MATLAB code was developed to estimate the center of curvature for each arc which describes the tank cross-section. Each circular arc is expressed in terms of its radius and coordinates of its center, such that:

$$(y - c_{yn})^2 + (z - c_{zn})^2 = R_n^2 \quad n = 1, 2, \dots, 8 \quad (2.12)$$

where c_{yn} and c_{zn} are the coordinates of the center of arc n , and R_n is the radius of the n^{th} arc. Intersection points of adjacent arcs are obtained through solving equations for arc n and arc $(n+1)$ simultaneously.

Figure 2.3 shows the steady-state roll plane model of a partly-filled modified-oval tank. Intersection points of the free surface with the tank geometry are estimated by simultaneously solving Eqn. (2.12) and the free surface equation (2.2). In the absence of roll motion and lateral acceleration, the algorithm compares the free surface height (Eqn. 2.3) with range of extreme z -coordinates of each arc, whereas in presence of tank roll and lateral acceleration the intersection coordinates are estimated through an iterative process. The volume per unit length of the tank is subsequently derived from Eqns. (2.7) and (2.8), and the cg coordinates, and the forces and moments are computed using moment integrals and Eqns. (2.9) and (2.10), respectively.

2.3 Dynamic Slosh Model of a Partly-Filled Tank

It has been suggested that the destabilizing forces and moments due to transient slosh are considerably higher than their respective steady-state values [5, 10]. Studies have revealed that the transient slosh effects can generate up to 70% and 50% higher

longitudinal and lateral forces, respectively, for a 40% filled tank subject to lateral acceleration of 0.3g. Furthermore, the quasi- static slosh models are limited only to clean-bore tanks and do not permit analysis of anti slosh effectiveness of baffles. A dynamic slosh model is thus vital for investigating transient slosh within clean-bore and baffled tanks.

Dodge et al. [9] developed a dynamic mechanical-equivalent model of liquid slosh within a tank. In this model sloshing liquid is conceptually represented by a mechanical system comprising of springs and masses or pendulums. The dynamic motions of the sprung masses or pendulums can provide good estimates of the oscillatory slosh forces generated by the moving liquid within the tank. However, such models are based on linear slosh. Alternatively, Ibrahim et al. [24] formulated a nonlinear pendulum analogy to model the dynamics of liquid sloshing, by considering slosh damping. Mechanical analogies of liquid slosh, however, involve considerable challenges and complexities in identifying the mechanical system parameters for varying tank geometry and fill levels.

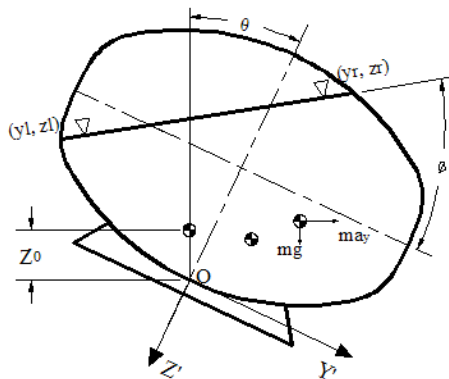


Figure 2.3: Liquid free surface intersections with the modified-oval cross-section tank.

A number of recent studies have investigated transient slosh using computational fluid dynamic (CFD) methods [26, 27, 28] and have demonstrated reasonably good validity with respect to experimental results [19]. The CFD methods have been applied for analysis of transient slosh within cylindrical [7] and RT [22] tanks with and without baffles under lateral as well longitudinal acceleration fields. The effect of sprung mass roll on the fluid slosh, however, has been ignored. Owing to suspension and tire compliance and dynamic load shift, considerable sprung mass roll is invariably evident in road vehicles. Integration of sprung mass roll in a dynamic slosh model is thus important to attain more realistic slosh responses.

A dynamic fluid slosh model is formulated to study the slosh responses under sprung mass roll and acceleration fields using computational fluid dynamic (CFD) software. The model is formulated in the FLUENT platform and solved using Volume-Of-Fluid (VOF) technique [7, 10]. Deformations of the free surface at each instant of time are derived from the concept of tracking the volume of fluid instead of the usual practice of assuming irrotational flow with no horizontal displacement of fluid particle at the free surface [7, 10]. Such a technique is extremely effective in simulating nonlinear fluid slosh within baffled tanks subjected to roll motion and time varying acceleration excitations. Sprung mass roll is simulated by constructing the complete geometry of the tank rolled with respect to the global axis (YZ) system. Figure 2.4 illustrates the global (YZ) and body-fixed (Y'Z') axis systems for the modified-oval tank geometry. The tank geometry is defined in the body-fixed axis (Y'Z') axis system, while the mesh is generated in the global axis system.

Studies have suggested that liquid motion within a partly-filled tank under a time varying excitation can be formulated as a two phase laminar flow: a liquid phase and an air phase [25, 27]. Furthermore, Lee et al. [27] have demonstrated negligible differences in fluid pressures derived from the laminar and turbulent computational fluid dynamic flow models.

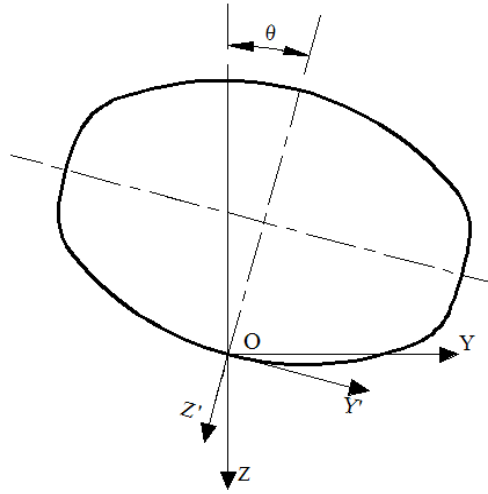


Figure 2.4: Global (YZ) and body-fixed (Y'Z') axis systems considered for the modified-oval tank.

Assuming constant viscosity and incompressible flows, three-dimensional fluid flow within the tank can be represented by the conservation of mass and momentum equations as:

$$\frac{\partial u}{\partial x} + \frac{\partial v}{\partial y} + \frac{\partial w}{\partial z} = 0 \quad (2.13)$$

$$\frac{\partial u}{\partial t} + u \frac{\partial u}{\partial x} + v \frac{\partial u}{\partial y} + w \frac{\partial u}{\partial z} = -a_x - \frac{1}{\rho} \frac{\partial P}{\partial x} + \gamma \left(\frac{\partial^2 u}{\partial x^2} + \frac{\partial^2 u}{\partial y^2} + \frac{\partial^2 u}{\partial z^2} \right)$$

$$\frac{\partial v}{\partial t} + u \frac{\partial v}{\partial x} + v \frac{\partial v}{\partial y} + w \frac{\partial v}{\partial z} = -a_y - \frac{1}{\rho} \frac{\partial P}{\partial y} + \gamma \left(\frac{\partial^2 v}{\partial x^2} + \frac{\partial^2 v}{\partial y^2} + \frac{\partial^2 v}{\partial z^2} \right)$$

$$\frac{\partial w}{\partial t} + u \frac{\partial w}{\partial x} + v \frac{\partial w}{\partial y} + w \frac{\partial w}{\partial z} = -a_z - \frac{1}{\rho} \frac{\partial P}{\partial z} + \gamma \left(\frac{\partial^2 w}{\partial x^2} + \frac{\partial^2 w}{\partial y^2} + \frac{\partial^2 w}{\partial z^2} \right) \quad (2.14)$$

where u , v and w are the X , Y and Z components of velocity of the liquid within the domain at an arbitrary point, P is the fluid pressure, γ is the kinematic viscosity and a_x , a_y and a_z are the unit body forces acting along X , Y and Z directions, respectively. Furthermore, it is also assumed that the body forces are homogeneous [25] and the flow is laminar. Velocity components of the liquid, normal and tangential to the wall, are reasonably assumed as zero, which accounts for the boundary condition [34].

2.3.1 Method of analysis

Navier-Stoke's equations are solved with appropriate boundary conditions to compute the velocity component and pressure distribution using the FLUENT software [35], which is a wide-ranging CFD code based of Finite Volume numerical method capable of solving wide range of transient flows encountered in many situations. For the transient fluid slosh in partly-filled tanks, governing equations are discretized in both time and space. A second-order upwind scheme is used for the spatial discretization, whereas an implicit scheme is employed for temporal discretization. Transient pressure and velocity responses are estimated using pressure-based segregated algorithm (PISO) [35] in conjunction with the liquid volume tracking to locate the interface between the two fluid phases [53]. For this purpose, a fluid fraction function is defined as 0 or 1, representing the fluid phase existing in a particular cell.

2.4 Response Characteristics

Reported studies on stability and directional dynamics of partly-filled tank vehicles have clearly suggested that the load shift directly affects both the stability and directional dynamics of the partly-filled tank vehicle [5, 17]. Further, the inertial forces attributed to acceleration excitation also contribute to the overturning roll and yaw moments and thereby affect the stability of the tank vehicle in an adverse manner. The transient slosh forces and moments could be derived from the instantaneous pressure distribution along the tank structure. User defined functions (UDF) are subsequently developed to estimate the slosh responses in terms of forces, moments and load shifts, expressed in terms of the mass center of the liquid cargo.

2.4.1 Load shift

The transient load shifts due to sloshing of liquid cargo is estimated from the volume integrals over the liquid domain within the partly-filled tank [10]:

$$X_{cg}(t) = \frac{\sum_c^{liquid} A_c x_c(t)}{\sum_c A_c}; \quad Y_{cg}(t) = \frac{\sum_c^{liquid} A_c y_c(t)}{\sum_c A_c}; \quad Z_{cg}(t) = \frac{\sum_c^{liquid} A_c z_c(t)}{\sum_c A_c} \quad (2.15)$$

where x_c , y_c and z_c are the instantaneous cg coordinates of the cell 'C' with respect to the origin 'O', A_c is the cell area in the desired plane and 'liquid' defines the integration domain of the liquid cargo.

2.4.2 Forces and moments

The resultant forces and moments due to sloshing are estimated from the pressure distribution along the wall of the clean-bore tank. The forces are estimated by integrating

the product of instantaneous distributed pressure and the wetted area of the desired planes, as [10]:

$$F_x(t) = \sum_c^{A_w} P_c(t) A_c \cdot i \quad F_y(t) = \sum_c^{A_w} P_c(t) A_c \cdot j \quad F_z(t) = \sum_c^{A_w} P_c(t) A_c \cdot k \quad (2.16)$$

Where $F_x, F_y,$ and F_z are the resultant forces acting on the tank, P_c is the pressure of the cell 'C' located on the on the tank wall and A_w is the wetted area. The moments are subsequently calculated as a product of the forces and the position vector of the cell C on the tank wall or the end cap:

$$\vec{M}(t) = \sum [\vec{P}_c(t) A_c] \cdot \vec{r}_c(t) \quad (2.17)$$

where $\vec{M}(t)$ the moment is the vector and $\vec{r}_c(t)$ is the position vector of the cell 'C' as shown in the Figure 2.5.

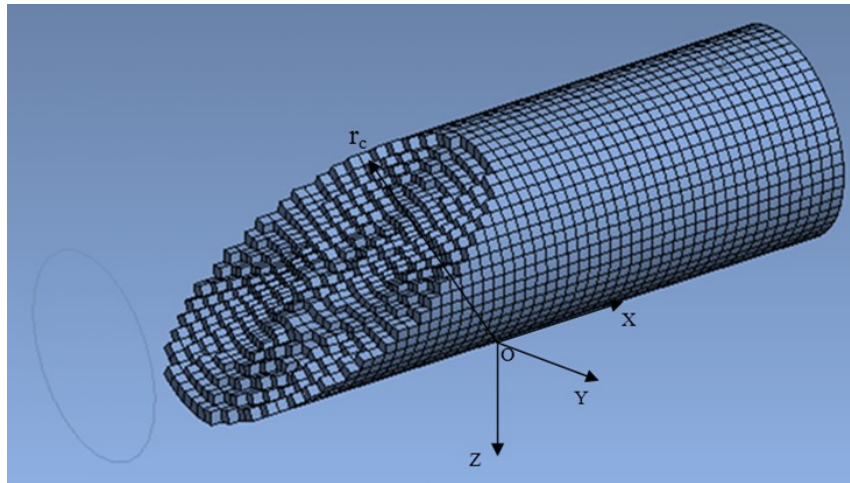


Figure 2.5: Position vector r_c of an arbitrary wet boundary cell.

2.5 Three-Dimensional Simulation Details

The transient fluid slosh models are developed for the three selected tank cross-sections by considering the geometry of each cross-sections and different excitations, which are described below. The cross-sections are chosen so as to achieve nearly identical cross-section area for all the tanks, as described earlier in section 2.2.

2.5.1 Tank geometry

The influence of tank cross-section on the transient slosh responses are analyzed for the three prevalent tank cross-sections, namely the circular, modified-oval and elliptic. Figure 2.6 illustrates the geometry of the clean-bore modified-oval tank used for the present study, three different baffle configurations are also analyzed in chapter 4.

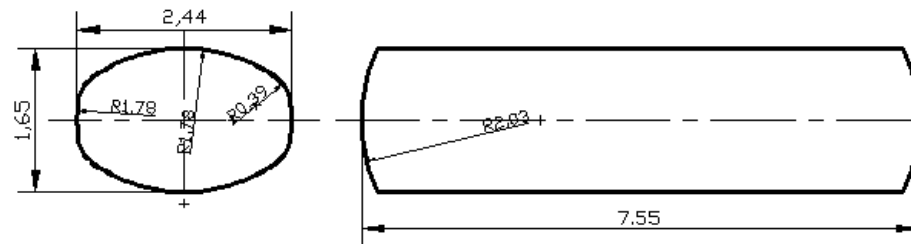


Figure 2.6: Clean-bore modified-oval tank geometry.

2.5.2 Discretization and time step

Gambit Tet/Hybrid scheme is used to mesh the tank geometries under consideration. The bulkhead surface is selected as the source face and the surface meshes are subsequently swept through the volume [36]. Further, desired grid densities are accomplished by assigning adequate numbers of nodes and specifying distribution of nodes on the edges. Earlier studies of transient slosh inside a partly-filled circular tank [7, 10] have established that such an analysis could be conveniently carried out with mesh densities of

1280 elements per cubic meter or more. For the present study meshes are generated, for all the three cross-sections, with mesh density of at least 1573 elements per cubic meter. Figure 2.7 illustrates the meshing of the two phase flows within the partly-filled cylindrical tank.

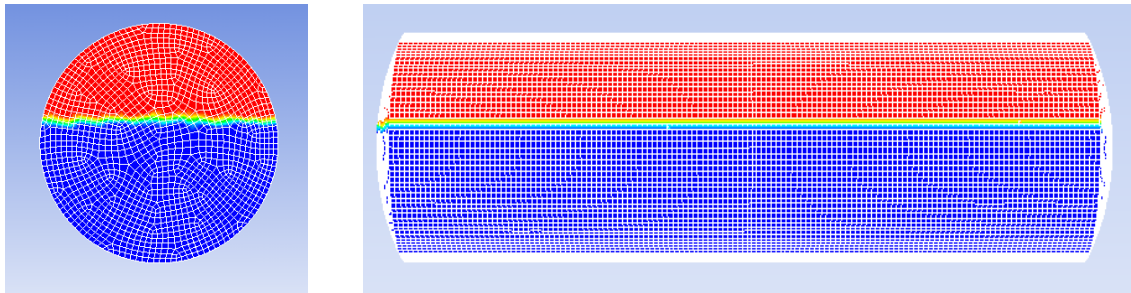


Figure 2.7: Two phase flow mesh in a partly-filled cylindrical tank.

Preliminary analyses were performed to investigate sensitivity of responses to mesh density for the modified-oval cross-section tank. For this purpose, three different mesh densities of 1573, 3039 and 7374 were considered for the 60% filled tank. The analyses were performed under $0.4g$ rounded ramp-step lateral acceleration (described in section 2.5.3) with a fixed time step of 0.01sec and simulation time of 10s. The means of the transient responses were derived and compared to those derived over the interval \dots , from the quasi-static model. The results in term of lateral slosh forces are summarized in Table 2.1, as an example. The results suggest that increasing the mesh density could reduce the error. However, considering computational time and given the fact that the present study focuses on comparative evaluations of various cross-sections, the relative error 1.39% for the chosen course mesh density of 1573 elements/m³ was considered acceptable.

Mesh density (Elements / m³)	Quasi-static Lateral force (N)	Mean dynamic Lateral force F_y (N)	Relative error (%)
1573	77763.72	76678.43	1.39
3039		76761.43	1.28
7374		77016.62	0.96
Table 2.1: Influence of mesh density on the resulting mean dynamic lateral force (modified-oval tank; <i>fill volume</i> = 60%; <i>a_y</i> = 0.4g)			

Furthermore, a previous work has suggested that influence of time step on the accuracy of the dynamic slosh measures is negligible in the range of 0.025s to 0.01s for circular cross-section tanks [13]. The present study also verified the same for a modified-oval and elliptic tank cross-sections. Simulations were conducted for the 40% fuel oil filled modified-oval and elliptic tanks subjected to 0.25g rounded ramp-step lateral acceleration using two different time steps: 0.025s and 0.01s and total simulation period of 10 s. The results revealed insignificant differences in all the transient slosh measures, namely, the lateral force, roll moment and the cg coordinates. A time step of 0.025s was thus selected for simulation so as to achieve greater computational efficiency.

2.5.3 Acceleration excitations

The analyses are performed considering lateral, longitudinal, and combined lateral and longitudinal acceleration excitations, in addition to the tank roll motion. These are considered to represent steering, braking combined steering and braking maneuvers, respectively. The lateral acceleration excitations are initially defined to simulate for turning and path change maneuvers. A turning maneuver is idealized by a rounded ramp-step function, while an exponentially decaying sine function is defined to idealize centrifugal acceleration encountered during a path- change maneuver. Figure 2.8

illustrates the time-histories of the lateral acceleration excitations employed in the study. The magnitudes of the excitations, however, are varied to study the effect of maneuver severity. Apart from the lateral acceleration excitation, a constant roll angle of 7° is imposed on the tank.

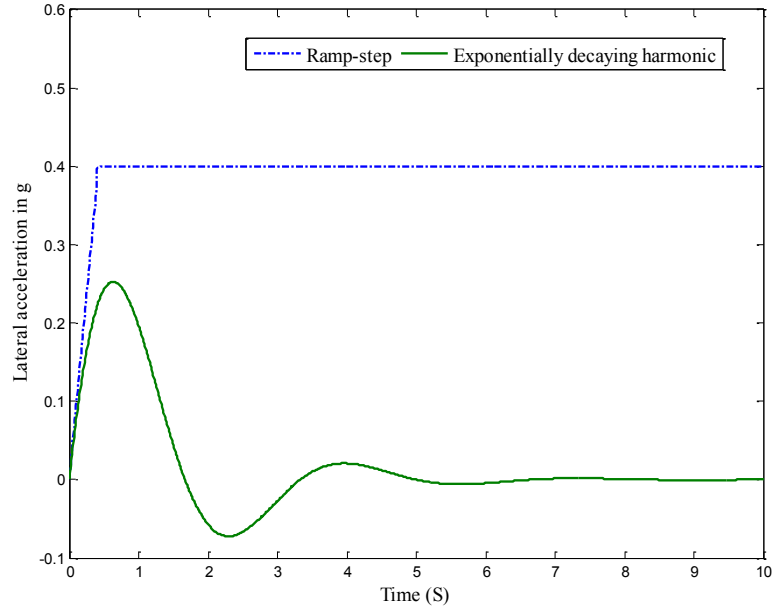


Figure 2.8: Time-histories of ramp-step and exponentially decaying harmonic lateral acceleration excitations.

2.5.4 Fill volume

Tank vehicles may encounter partial fill conditions either due to variation in the product density or while in local delivery route. These two conditions are characterized by partial fill with a constant payload, and partial fill with varying payload. The analyses are performed by considering three fill conditions, defined by the ratio of fill height (c_o) from the origin 'O' to the overall tank height, namely 40%, 60% and 80%. For constant payload, the total cargo load is taken for a completely-filled fuel oil tank ($\rho = 850 \text{ kg/m}^3$;

$\gamma = 0.0867 \text{ kg/m s}$). The Mass density was varied to achieve the selected fill height, so as to ensure a constant payload.

2.6 Summary

Quasi-static and transient roll plane slosh models of the partly-filled tanks are developed considering the industry prevalent tank cross-sections. The method of analysis is presented to investigate effect of tank cross-section on transient slosh responses in terms of slosh forces and moments. Furthermore, the chosen mesh density and time step together with the roll-plane excitations are discussed for the simulations. The models are used to study the effects of tank geometry and the baffle arrangements in the subsequent chapters.

CHAPTER 3

ROLL PLANE FLUID SLOSH ANALYSIS IN CLEAN-BORE TANKS

3.1 Introduction

The roll stability limit of commercial vehicles is widely expressed in terms of static rollover threshold (SRT), defined as the maximum magnitude of lateral acceleration that the vehicle could withstand prior to overturning [19, 51]. The SRT thus directly relates to the centrifugal force or acceleration encountered during the steady turn and path-change maneuvers. In case of partly-filled road tankers, the cargo shift in the roll plane would impose an additional roll moment on the vehicle, as described in section 2.2. The roll plane fluid slosh and its potential contribution to the SRT of the vehicle can thus be evaluated in terms of: (i) cargo shift, expressed in terms of instantaneous cg coordinates; (ii) lateral slosh force, F_y ; and (iii) roll moment, M_x . The roll moment strongly depends on the magnitude of the cargo shift, as seen in Eqn. (2.10). The cargo shift on the other hand is strongly dependent upon the tank cross-section [5, 6]. A wider cross-section yields lower cg height and thus greater stability limit. The lateral load shift in a wider tank, however, is significantly larger, which causes the roll stability limit to decrease.

The three-dimensional dynamic fluid slosh model, presented in chapter 2, could be used to derive the above mentioned roll stability measures. In this chapter, the dynamic slosh model is solved under lateral acceleration and roll angle excitations to determine transient as well as steady-state responses in terms of the roll stability measures. The effect of the tank cross-section on the performance is particularly emphasized, which could yield guidance on operation and design of tank vehicles.

Furthermore, the variations in the fundamental slosh frequency as a function of tank cross-section and fill level are evaluated and discussed. The contribution of sprung mass roll motion to various pertinent measures of transient slosh in the roll plane is also presented.

3.2 Measures of Dynamic Slosh in Roll Plane

The primary purpose of the transient fluid slosh analysis is to identify response quantities that could be related to roll stability limits of the vehicle. These include the dynamic load shifts, lateral slosh force and roll moment. Apart from these, the cargo movement would also affect the roll mass moment of inertia of the liquid cargo, which is also known to influence the dynamic roll response of the vehicle and its directional dynamics [13]. The CDF fluid slosh model is thus solved to derive these measures under tank roll motion and lateral acceleration excitations. Furthermore, these measures would facilitate relative performance evaluations of different cross-section tanks. These performance measures are described below.

3.2.1 Dynamic load shifts

Dynamic load shifts directly influence roll moment imposed on the vehicle and roll mass moment of inertia of the fluid cargo, and thus the roll stability of partly-filled tank vehicles. While the lateral load shift results in an offset between vertical axis of the vehicle and the cargo cg thereby augmenting the existing inertial overturning moment due to maneuver-induced lateral acceleration, the variation in vertical cg coordinate also contributes to the overturning moment, as seen in Eqn. (2.10). The analyses are performed to identify steady-state as well as transient load shift. The transient load shift

response is analyzed to identify the variation in peak load shift, which signifies the effect of tank cross-section on the transient slosh. Modaressi et al. [10] suggested that the transient slosh responses may be expressed by an amplification factor representing the relative significance of a transient response in relation to the steady-state response. The amplification factor is defined as the normalized peak cargo response to the mean dynamic response, which is identical to that derived from the quasi-static model, such that:

$$K_q = \frac{\text{Max}[q(t)]}{\bar{q}} \quad (3.1)$$

where K_q is the normalized transient response of quantity q and \bar{q} is the steady-state response quantity.

The cargo load shift is particularly described in terms of normalized deviation in the lateral K_y cg coordinates and peak variation in the vertical cg coordinates (ΔZ), given by:

$$K_Y = \frac{\text{Max}[Y_{cg}(t)]}{\bar{Y}_{cg}} \quad (3.2)$$

$$\Delta Z = \text{Max}[Z_{cg}(t) - Z_0] \quad (3.3)$$

where Z_0 is the cg height of the cargo with respect to the tank base ‘O’ in the absence of external excitations, and \bar{Y}_{cg} is the mean lateral cg coordinate of the cargo, and $Z_{cg}(t)$ is the transient vertical coordinate of the cargo cg. It should be noted that the vertical cg deviation is not normalized due to considerably different Z_0 values of the selected tanks.

3.2.2 Dynamic slosh forces and moments

It has been suggested that stability and controllability of partly-filled tank vehicles are directly affected by the dynamic slosh forces and moments [2]. A higher value of dynamic slosh force and moment due to a maneuver-induced excitation yields a relatively lower stability and controllability of the tank vehicle, as seen in the section 2.2.1. Shape effect of different tank cross-sections on slosh forces is investigated in terms of normalized in lateral slosh force K_{F_y} and roll moment K_{M_x} for the selected fill levels and ramp-step excitation. Normalized or dynamic lateral slosh force and roll moment amplification factors are defined as:

$$K_{F_y} = \frac{Max(F_y)}{\bar{F}_y} \quad (3.4)$$

$$K_{M_x} = \frac{Max(M_x)}{\bar{M}_x} \quad (3.5)$$

where \bar{F}_y and \bar{M}_x are the mean dynamic slosh force and dynamic roll moment, respectively, which are the steady-state values. However, for the path-change maneuver, effect of different tank cross-sections on lateral slosh forces and roll moments are studied in terms of variation in the peak transient lateral slosh force $\max(F_y)$ and peak transient roll moment $\max(M_x)$ for the selected fill level range

3.2.3 Variation in roll mass moment of inertia

Variation in mass moments of inertia of the sprung mass due to a maneuver-induced excitation could also affect the directional response characteristics of a heavy vehicle [13]. Unlike the conventional freight vehicles, the partly-filled tank vehicles would exhibit considerable variation in the effective mass moment of inertia, which is attributed

to the fluid cargo movement. A few studies have applied the kineto-static and CFD models to identify variations in the mass moments of inertia of circular and RT tank cross-sections [10, 17], a relative analysis of mass moments of inertia of cargo within partly-filled industry prevalent cross-sections has not yet been reported. The variations in peak roll mass moment inertia of the deflected cargo are compared for different tank cross-sections and fill levels to illustrate the influences of tank cross-section.

3.3 Model Validation

Validation of the dynamic fluid slosh model is examined in sequential stages. In the first stage, the steady-state load shift responses \bar{Y}_{cg} and \bar{Z}_{cg} of the partly-filled circular tank under a roll motion alone are derived from the transient responses and compared to those derived from the quasi-static model. In the second stage, the steady-state responses in terms of lateral load shift \bar{Y}_{cg} and slosh force \bar{F}_Y of the same tank are evaluated under 7° roll motion and $0.4g$ ramp-step lateral acceleration and various fill levels. These responses are compared with respective quasi-static values to demonstrate validity of the dynamic slosh model. The simulations are performed for the partly-filled clean-bore circular tank of unit length with mesh density greater than 1280 elements per square meters and a time step of 0.01s. The simulations were performed for a duration of 10s, and the steady-state solutions were obtained through averaging of the transient response over an interval of .

Figure 3.1 illustrates correlations between the mean dynamic and quasi-static lateral cg coordinates of the partly-filled circular tank subjected to tank roll alone for three different fill conditions in the 40 to 80% fill range. The mean dynamic values,

evaluated from time integral of transient lateral load shift response, agree very well with the corresponding quasi-static values over the entire fill range considered. A closer examination of the responses revealed only minor differences (<4%) between the responses, which could be attributed to possible error in estimating the mean values of the dynamic responses. Results in Figure 3.1 further show that an increase in fill yields relatively lower lateral load shift. This trend has also been reported in a few earlier studies based on kineto-static slosh analysis [1, 6]

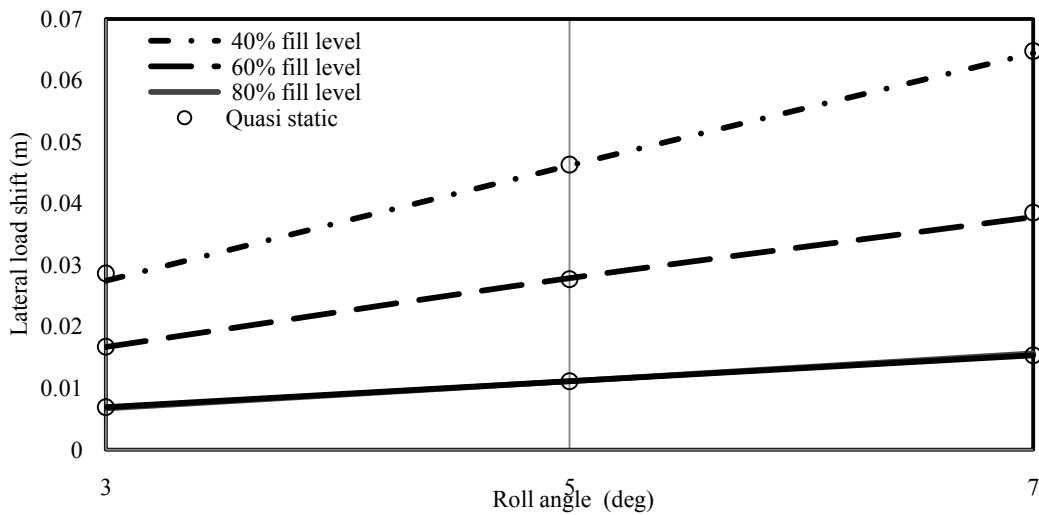


Figure 3.1: Comparison of lateral cg coordinates (Y_{cg}) of the liquid cargo in a circular tank subjected to roll motions.

Figure 3.2 illustrates the comparisons of lateral and vertical load shifts of the partly-filled circular tank subjected to 7° tank roll and $0.4g$ ramp-step lateral acceleration under various fill levels in the 40 to 100% range. The mean dynamic responses agree very well with the quasi-static values for all the fill levels considered. The mean dynamic values are also in reasonably good agreement with those reported in an earlier study [6]. The results show that both the lateral and vertical load shifts decrease with increase in fill level and become negligibly small at very high fill levels. Figure 3.3 compares the

steady-state lateral and vertical slosh forces with the corresponding quasi-static forces for different fill levels. Comparisons reveal good agreements between the slosh forces estimated from the dynamic slosh model and the quasi-static analysis. Small deviations between the two are attributed to error in estimation of mass by the dynamic slosh model. The results show nearly linear increase in steady-state slosh forces and moments with increasing fill under low to medium fill levels. The responses tend to saturate at higher fill levels.

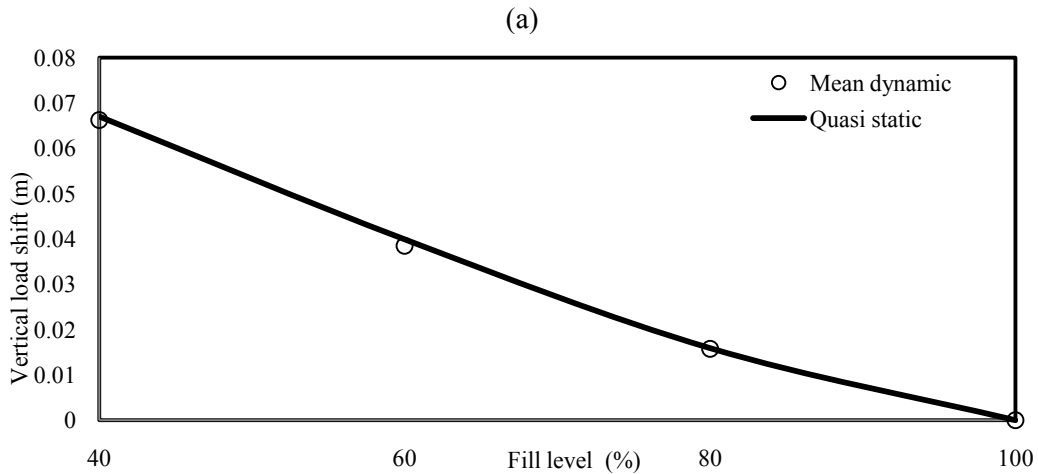
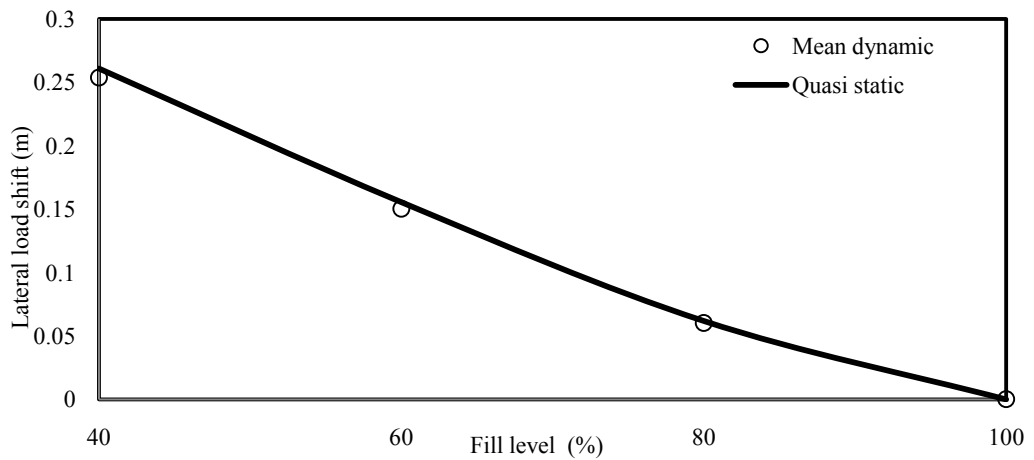


Figure 3.2: Comparisons of mean dynamic and quasi-static lateral and vertical shifts in the cargo cg for a circular tank subjected to 7° roll and $0.4g$ lateral acceleration at various fill levels: (a) lateral; and (b) vertical.

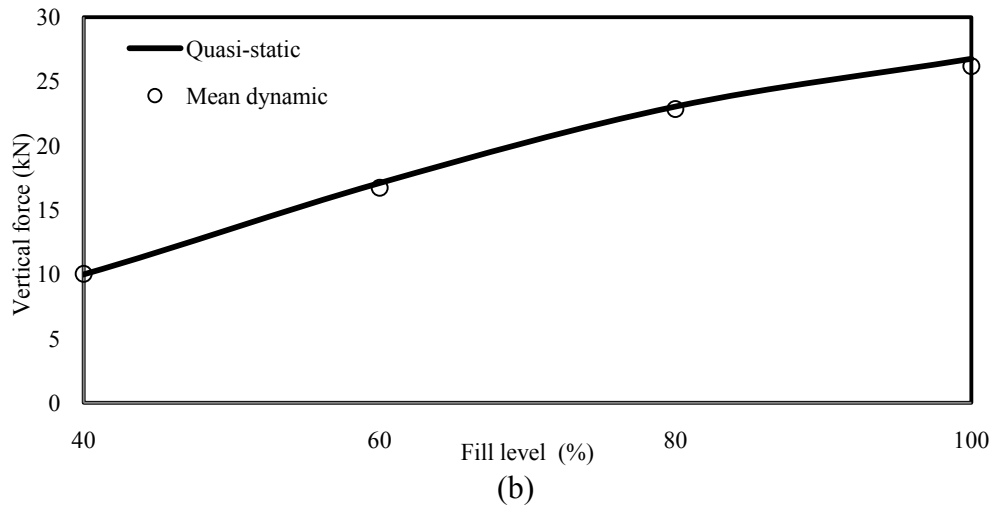
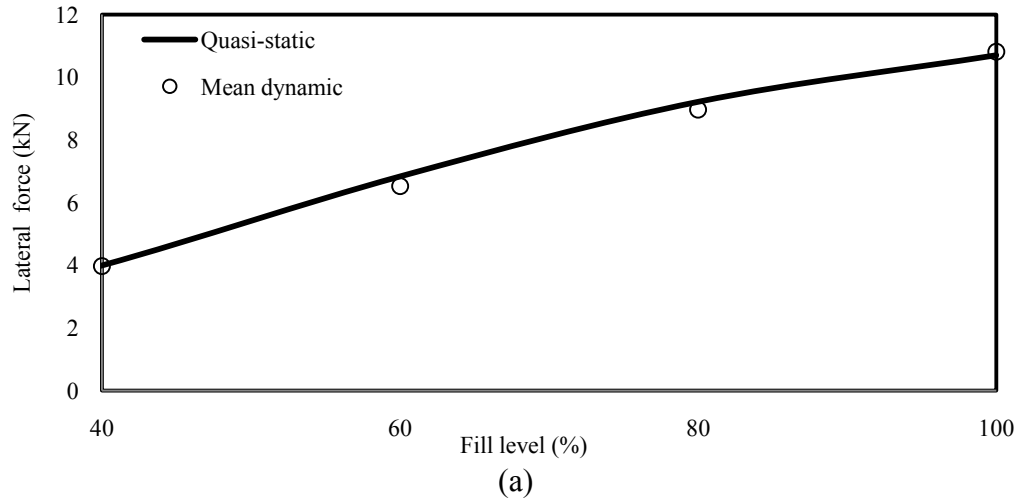


Figure 3.3: Comparisons of mean dynamic and quasi-static lateral and vertical slosh forces for a circular tank subjected to 7° roll and $0.4g$ lateral acceleration at various fill levels; (a) lateral; and (b) vertical.

3.4 Effects of Tank Cross-Sections

The dynamic fluid slosh model is used to study the transient responses of partly-filled circular, modified-oval and elliptic cross-section tanks. The analyses are performed under ramp-step and sinusoidal lateral acceleration excitations, described in section 2.5.3, together with tank roll motion. In order to study the effect of tank cross-section, the simulations are performed assuming constant cargo load of 20383kg, which represents

the cargo mass corresponding to a completely-filled tank of length 7.55m with the fuel oil. Shape effects of these prevalent cross-sections are analyzed through a relative study of transient slosh measures, described in section 3.2, under fill levels of 40, 60 and 80%, which were realized by varying the mass density.

3.4.1 Effect of tank cross-section on dynamic load shift

Idealized path-change lateral acceleration

Figure 3.4 illustrates the variations in the lateral cg coordinate of the liquid cargo within the 40% filled tanks subjected to the path-change maneuver at 0.3Hz and sprung mass roll of 7°. The initial deviation in the lateral cg coordinate, as seen in figure 3.4, at time $t=0$, is attributed to the sprung mass roll. The results show harmonic variations in the cg coordinate at the frequency of 0.3Hz. The peak values of variations in both transient and steady-state are significantly greater for the wider modified-oval tank compared to that of the circular tank. These suggest that wider tank permits greater lateral load shift, which would impose a relatively greater roll moment on the vehicle. Furthermore, owing to the differences in the width of the tank cross-sections a phase shift between the responses can also be observed in Figure 3.4. Peak values of lateral cg coordinates, $\max Y_{cg}$, within all the considered tank cross-sections are compared in Figure 3.5. The results show that wider modified-oval tank yield considerably greater peak lateral cg coordinates for the entire fill range when compared to that of circular cross-section tank. Moreover, due to comparable dimensions of circular and elliptic tank cross-sections as described in section 2.2, variations in peak lateral cg coordinates of these two cross-sections are comparable. The magnitude of the lateral load shift decreases with increase in fill level. The results

also reveal that the peak lateral cg shift within modified-oval tank is nearly 50% more than that within a circular tank at a lower fill level of 40%. This difference in the peak values, however, reduces to nearly 12% at a high fill level of 80%. This is attributed to the lower free surface length under high fill levels.

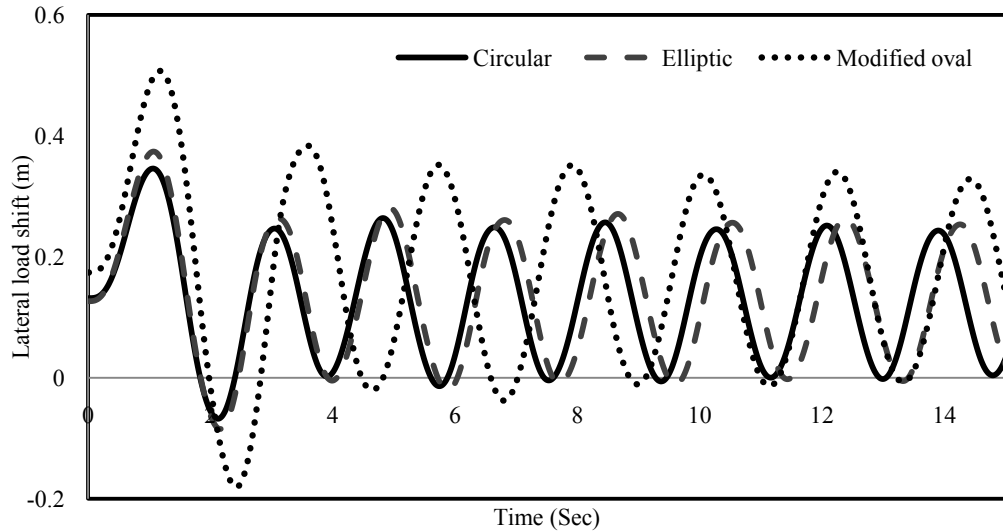


Figure 3.4: Time-histories of lateral load shift of the cargo within various tank cross-sections subjected to idealized path-change maneuver and 7° sprung mass roll (40% fill level).

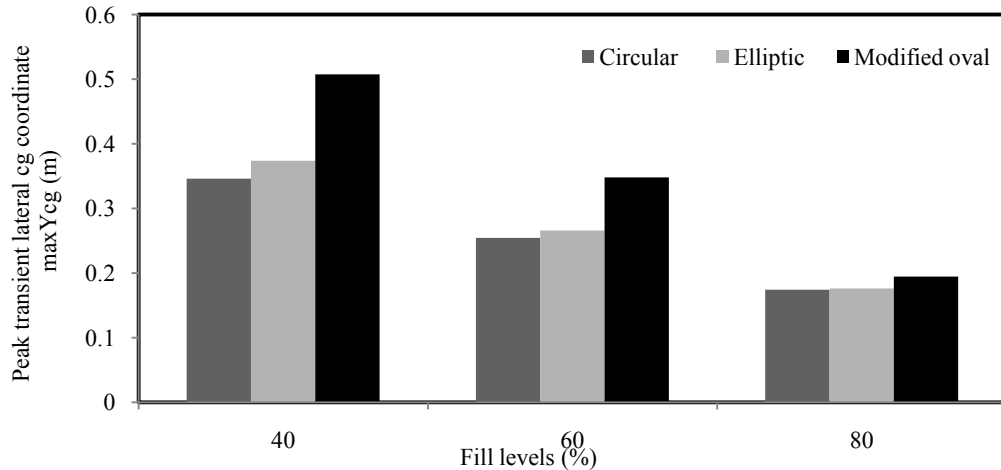


Figure 3.5: Comparisons of peak values of transient lateral cg coordinate of the cargo within various tank cross-sections subjected to idealized path-change maneuver and 7° sprung mass roll.

Figure 3.6 compares the peak deviation of the deflected cargo vertical cg coordinate \bar{z}_{cg} from the static cg height z_0 under the described path-change maneuver and sprung mass roll. These deviations signify the effect of tank cross-section on transient variations in the vertical cg coordinate of the cargo. Although a wider cross-section tank yields lower cg height compared to the less wide tanks, the wider cross-sections generate greater relative variation in the cargo cg coordinate in the vertical axis. This is also evident from the lateral cg coordinate (Figure 3.5). However, it is note-worthy that both static and transient peak vertical cg coordinates of liquid cargo within the modified-oval and elliptic tanks are smaller than that so the cargo within the circular tank.

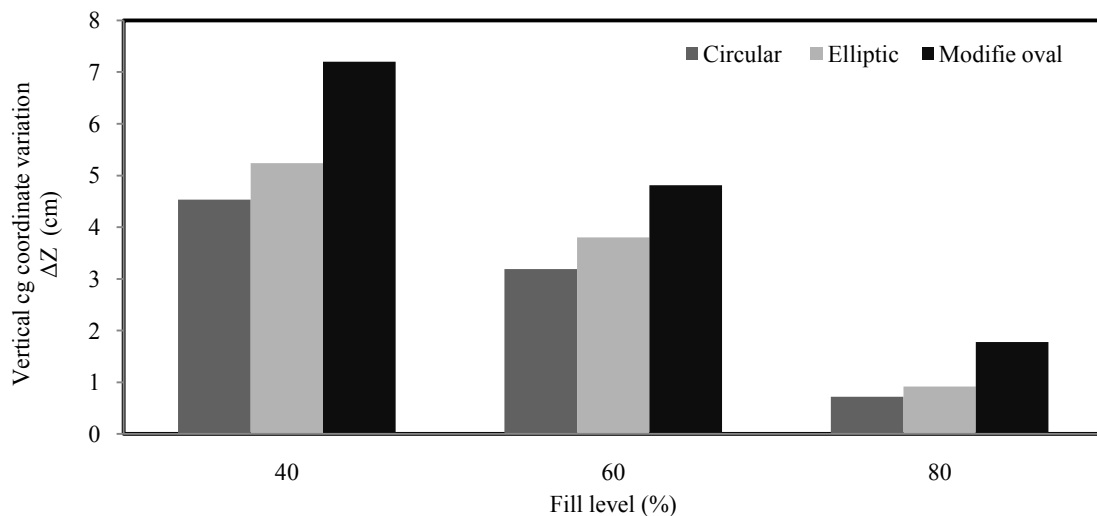


Figure 3.6: Comparisons of variation in vertical cg coordinate within various tank cross-sections subjected to idealized path-change maneuver and 7° sprung mass roll

Ramp-step lateral acceleration

Figure 3.7 shows the deviation in normalized lateral cg coordinate (K_Y) of the liquid cargo as a function of fill level and tank cross-section under $0.25g$ ramp-step acceleration excitation. The modified-oval and elliptic tanks, being wider than the circular tank, yield

greater normalized lateral load shifts for the entire range of fill levels considered in the study. It is also seen from the results that the magnitudes of normalized lateral cg coordinate decreases with increase in fill level. This is primarily attributed to the decrease in available sloshing volume and free surface length at higher fill levels. Further, wider elliptic and modified-oval tanks yield larger peak and mean lateral cg coordinate when compared to those of the circular tank.

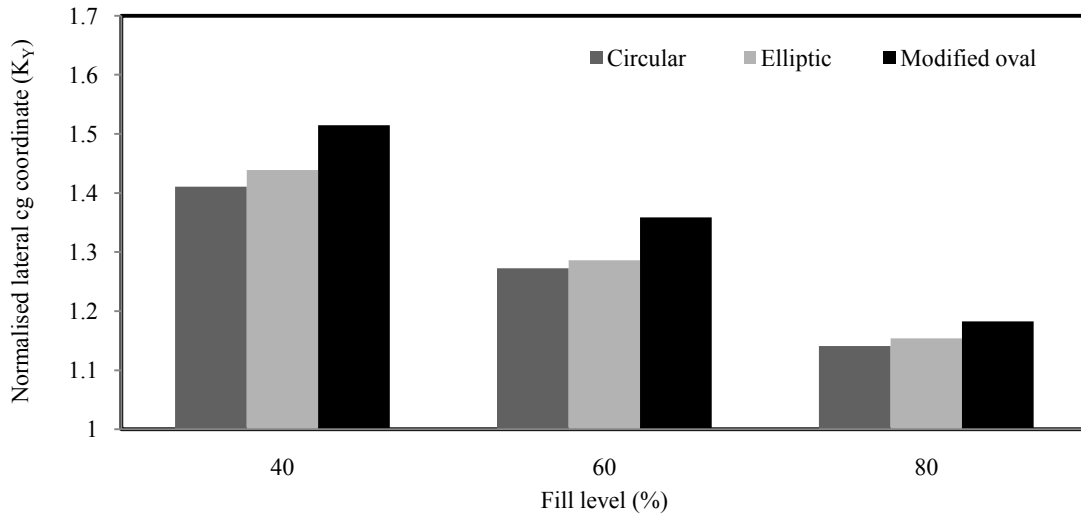


Figure 3.7: Comparisons of normalized lateral cg coordinates for various tank cross-sections subjected to steady-turning maneuver and 7° sprung mass roll.

Figure 3.8 compares the peak variation in the vertical cg coordinate with respect to the static cg height, as described in Eq. 3.3, under different fill levels subject to idealized steady-turning maneuver excitation of $0.25g$ amplitude for the tank cross-sections considered in the study. Results reveal that wider tank cross-sections yield larger variation in vertical cg height when compared to the circular tank cross-section. The large difference in the vertical cg variations between the modified-oval and circular tank cross-sections is due to the combined effects of greater load shifting in the wider tank cross-section and relatively lower static cg height of wide modified-oval tank cross-sections.

This subsequently justifies the considerably large vertical cg coordinate variation of modified-oval tank when compared to circular and elliptic tanks at 80% fill level.

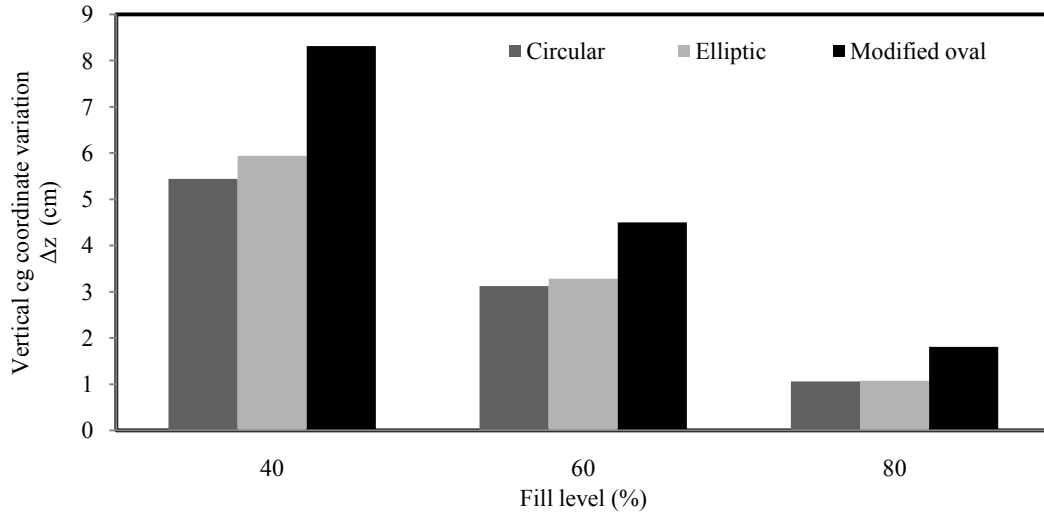


Figure 3.8: Comparisons of variation in vertical cg coordinate within various tank cross-sections subjected to steady-turning maneuver and 7° sprung mass roll.

Figure 3.9 compares the static vertical cg coordinates as a function of the fill level and the tank cross-section considered in the present study. The wider modified-oval tank yields 16% to 18% lower cg height compared to the circular cross-section tank

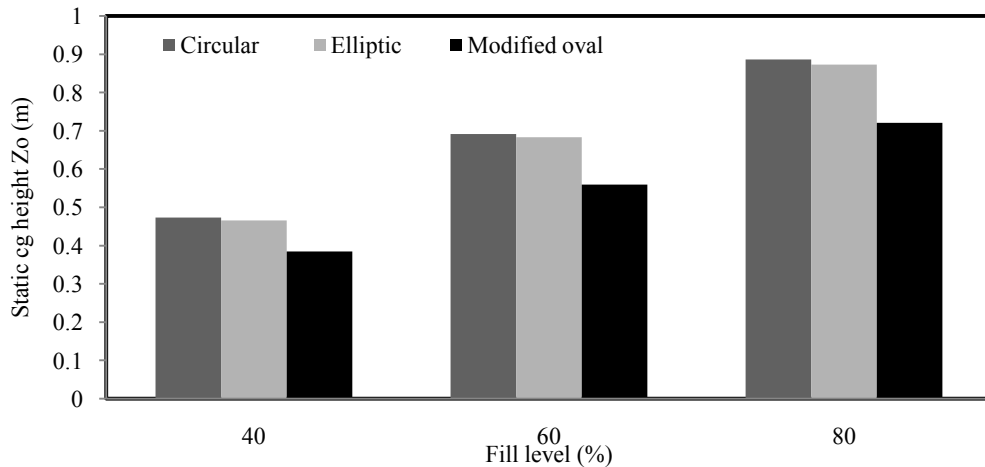


Figure 3.9: Comparisons of static cg height of liquid cargo of selected tank cross-sections for different fill levels.

corresponding to 40 and 80% fill levels, respectively. A wider tank would thus be expected to exhibit relatively higher SRT under partly-filled conditions, the greater lateral load shift however tends to deteriorate the SRT values.

3.4.2 Effect of tank cross-section on dynamic slosh forces

Idealized path-change lateral acceleration

The effect of tank cross-section on transient slosh force under path-change maneuver and 7° sprung mass roll is analyzed in terms of peak transient lateral slosh force. Figure 3.10

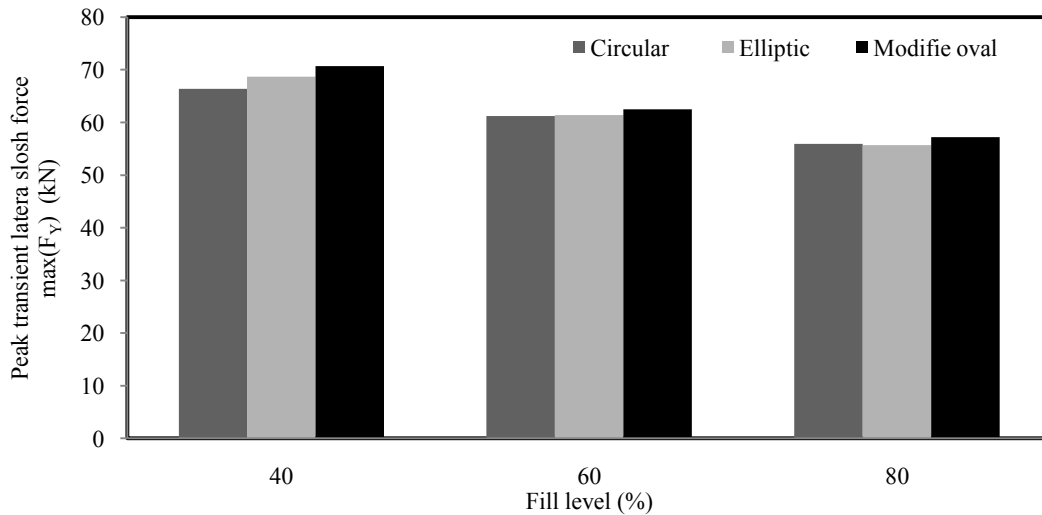


Figure 3.10: Comparisons of peak transient lateral slosh force of the cargo subjected to idealized path-change maneuver and 7° sprung mass roll for different fill levels.

compares the peak transient lateral slosh force $\max F_y$ as a function of the fill level and tank cross-section. The results show that the wider modified-oval tank yields slightly greater lateral slosh force compared to circular and elliptic tanks in the range of fill levels considered in the present study. At a lower fill level of 40%, the modified-oval tank yields a maximum of nearly 8% higher peak lateral slosh force than that of circular tank at the same fill level. Due to lateral boundary constraints, the circular tank tends to limit the

lateral cargo motion better than the wider elliptic and modified-oval tanks. A closer analysis of the results revealed a slightly higher peak lateral slosh force for the circular tank compared to that of elliptic tank for the 80% fill condition. This is ascribed to an error (0.05%) in estimation of cargo weight by the dynamic fluid slosh model. It is also seen from the results that the peak transient lateral slosh forces decrease with increase in fill level for all the selected cross-sections. This trend is attributable to decrease in available space for cargo movement at higher fill levels.

Ramp-step lateral acceleration

Variations in lateral force amplification factor, K_{F_y} , under the described idealized steady-turning maneuver excitation are illustrated in Figure 3.11 as a function of fill level for different cross-sections. The result show relatively small differences in K_{F_y} across the selected tank cross-sections and fill levels. This is attributed to consideration of constant fluid mass, irrespective of the fill volume. The results, however, suggest that the peak

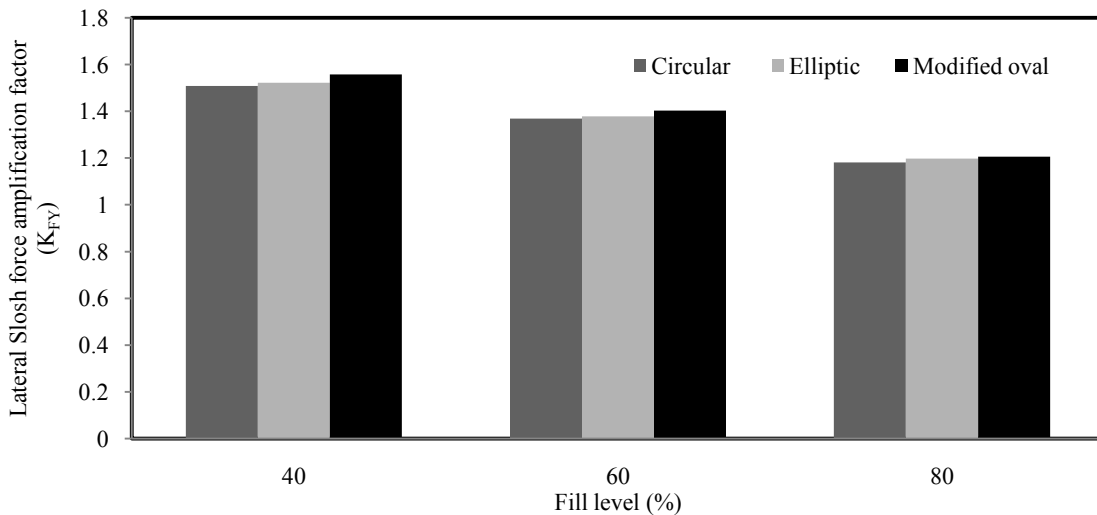


Figure 3.11: Comparisons of lateral slosh force amplification factor of the selected tank cross-sections with different fill levels subjected to steady-turning maneuver and 7° sprung mass roll.

lateral slosh forces could be 18 to 58% higher than those predicted from the kineto-static fluid cargo shift model. The normalized peaks tend to decrease with fill levels. This is due to the fact that boundary constraints help limit the fluid slosh under higher fill levels, as it is evident from the normalized lateral cg coordinate in Figure 3.7.

3.4.3 Effect of tank cross-section on roll moment

Idealized path-change lateral acceleration

The effect of tank cross-section on the roll moment developed by fluid slosh is shown in Figure 3.12. The figure compares the peak roll moment, caused by the moving cargo, for different tank cross-sections and fill levels under 0.3Hz exponentially decaying harmonic acceleration with peak amplitude of $0.25g$. The results reveal that wider modified-oval and elliptic tanks yield higher roll moment compared to the circular tank at low and moderate fill levels. This is attributed to the combined effects of larger peak lateral load shift and greater peak lateral slosh forces within the wider tanks under low to moderate fill ranges, as observed in Figure 3.5 and Figure 3.10, respectively. On the contrary, at the higher fill level, the wider tanks yield lower peak roll moment compared to the circular tank. This is ascribed to the lower cg height of the wider tanks, as shown in Figure 3.9. Results show that modified-oval tank yields nearly 7% lower roll moment compared to the circular tank for the 80% fill level. Thus, suggesting greater SRT and stability limits for wider tanks at higher fill levels.

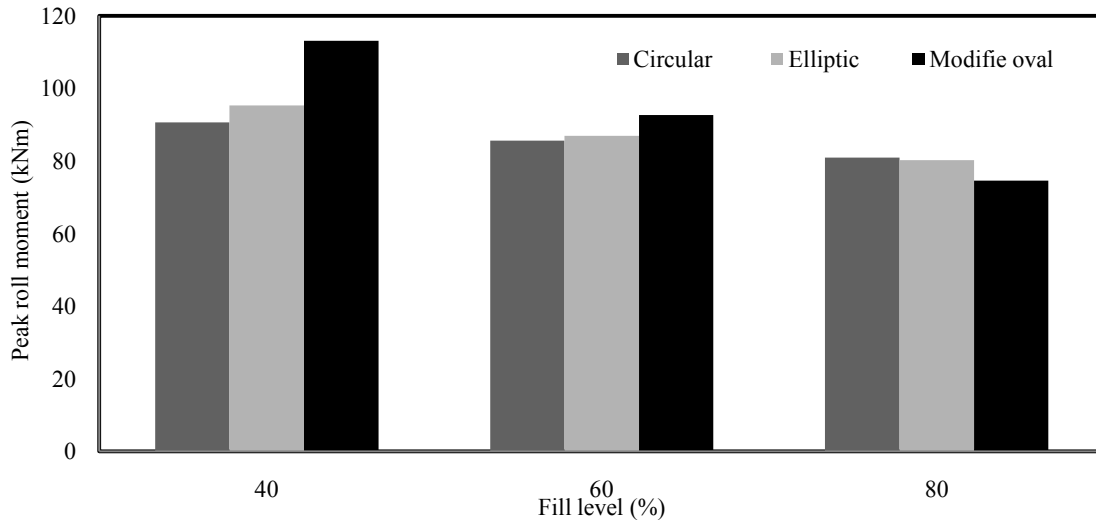


Figure 3.12: Comparisons of peak roll moment caused by fluid slosh within partly-filled tanks subjected to idealized path-change maneuver and 7° sprung mass roll.

Ramp-step lateral acceleration

Unlike the lateral force amplification factors, roll moment due to fluid slosh is strongly influenced by the tank cross-section. This is attributable to greater lateral load shift in wider elliptic and modified-oval tanks compared to the circular cross-section tank, as observed in Figure 3.7. The roll moment resulting from a maneuver-induced lateral acceleration and sprung mass cg offset could be the primarily overturning moment responsible for potential roll instability, considering the trailer structure sprung mass is smaller than the fluid cargo mass. Variations in the roll moment, estimated from the slosh forces, are illustrated in Figure 3.13. The results suggest that circular and elliptic tank cross-sections yield lower peak and steady-state overturning moments compared to the modified-oval cross-section tank at the lower fill level of 40%. Oscillations also show slightly lower frequency of the roll moment caused by the slosh in the modified-oval tank compared to the other tanks. Further, the roll moment oscillation frequency for the circular and elliptic tanks is estimated to be nearly 0.54Hz, while that estimated

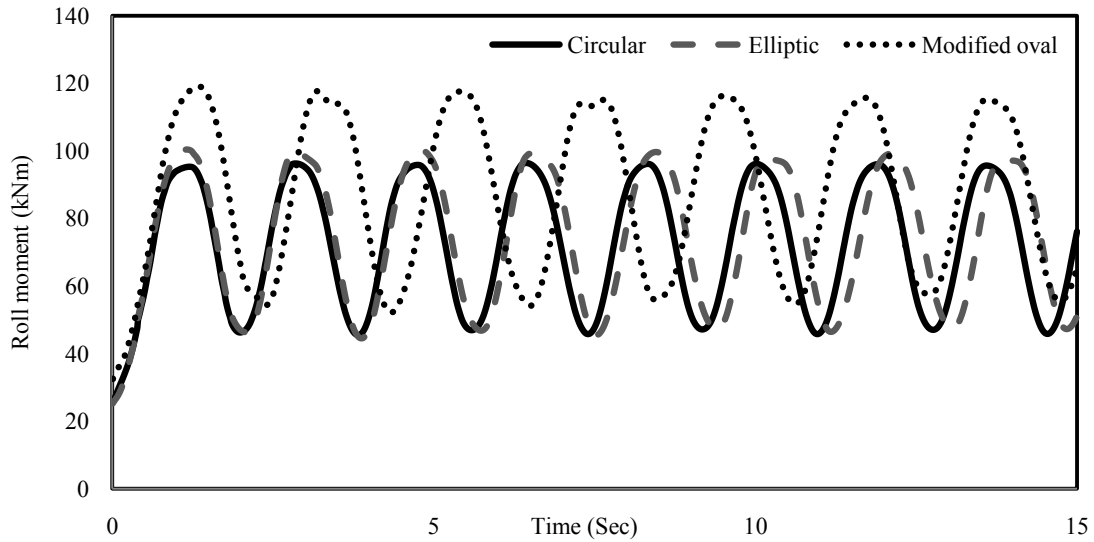


Figure 3.13: Time-histories roll moment caused by fluid slosh within 40% filled tanks subjected selected steady-turning maneuver and 7° sprung mass roll.

for modified-oval tank is 0.48Hz. A number of studies have also reported similar fundamental slosh frequencies for 40% filled circular tanks [11, 13, 43]. The time history of the roll moment due to cargo slosh within the modified-oval tank also reveals slight dipping during the second and fourth cycles, which was related to slight flow separation from the tank surface.

Figure 3.14 illustrates variations in the roll moment amplification factor K_{M_x} as a function of the fill level and the tank cross-section. Results show that modified-oval tank yields higher normalized roll moment under lower and moderate fill conditions compared to the elliptic and circular cross-section tanks. The modified-oval tank, however, yields lesser roll moment under 80% fill condition. This trend can be directly related to deviation in lateral and vertical cg coordinates of the sloshing cargo. It should be noted

both the lateral and vertical cg coordinates contribute to the net roll moment, as seen in Eqn. (2.10).

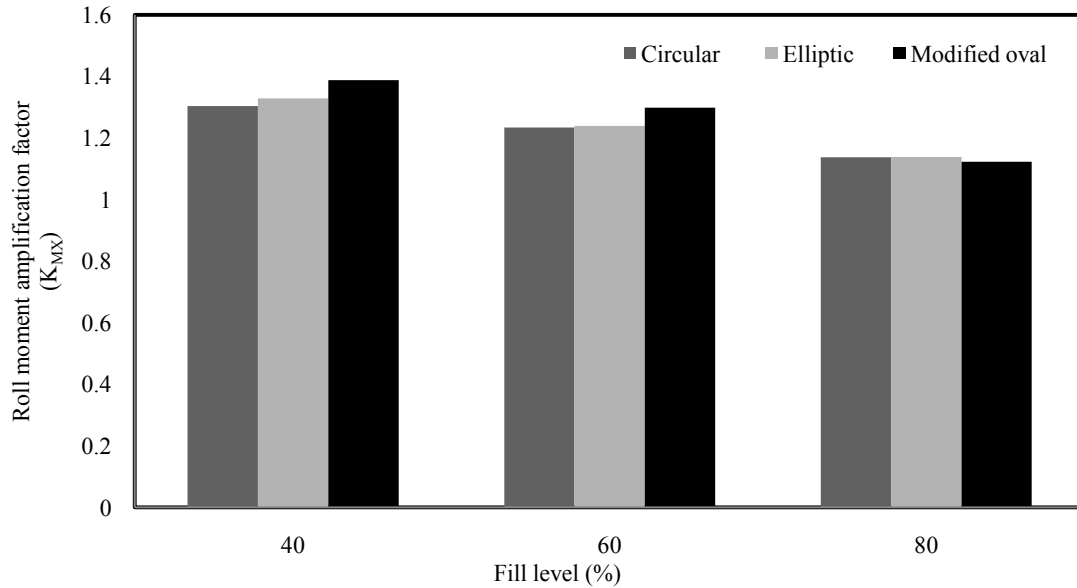


Figure 3.14: Comparisons of variation in roll moment amplification factor for tanks of various cross-sections subjected to selected steady-turning maneuver and 7° sprung mass roll.

Under high fill levels, the vertical cg cargo yields a greater contribution to the roll moment than the lateral cg coordinate. The lower cg height of the modified-oval tank thus results in lower magnitude of roll moment under the high fill level.

3.4.4 Effect of tank cross-section on roll mass moment of inertia

The roll mass moment of inertia of the vehicle sprung mass is directly related to the directional characteristics of the tank vehicles. The free surface movements of the cargo tends to alter the mass moment of inertia in the pitch, roll and yaw planes, which could significantly alter the directional behavior of the vehicle. Variations in peak mass moment of inertia, $\max(I_X)$, about the roll axis of the tank are illustrated in Figure 3.15 for different fill levels and cross-section tanks subjected to idealized steady-turning

maneuver excitation. The results show that wider elliptic and modified-oval cross-sections yield higher roll mass moment of inertia of the sloshing

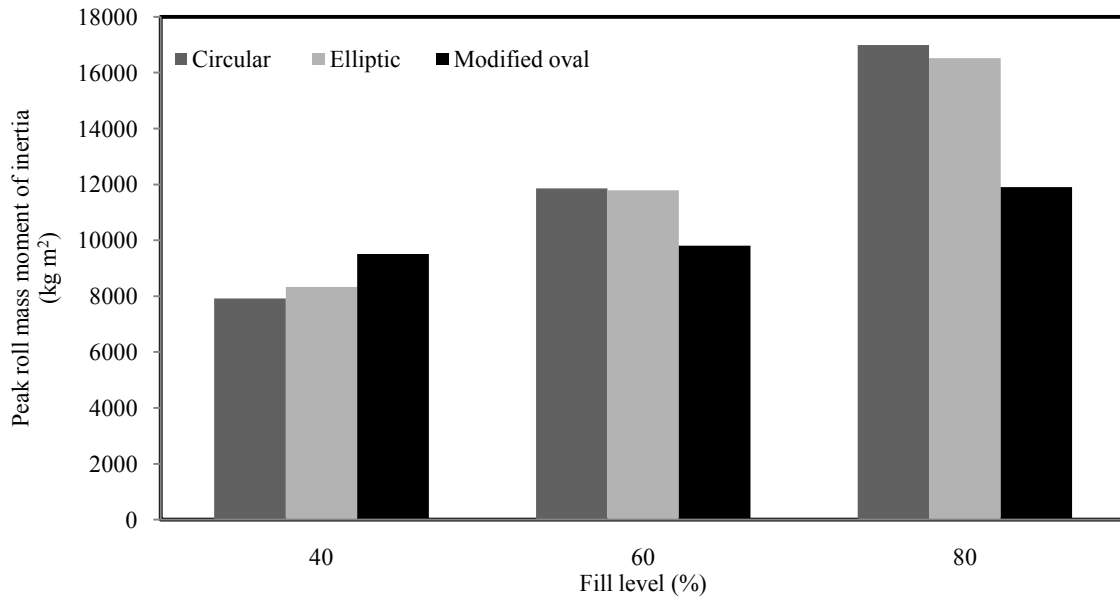


Figure 3.15: Illustrates the variations in peak deviation of roll mass moment of inertia ($max I_x$) as a function of tank cross-section and fill level under idealized path-change maneuver and 7° sprung mass roll.

cargo under low fill conditions, while under moderate and high fill levels these tank cross-sections yield considerably lower roll mass moment of inertia. Under low fill conditions, lateral cg coordinate contributes significantly to the roll mass moment of inertia for wider tank cross-sections. However, with increase in fill conditions, the contribution of vertical cg coordinate to roll mass moment of inertia become overriding and thus elliptic and modified-oval tanks yields considerably lower roll mass moments of inertia under high fill conditions. Although the deflection of cargo is greater in wider tank cross-sections, as seen from Figure 3.7 and Figure 3.8, cargo mass moments of inertia within wider tanks are lower at high fill levels. Table 3.1 compares the peak vertical cg coordinate which justifies the lower roll mass moments of inertia of wider tanks at

moderate and high fill levels. Comparisons of roll mass moment of inertia under a path-change maneuver yield similar trends in results and re-emphasize higher stability limits of wider tanks under high fill conditions.

Tank cross-section	Peak vertical cg coordinate of deflected cargo (m)		
	40%	60%	80%
Circular	0.5185	0.7206	0.8958
Elliptical	0.5180	0.7211	0.8825
Modified-oval	0.4570	0.5999	0.7387

Table 3.1: Comparisons of peak vertical cg coordinate of deflected cargo within tanks various cross-sections and fill levels subjected to steady-turning maneuver and 7° sprung mass roll.

3.5 Fundamental Slosh Frequency

Fundamental slosh frequencies of the cargo within circular tank at different fill conditions were investigated by Dodge [9]. Similar results were also demonstrated by Modaressi et al. [14] on the basis of the dynamic slosh responses of partly-filled circular tanks. This study also reported that directional maneuvers with frequencies in the vicinity of liquid slosh natural frequency would yield considerably large slosh force and moment responses. The fundamental slosh frequency is also influenced by the tank cross-section. Romero et al. [43] proposed a semi-empirical approach to estimate the fundamental slosh frequencies of alternate tank cross-sections on the basis of experiments conducted on very small tanks. In this study, the fundamental slosh frequencies are identified from Fourier analysis of the transient slosh responses to a 0.4g ramp-step lateral acceleration excitation. Figure 3.16 presents the fundamental frequencies obtained for different fill levels in the selected tank cross-sections. Results show that increase in tank width yields lower fundamental slosh frequency for a given fill level. The modified-oval cross-section

yields lowest fundamental slosh frequency for all fill conditions considered. This is attributed to the fact that wider tanks produce longer roll plane free surface length compared to that in the less wide tanks. Furthermore, a low fill volume yields relatively lower fundamental frequency, irrespective of the tank cross-section. This trend has been widely reported in studies based on linear slosh, experiments, and nonlinear dynamic slosh [43, 19, 13].

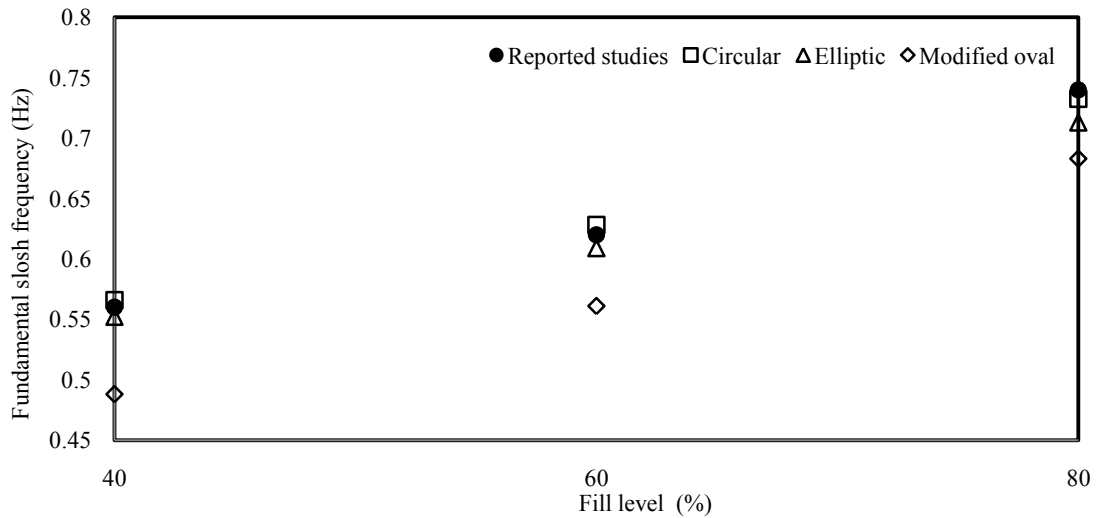


Figure 3.16: Comparison of fundamental frequency of slosh as a function of fill level and tank cross section.

3.6 Effect of Sprung Mass Roll Motion on Dynamic Slosh Measures

The reported studies on dynamic fluid slosh invariably considered excitations arising from lateral and longitudinal accelerations, while the effects of tank roll and pitch motions have been entirely ignored [7, 8, 13]. The roll and pitch motions of the sprung mass also cause dynamic load shift and would contribute to the resulting roll and pitch moments. The dynamic slosh model is analyzed to study the effect of tank roll motion on the dynamic slosh measures. The effects of sprung mass roll are studied by evaluating

response characteristics with respect to the global axis system (YZ), as shown in Figure 2.4, and comparing the responses under roll and no-roll conditions. The results are presented for all the tank cross-sections considered under 0.25g ramp-step lateral acceleration. Further, to investigate the effect of sprung mass roll exclusively, simulations are carried out at a constant axle load of 20,383kg representing the full load condition.

3.6.1 Effect of roll motion on dynamic load shift

Figure 3.17 compares the steady-state lateral load shift of partly-filled tanks subjected to selected lateral acceleration measured from the global axis. The results are obtained for 0° and 7° roll angles of the sprung mass. The results clearly show that lateral load shift increases with increase in the sprung mass roll angle, and approaches substantially higher values for lower fill levels. The results further show that the variations in the lateral cg coordinates for the selected cross-sections occur in a decreasing linear manner with the fill level. A closer examination of the results further revealed that wider elliptic and modified-oval tanks yields higher lateral load shifts compared to that of circular tank in the presence of tank roll motion. The results evidently show that sprung mass roll would yield substantially higher load shift and cause considerable contribution to the roll moment. The effect of tank roll on the vertical cg coordinate, however, was observed to be very small, irrespective of the fill level. The consideration of tank roll angle causes the vertical cg coordinate to be slightly lower compared to the no-roll condition.

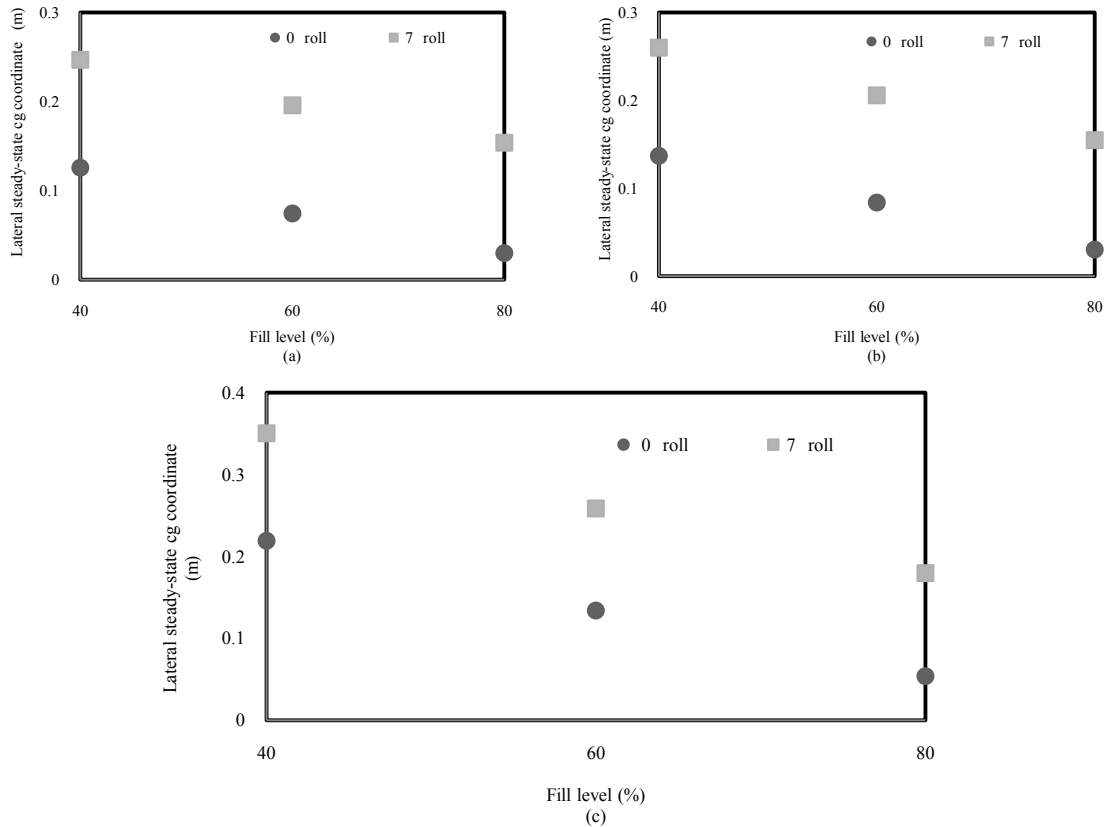


Figure 3.17: Influence of tank roll motion on the steady-state lateral cg coordinates of liquid cargo within the partly-filled tanks subjected to $0.25g$ lateral: (a) Circular; (b) Elliptic and (c) Modified-oval.

3.6.2 Effect of sprung mass roll on dynamic slosh forces

The effect of sprung mass roll on dynamic slosh is analyzed by comparing the steady-state lateral force under 7° tank roll with quasi-static lateral force for various cross-sections. Unlike dynamic load shift, a lateral force due to fluid slosh is negligibly influenced by the sprung mass roll motion. Figure 3.8 illustrates the effect of tank roll on the lateral slosh force under partly-filled tanks subjected to $0.25g$ ramp-step lateral acceleration excitation. Results show negligible effect of sprung mass roll on the lateral slosh force. Slight variations between the quasi-static and steady-state forces are observed with a maximum error magnitude of about 4%. Similar differences between the quasi-

static and steady-state forces have been reported in earlier studies [7, 13, 19]. This difference is attributable to the error in numerical estimation of mass by the dynamic fluid slosh model.

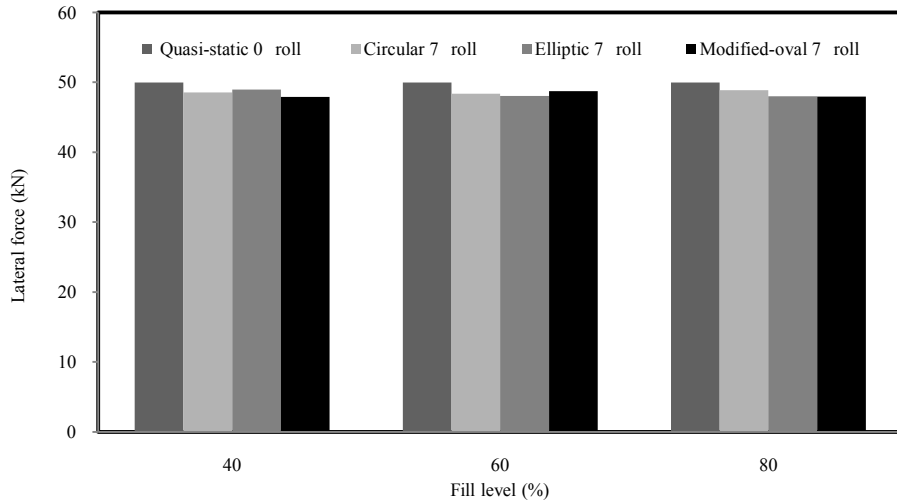


Figure 3.18: Comparisons of lateral force amplification factor due to cargo shift within partly-filled tanks subjected to $0.25g$ lateral acceleration and sprung mass roll motion.

3.6.3 Effect of sprung mass roll on roll moment

Effect of sprung mass roll on roll moment could be directly associated with the dynamic load shift due to roll motion of the sprung mass. Effect of tank roll motion on the dynamic roll moment is studied in terms of variations in peak roll moment within the tank cross-sections considered under $0.25g$ ramp-step lateral acceleration excitation with and without sprung mass roll motion. Figure 3.19 compares the variations in peak roll moment for different fill levels and tank cross-sections. Results reveal nearly linear effect of sprung mass roll on peak roll moment caused by the liquid cargo movement within the tanks. The results suggest that sprung mass roll of 7° could yield as high as 24% greater roll moment compared to no-roll condition.

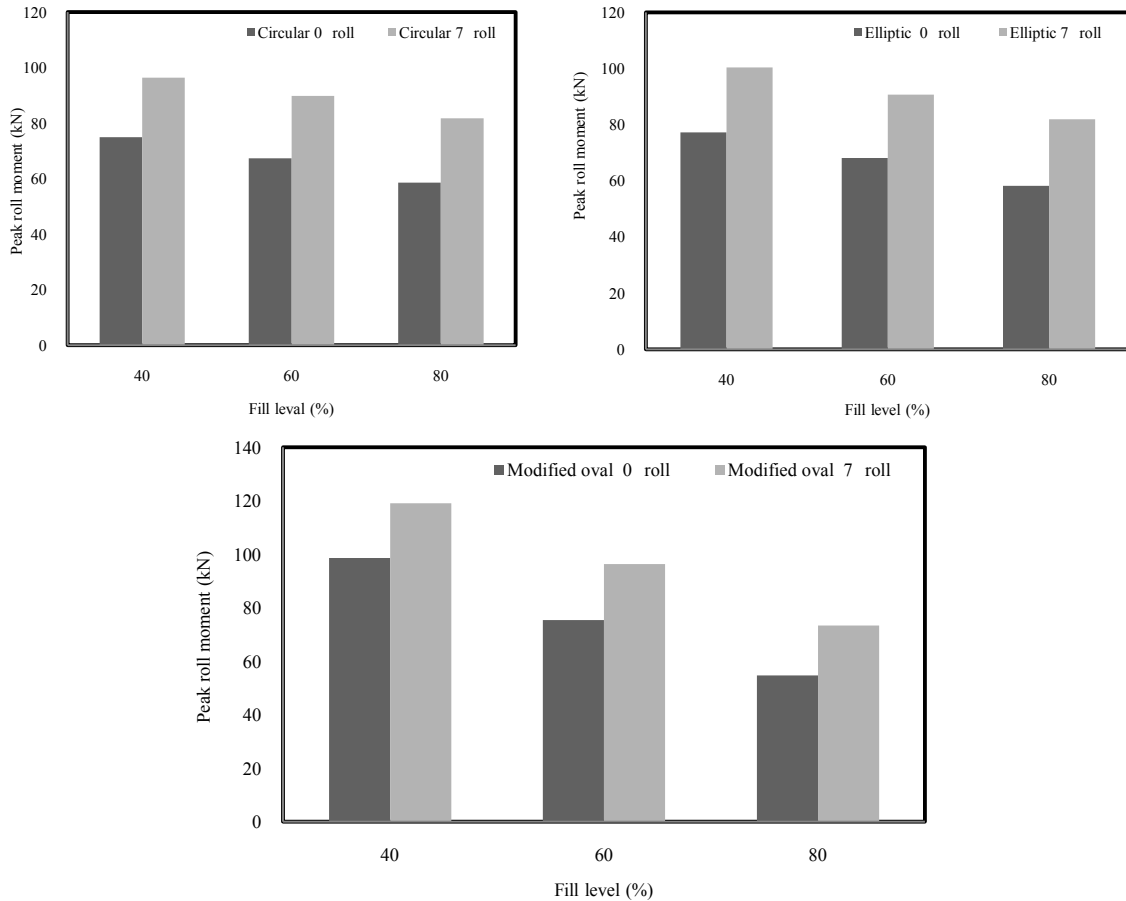


Figure 3.19: Illustrates the variations in peak roll moment for partly-filled tanks subjected to $0.4g$ lateral acceleration with and without roll under constant load at various fill levels.

The same is ascribed to the combined effects of higher lateral load shift, which was observed in Figure 3.17 under constant load condition. Time-histories of roll moment due to sloshing cargo within the 40% filled modified-oval tank under $0.25g$ lateral acceleration excitation as a function of roll angle are shown in Figure 3.20. The results clearly show the increase in both the peak and the steady-state roll moment magnitudes with sprung mass roll. It is also seen from the figure that tank with roll motion yields higher initial ($t=0$) roll moment compared to tank at no-roll condition. The time-histories also reveal that modified-oval tank with 7° roll yields marginally higher fundamental

frequency of slosh compared to the 0° roll angle. This is attributed to the reduced roll plane free surface length of modified-oval tank under 7° roll condition. It can thus be safely concluded that sprung mass roll motion further increases the dynamic lateral load shift and roll moment caused by the cargo movement within the partly filled tanks under maneuver-induced excitations. Moreover, in terms of safety dynamics of partly-filled tank vehicles, the sprung mass roll further reduces the SRT and stability limits of partly-filled road tankers.

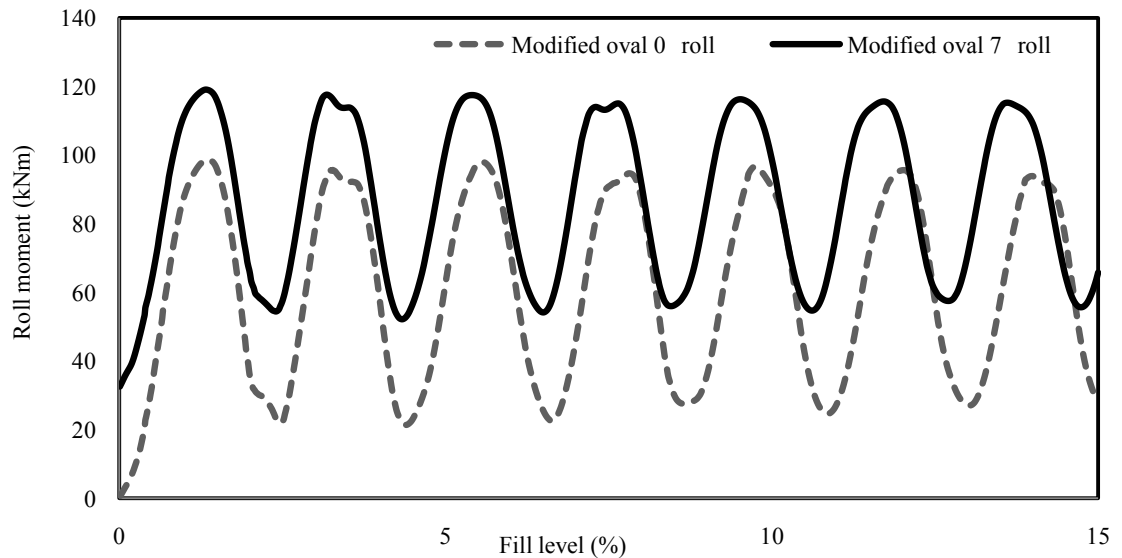


Figure 3.20: Time histories of roll moment caused by sloshing cargo within partly-filled modified-oval tank subjected to $0.25g$ lateral acceleration and sprung mass roll at 40% fill level.

3.7 Summary

Transient slosh in the roll plane of the partly-filled tanks of different cross-sections subjected to idealized directional maneuvers is investigated. Dynamic slosh responses in terms of load shifts, slosh forces and moments and roll mass moment of inertia are evaluated. Results demonstrated good agreements of steady-state slosh responses with those estimated from quasi-static model. Due to free surface deformation and flow

separation in the dynamic slosh only minor deviations between the two were also observed.

Effects of tank cross-section on the transient slosh are particularly emphasized by comparing the dynamic response measures of the selected tanks under different fill levels, subjected to idealized path-change and turning maneuvers lateral accelerations. Results reveal that maneuver-induced transient slosh could severely impair the directional dynamics of wider elliptic and modified-oval tank vehicles at low and medium fill levels, while at higher fill level the wider tanks could yield enhanced directional dynamic characteristics. While at lower fill levels wider modified-oval tank yields nearly 25% higher magnitude of peak roll moment compared to the circular tank. At a higher fill level of 80%, the modified-oval tank yields 8% lower peak roll moment compared to the circular tank under an idealized path-change maneuver excitation

Effects of sprung mass roll are also evaluated in terms of transient slosh measures. Results showed that the sprung mass roll could have considerable affect on all the transient slosh measures. The effect of sprung mass roll was observed to be relatively greater for wider modified and elliptic tank cross-sections then that for the less wide circular tank. Moreover, the fundamental frequency of slosh is also investigated to be affected by the sprung mass roll. The fluid slosh in both the pitch and roll planes are analyzed in the subsequent chapter using three-dimensional CFD model to study the anti slosh effectiveness of baffles arrangements.

CHAPTER 4

THREE-DIMENSIONAL FLUID SLOSH ANALYSIS IN BAFFLED MODIFIED-OVAL TANK

4.1 Introduction

The results presented in chapter 3 showed that the wider cross-section tank (MC-406, modified-oval) subjected to lateral acceleration and sprung mass roll motion yields higher transient and steady-state roll moment under low and moderate fill levels compared to the circular tanks. Furthermore, the presence of sprung mass roll causes relatively higher initial ($t=0$) roll moment for the modified-oval tank compared the less wide circular tank. These suggest that a road tanker with a partly-filled modified-oval tank is more susceptible to rollover compared to that with a circular tank. This is also supported by the accident data reported by the Motor Carrier Management Information System (MCMIS), which suggests that road tankers with modified-oval cross-section tanks (MC-406) are involved in 73% of the reported rollover crashes, while those with circular cross-section tanks (MC-407) account for the remaining rollover crashes [3]. The disparity in number of rollover accidents between the two tank geometries may in-part be attributed to difference in operating pressures of the MC-406 and MC-407 vehicles [39].

Although the current tank designs, except for those employed in general purpose bulk transportation, generally employ transverse baffles that tend to limit slosh in longitudinal direction. Such baffles do not help reduce the lateral load shift and thus the roll moment. In recent years Yan [14] has reported an analysis of transverse baffles effectiveness within partly-filled RT tanks. The study concluded that transverse baffles increased the longitudinal fundamental slosh frequency up to three times than that of

clean-bore tanks, while effectively limiting the longitudinal load shift and pitch moments. Ervin et al. [54] used Strandberg's experimental results [21] to highlight relative benefits of different longitudinal baffle arrangements to limit the lateral slosh force. The study illustrated the potential benefits of longitudinal baffles in terms of side force amplification and fundamental slosh frequency for a 50% filled scaled elliptic tank. Miralbes et al. [8] numerically investigated effectiveness of split longitudinal baffle arrangements within circular tanks. The proposed arrangements, however, did not yield considerable reduction in the roll moment, which was attributed to the poor baffle design. In this study, a few arrangements of transverse-longitudinal baffles are presented to study their effectiveness in limiting fluid slosh in both roll and pitch planes. For this purpose, the three-dimensional CFD model of the partly-filled modified-oval tank is applied under selected lateral and longitudinal accelerations excitations. The slosh responses are presented and discussed in terms of load shift, slosh forces and moments.

4.2 Baffle Design Concepts for Modified-oval Tank

Transverse baffle arrangements are commonly used in tank vehicles to impede the fore/aft movement of liquid cargo thereby enhancing its braking performance limits apart from integrity of the tank structure. On the other hand, transverse baffle arrangements have practically negligible effect in attenuating lateral slosh affecting roll stability of the tank vehicles. The transverse baffle arrangements used in current designs attenuate liquid cargo sloshing through damping of fluid flow energy and reduction in effective sloshing mass, while horizontal split baffle arrangements provided only damping of fluid flow energy via directing the moving cargo away from the outer walls of the tank. Horizontal

split baffles, however, pose considerable challenges in terms of design, dimensioning and positioning within the tank. Alternately, a simple concept of a vertical baffle along the longitudinal center line of the tank could help reduce the lateral load shift and provide two equal compartments. Such a longitudinal baffle would not only effectively dampen the fluid flow energy but also reduce the effective sloshing mass. Although such a longitudinal baffle arrangements would include additional baffle weight of nearly 19% for a 7.55m long tank, optimal baffle perforation and diligent design could significantly reduce the additional baffle weight. Further, provisions for cleaning tanks equipped with such baffles can also be devised, provided these baffle arrangements successfully impede lateral movement of the cargo thereby producing considerable improvement in roll stability of modified-oval tank vehicles.

This chapter presents a preliminary attempt in investigating the relative improvement in dynamic slosh responses within partly-filled modified-oval tanks with four different baffle arrangements. These consist of a conventional transverse baffled tank, and three different transverse and longitudinal baffled configurations described below:

1. Modified-oval tank with conventional transverse baffle arrangement as shown in Figure 4.1(a), hereafter referred to as tank ‘A’;
2. Modified-oval tank with conventional transverse baffles and a vertical partition along the longitudinal center line of the tank as shown in Figure 4.1 (b), hereafter referred to as tank ‘FT-FL’;
3. Modified-oval tank with conventional transverse baffles and a partial vertical partition along the longitudinal center line of the tank as shown in Figure 4.1(c), hereafter referred to as tank ‘FT-PL’; and

4. Modified-oval tank with partial transverse baffles along with a partial vertical partition along the longitudinal center line of the tank as shown in Figure 4.1(d), hereafter referred to as tank 'PT-PL'.

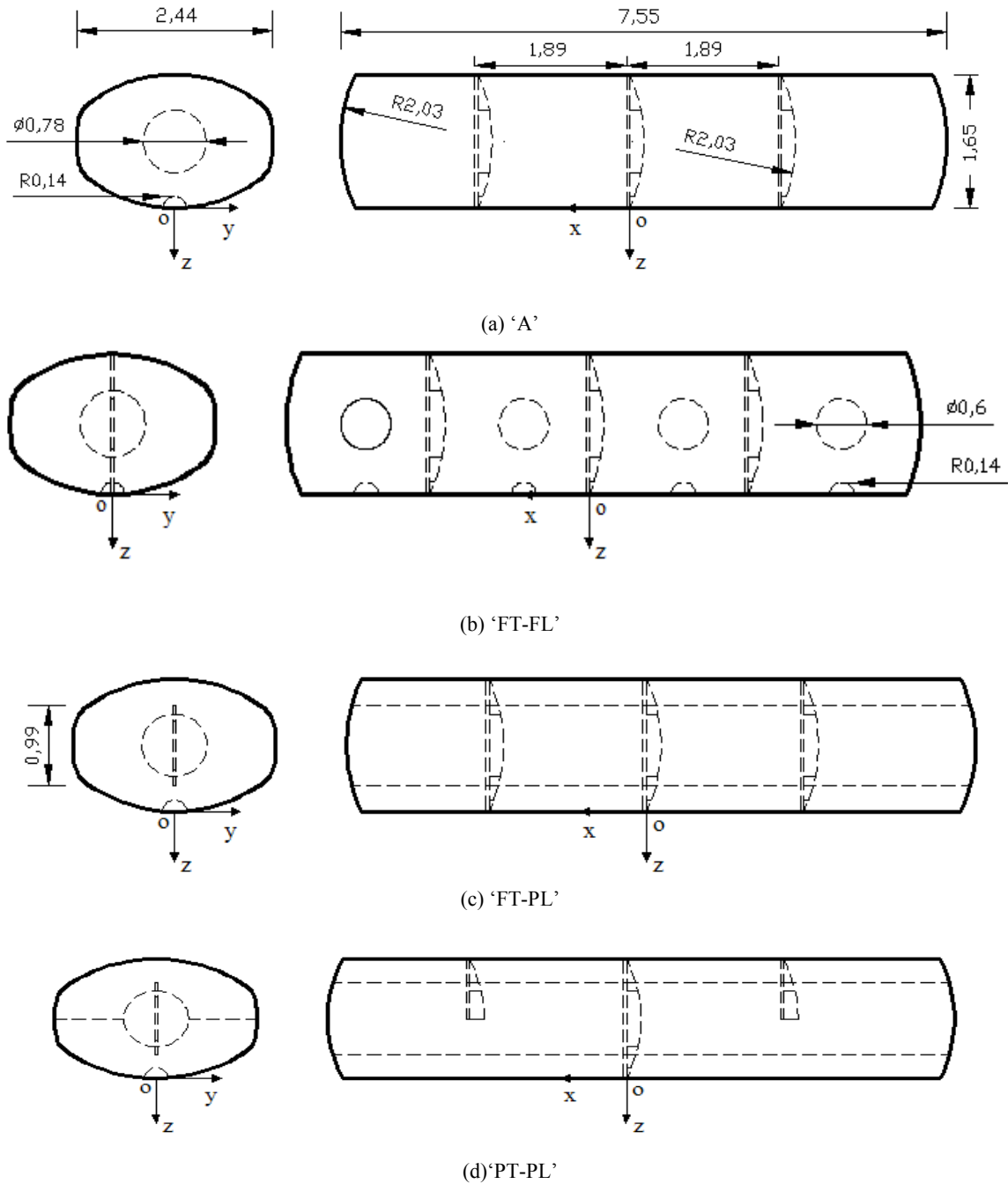
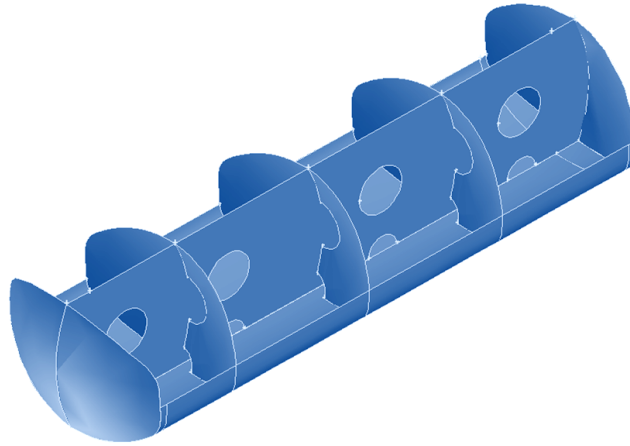


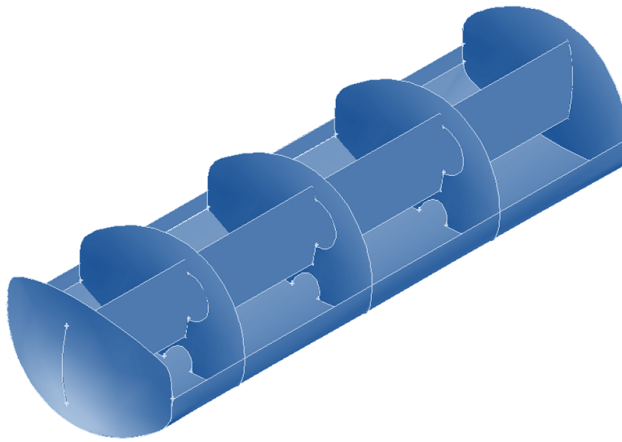
Figure 4.1: Schematics of different baffle arrangements considered in the present study.

Figure 4.2 illustrates the three-dimensional sectional views of the tank with proposed baffles arrangements, FT-FL, FT-PL and PT-PL. The tanks FT-PL and PT-PL represent preliminary concept towards reducing the baffles weight. Height and positioning of the partial longitudinal baffle in FT-PL and PT-PL configurations is chosen such that it covers 20 to 80% of fill levels, although analysis with different heights would also be desirable. The height is based on the facts that fill levels up to 20% are unlikely to occur in practice, while the fill levels of 80% and above yield relatively lower cargo sloshing due to higher boundary constraints, as observed in results in chapter 3. Further, baffles employed in the present study have an overall baffle opening area of nearly 15% and 10% of the transverse and longitudinal baffle cross-section areas respectively, which are within the 20% limit specified in the CFR [42]. Spacing between transverse baffles is set to be 1.89 m to have equal compartment length [32].

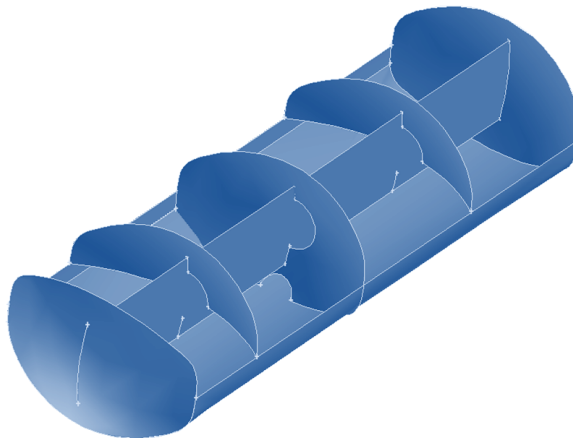
The analyses are limited only to modified-oval cross-section in order to explore the relative performance potentials of the proposed baffle design concepts. The transverse baffles are considered with curvature identical to that of the endcap, while the simulations are performed for constant load of 20383kg to analyze anti slosh properties of these baffle configurations subjected to lateral ($a_y=0.25g$), and simultaneous lateral and longitudinal ($a_y=0.25g$, $a_x=0.6g$) accelerations idealizing steady-turning and braking-in-turn maneuvers, respectively. Owing to complex baffled tank geometries and convergence criteria for residuals of 10^{-5} , the time step of 0.25ms is selected. Two fill levels, 40 and 60% are considered for the analysis, since these represent the fill conditions with greatest load shift potential.



(a)



(b)



(c)

Figure 4.2: Illustrates three-dimensional sectional views of baffled tank configurations; (a) FT-FL; (b) FT-PL; and (c) PT-PL

Three-dimensional CFD models of the four tanks are formulated with mesh density of 1573 elements per meter cube or greater. A processor sensitivity analysis is also conducted to investigate the computational time dependence of the solutions on number of processors used. Table 4.1 describes the time dependence of the solution for single and two processors. It is seen from the Table 4.1 that using parallel computation with just two processors significantly reduces the computing time. Parallel computation, with two processors, of the described slosh problem requires nearly 60% lesser time. Consequently, parallel computation with two processors is selected over serial computation mode for all baffled tank configurations.

Computation details	Single processor series computation	Two processors parallel computation
Simulation time 1 s	13hrs 42min	6hrs 21min
Simulation time 15 s	8days 12hrs 32min	3day 23hrs 16min

Table 4.1: Comparisons of overall computation time requirement for simulating a 40% filled modified-oval tank configuration subjected to $0.25g$ lateral acceleration with a time step of 0.25ms.

4.3 Responses to Lateral Acceleration

4.3.1 Dynamic load shift

Lateral and vertical cg coordinates are one of the most critical slosh responses that can be directly related to the overturning moment, as described in Eqn. (2.10), of a partly-filled tank vehicle. Anti slosh effectiveness of the alternate baffle design concepts is investigated in terms of time-histories of the lateral cg coordinate. Figure 4.3 compares time-histories of lateral cg coordinates for the 40 and 60% filled baffled modified-oval tank configurations (FT-FL, FT-PL and PT-PL) under $0.25g$ ramp-step lateral

acceleration and 7° sprung mass roll motion. Results clearly show that conventional lateral baffle arrangement yields not only a higher peak lateral cg coordinate but also significantly lower cargo slosh damping compared to the tanks with proposed baffle arrangements for both the fill conditions. Evaluation of damping ratio employing logarithmic decrement method reveals that the proposed longitudinal baffle arrangements invariably yield higher effective damping ratio. The increase in damping ratio was estimated to be maximum for tank configuration FT-PL ($\xi=0.0774$), which is nearly 3 times that of the configuration A ($\xi=0.0266$), suggesting high roll plane slosh attenuation efficiency of the baffle arrangement FT-PL. A closer inspection of the result reveals that proposed baffled configurations yield lower initial lateral cg coordinate compared to conventional baffled tank. These are attributed to the fact that longitudinal baffles effectively impede the lateral movement of the cargo under external excitations. Results further indicate an increase in the roll plane fundamental frequency of slosh for the proposed configurations, the increase is most significant for the FT-FL design. Moreover, configurations FT-FL, FT-PL and PT-PL, yield relatively lower instantaneous vertical cg coordinate compared to the conventional baffled modified-oval tank. The results suggest that proposed longitudinal baffle configurations would yield relatively lower the overturning moment compared to the conventional tank A and subsequently improve the stability and controllability limits of the partly-filled fluid cargo tank vehicles.

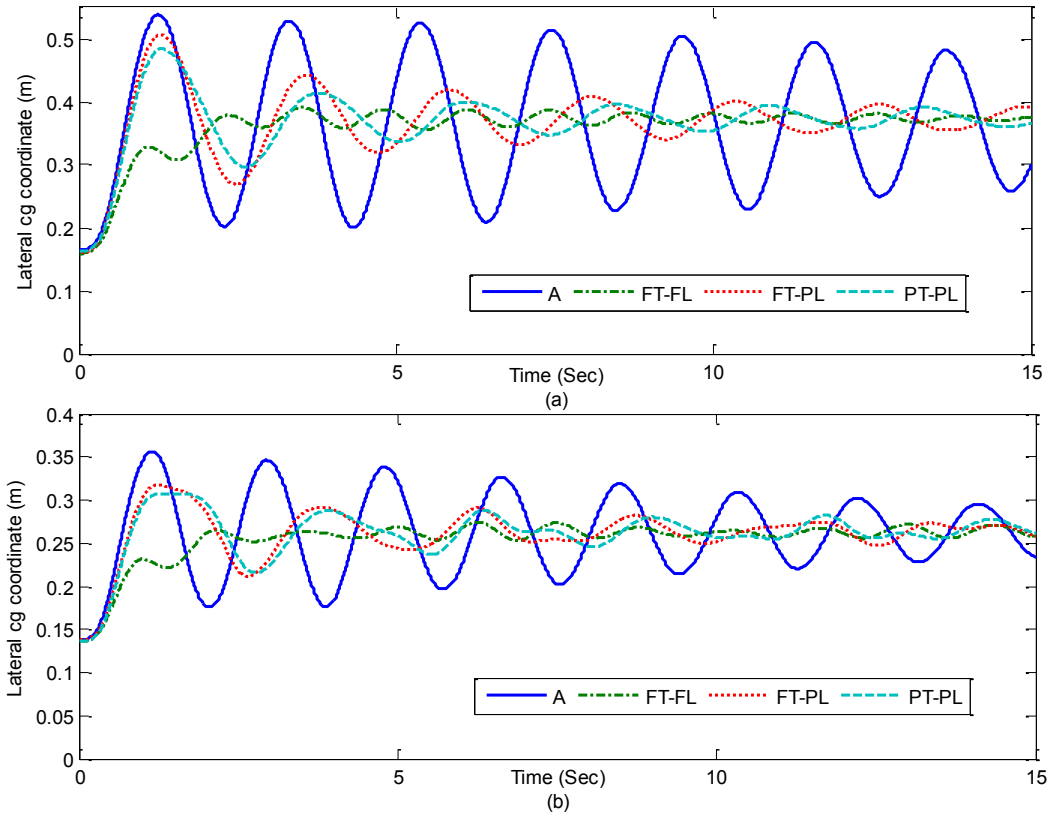


Figure 4.3: Comparisons of the time-histories of instantaneous lateral cg coordinates of fluid cargo within 40 and 60% filled modified-oval baffled tank configurations under $0.25g$ ramp-step lateral acceleration and 7° sprung mass roll motion; (a) 40% fill; and (b) 60% fill.

4.3.2 Dynamic forces and moments

The effects of longitudinal baffle configurations on dynamic slosh forces and roll moments are investigated in terms of normalized lateral slosh force (K_{F_y}) and roll moment (K_{M_x}) for the partly-filled baffled modified-oval tanks under $0.25g$ lateral acceleration and 7° roll motion. Figure 4.4 illustrate variations in the lateral and vertical slosh force amplification factors as a function of fill level and baffle configuration. Figure 4.4(a) clearly shows that lateral slosh force amplification factor decreases with higher fill level owing to greater boundary limitation at higher fill levels. The results further demonstrate that the lateral slosh force amplification factor is considerably lower in the

presence of the longitudinal baffle, with peak reduction in amplification factor of nearly 19% at 40% fill level. Results from Figure 4.4(a) also highlight the relative significance of transient lateral slosh force which is nearly 48% higher than that of the mean dynamic slosh force at the 60% fill level. Although the effect of longitudinal baffle configurations is not quite significant on the vertical force amplification factor, the longitudinal baffles tends to reduce the variation in vertical force amplification factor by 4% under 40% fill levels.

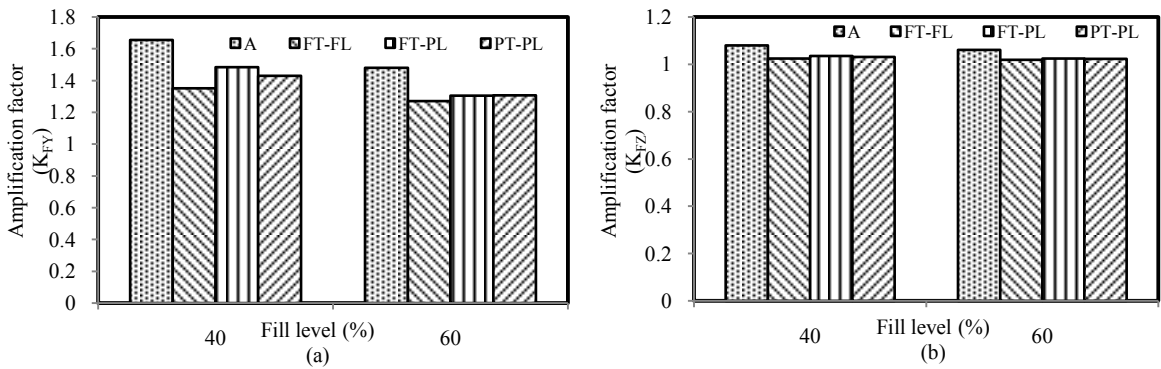


Figure 4.4: Comparisons of slosh force amplification factors of different configurations under $0.25g$ lateral acceleration and 7° sprung mass roll motion; (a) lateral force amplification; and (b) vertical force amplification.

Figure 4.5 shows the time-histories of roll moment responses of the tank configurations under same excitation at 40% fill level. The FT-PL and PT-PL configurations exhibit reduction in peak transient roll moments of 5.5 and 8.9%, respectively, while configuration FT-FL yields nearly 22% lower peak moment compared to the conventional configuration A. The proposed longitudinal baffle configurations prove to be highly efficient in damping the roll moment oscillations when compared to the conventional baffle tanks. The results further show roll moment oscillation frequency of nearly 0.47Hz for tank A, while those of other configurations are considerably higher.

The configuration FT-FL responses exhibit the highest oscillation frequency of 0.76Hz. This is attributed to the partial longitudinal baffle for tank FT-PL and PT-PL, while that for tank FT-FL being an entire longitudinal baffle with openings and equalizers only. Moreover, the dipping around the peak responses is attributed to partial flow separation. The roll moment of tanks A, FT-PL and PT-PL exhibit dipping in the peak response, while it is not evident in the response of tank FT-FL. Figure 4.6 shows the variation in roll moment amplification factors of the tank configurations and the two fill levels. The results show that the proposed baffle arrangements invariably reduce the roll moment amplification factor relative to the conventional baffled modified-oval tank, while configuration FT-FL yields lowest peak roll moment.

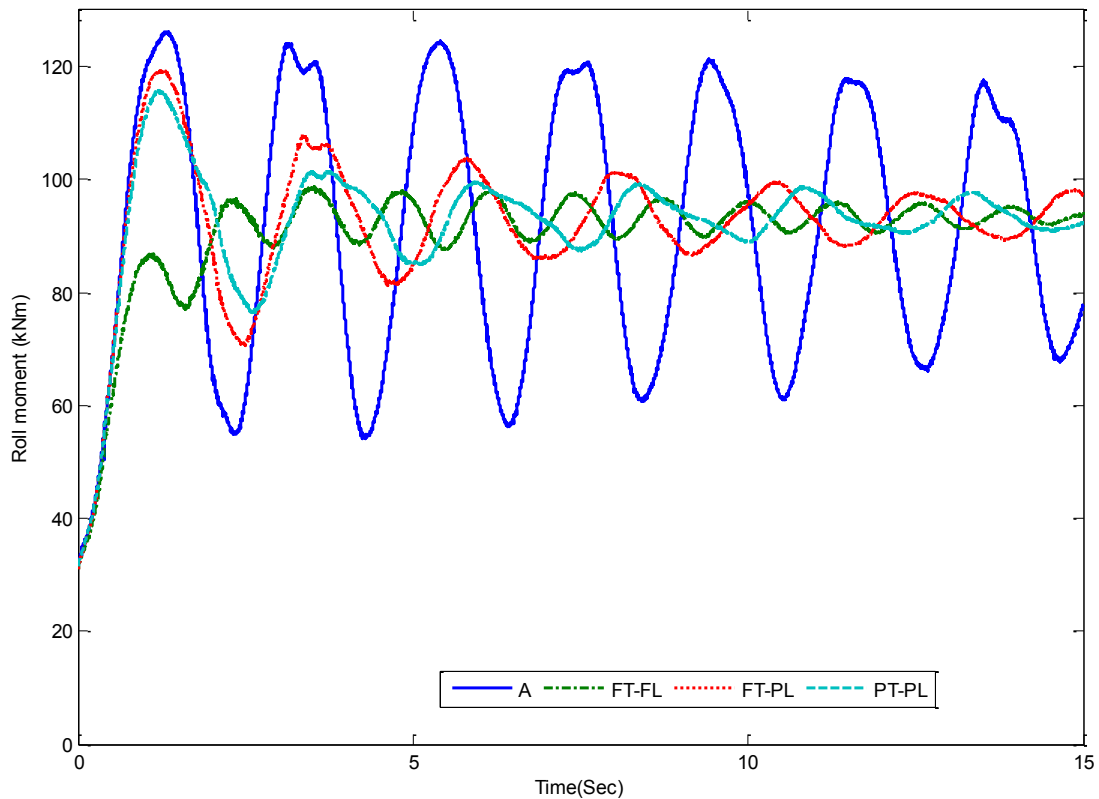


Figure 4.5: The time-histories of roll moment responses of the configurations with 40% filled tanks under idealized constant lateral acceleration and 7° sprung mass roll motion.

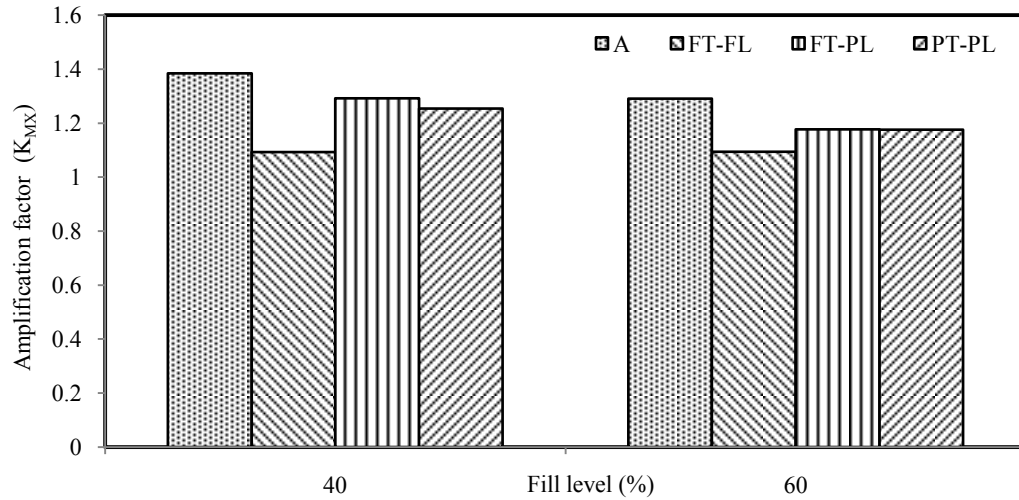


Figure 4.6: Comparisons of roll moment amplification factors (K_{M_x}) of tank configurations subject to $0.25g$ lateral acceleration and 7° sprung mass roll motion (40 and 60% fill conditions).

4.3.3 Fundamental slosh frequency

Apart from dynamic slosh measures, discussed above, the baffles also influence the fundamental slosh frequency. It has been suggested that an excitation steering frequency in the vicinity of the fundamental slosh frequency could cause large magnitude resonant slosh [13, 19]. The frequency of an emergency path-change maneuver may approach a fundamental slosh frequency under low fill level. The relative effect of longitudinal baffle configurations on fundamental slosh frequency is shown in Figure 4.7 for 40 and 60% filled tanks. It is observed from the figure that addition of a longitudinal baffle necessarily results in increased in fundamental slosh frequency in the roll plane. While configuration FT-FL yields the largest increase of nearly 65% in roll plane fundamental slosh frequency, configurations FT-PL and PT-PL exhibit moderate increase of 12.5% compared to conventional tank A at 40% fill level. The significantly higher frequency of FT-FL configuration is attributed to the fact that the baffle configuration reduces the roll plane free surface length most significantly.

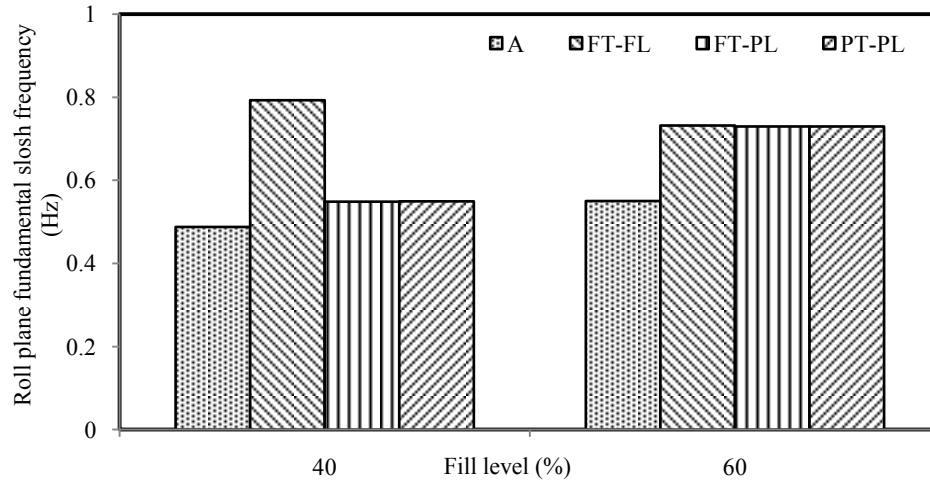


Figure 4.7: Comparisons of roll plane fundamental slosh frequency for baffled tank configurations under idealized steady-turning and 7° sprung mass roll motion.

4.4 Response to Simultaneous Lateral and Longitudinal Accelerations

Three-dimensional dynamic slosh model is solved under idealized braking-in-a-turn maneuver characterized by simultaneous lateral and longitudinal accelerations: $0.25g$ ramp-step lateral and $0.6g$ ramp-step longitudinal accelerations with 7° sprung mass roll angle. It has been shown by Yan et al. [19] that even standard straight line braking treadle pressure could induce an acceleration of nearly $0.6g$ to fluid within the partly-filled un-baffled tank. Thus a high longitudinal acceleration of $0.6g$ was selected. Moreover, such a maneuver would allow a comprehensive analysis of the proposed baffle configurations in both the roll and pitch planes.

4.4.1 Dynamic load shift

Figure 4.8 shows the comparison of time-histories of lateral cg coordinate for all baffled tank configurations considered in the present study under described idealized braking-in-

turn maneuver coupled with 7° sprung mass roll motion. It is clear from the Figure that introduction of the longitudinal baffle reduces the peak transient lateral load shift considerably compared to conventional baffled tank. For reasons of high effective sloshing mass and space offered by configuration PT-PL, the overall lateral cg coordinate variation at 40% fill level is considerably greater than that of other proposed configurations. It is further observed from Figure 4.8, that amplitude of oscillations reduces quite rapidly after a couple of oscillations. Owing to relatively higher longitudinal acceleration, the fluid cargo within the tank move towards one end of the tank consequently reducing lateral load shift. Thus, partly-filled cargo tanks subjected to simultaneous accelerations could yield lower mean lateral load shift compared to tanks subjected to similar lateral acceleration alone. However, this gain in terms of lower mean lateral load shift, for tanks subjected to simultaneous accelerations, is compensated by the associated longitudinal load shift. Furthermore, the proposed baffle configurations yields considerable reduction in the peak transient lateral cg coordinate, tank FT-FL yields nearly 18.5 and 13.6% lesser lateral cg coordinates compared to tank A at 40 and 60% fill levels respectively. Figure 4.9 shows two phase flow views of tank A subject to simultaneous lateral and longitudinal acceleration excitations under 40% fill level after 15s. The views in figure show the liquid cargo accumulating at one end of the tank and this further explains the convergence of the lateral cg coordinate under simultaneous acceleration excitation for all the tank configurations as seen in Figure 4.8.

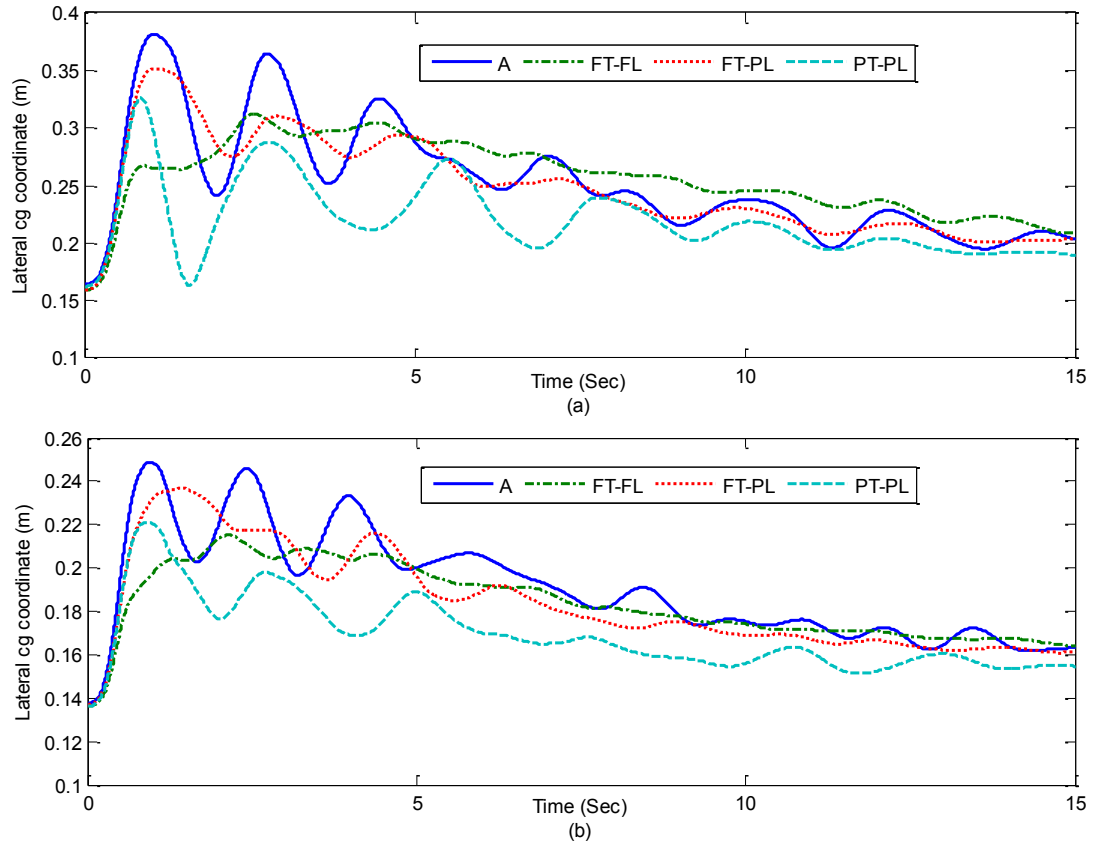


Figure 4.8: Comparisons of time-histories of lateral cg coordinate of the cargo in partly-filled tanks with different baffle subject to $a_x=0.6g$, $a_y=0.25g$ and $\theta = 7^\circ$; (a) 40%; and (b) 60% fill level.

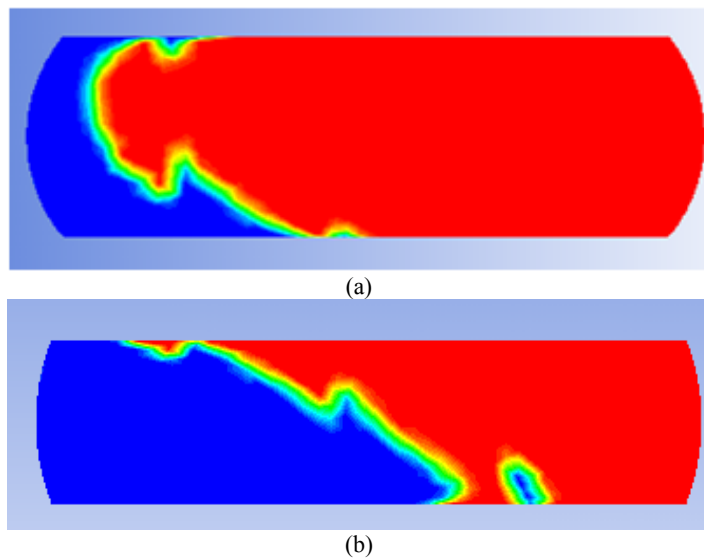


Figure 4.9: Shows the two phase flow view of 40% filled tank A under $a_x=0.6g$, $a_y=0.25g$ and $\theta = 7^\circ$ at $t=15s$ where blue and red colors represent fuel I oil and air respectively; (a) Top view; (b) Side view.

Longitudinal load shift due to fore-aft motion of the sloshing cargo is known to adversely affect the braking distance and pitch plane stability of the tank vehicle. The longitudinal load shift is thus also investigated in terms of longitudinal cg coordinate variations. Figure 4.10 shows the time-histories of instantaneous longitudinal cg coordinates of the cargo within different tank configurations under idealized braking-in-a-turn maneuver together with sprung mass roll under 40 and 60% fill conditions. Results show similar trends in variations in the longitudinal cg coordinate for all configurations due to similar transverse baffle arrangements for tanks A, FT-FL and FT-PL. However,

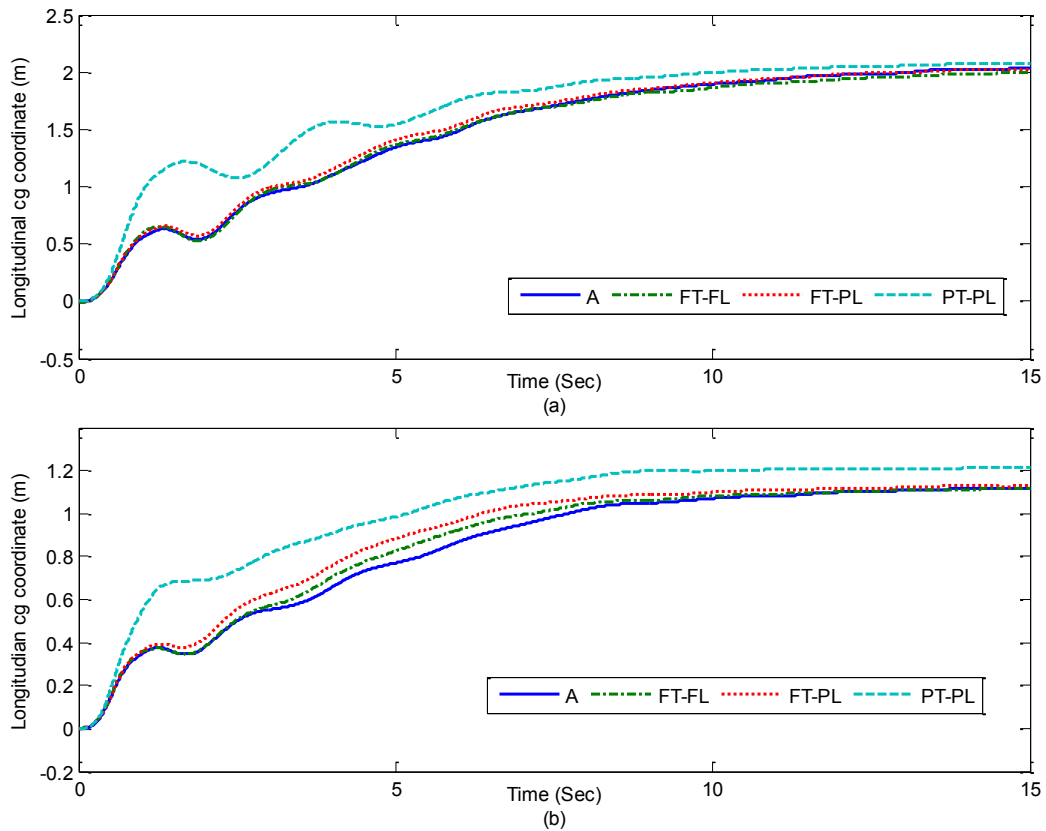


Figure 4.10: Comparisons of variation in instantaneous longitudinal cg coordinate of cargo in tanks with different baffle arrangements subject to $a_x=0.6g$, $a_y=0.25g$ and $\phi = 7^\circ$; (a) 40; and (b) 60% fill level.

owing to higher effective sloshing mass and reduced boundary constraints, the arrangement PT-PL yields higher peak and mean dynamic longitudinal load shift magnitudes compared to the other configurations. The results further suggest that longitudinal baffle arrangements FT-FL, FT-PL and PT-PL offer negligible gain in slosh suppression in the pitch plane. Furthermore, the oscillation frequency of longitudinal cg coordinates for configurations A, FT-FL and FT-PL is observed to be higher than that of configuration PT-PL. At a lower fill level of 40% oscillation frequency of longitudinal cg coordinates for configurations PT-PL is estimated to be nearly 10% lower than the rest of the configurations. This is attributable to the partial transverse baffle arrangement in tank PT-PL.

4.4.2 Dynamic slosh forces

Figure 4.11 illustrates the comparisons of lateral (K_{F_y}) and longitudinal (K_{F_x}) slosh force amplification factors for baffled tank configurations considered in the study under simultaneous lateral and longitudinal acceleration excitation. Due to consideration of constant load condition irrespective of the fill level, force amplification factor would signify the anti slosh effectiveness of proposed baffle configurations. While tanks FT-FL and FT-PL yield nearly 10% lower lateral force amplification factor compared to tank A, tank PT-PL yields considerably higher magnitude of lateral force amplification factor at 40 % fill level. This is attributable to the fact that under low fill levels partial transverse and longitudinal baffles allow greater effective sloshing of cargo compared to rest of the configurations. However, at high fill levels tank PT-PL yields comparable lateral forces amplification factor due to the presence of transverse baffles in the upper half of the tank.

The results further emphasize the significance of transient slosh effect, it is seen that even with the complete longitudinal baffle, for tank FT-FL, transient peak lateral force could be 34% higher than that of the mean dynamic lateral force at 40% fill. On the other hand all the tank configurations considered in the study yield comparable longitudinal force amplification factor.

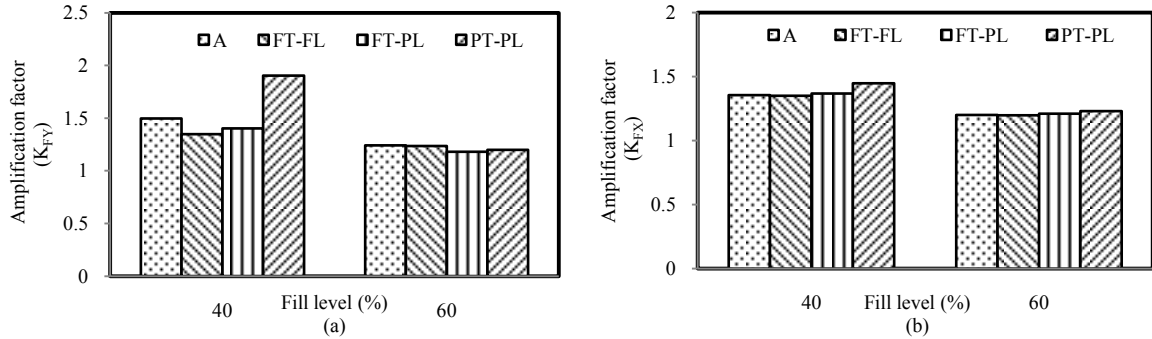


Figure 4.11: Comparisons of force amplification factors for all baffled tank configurations subject to $a_x=0.6g$, $a_y=0.25g$ and $\theta = 7^\circ$; (a) Lateral; and (b) Longitudinal.

Conversely owing to two partial transverse baffles in configuration PT-PL, it yields slightly higher longitudinal force amplification factor compared to other configurations under both 40 and 60% fill levels.

4.4.3 Dynamic slosh moments

Figure 4.12 shows time-histories of the roll moment for all tank configurations under 40% fill level subject to simultaneous acceleration excitations and 7° sprung mass roll motion. It is seen from the figure that all configurations have an initial roll moment ($t=0$) which is due to the sprung mass roll. Further, A and PT-PL tanks yield greater peak roll moment compared to FT-FL and FT-PL. This is attributed to the absence of longitudinal baffle in conventional tanks, while that for configuration PT-PL is attributed in-part to its significantly higher force amplification at low fill level of 40%, and partial transverse

baffles considered for this configuration. Moreover, due to lower boundary constraints and subsequent high effective sloshing cargo mass associated with A and PT-PL tanks, the overall amplitude of oscillations for these tanks are greater compared to tanks FT-FL and FT-PL. Results also reveal greater damping of roll moment oscillations for all tanks compared to tanks under identical lateral acceleration alone. This is ascribed to the relatively higher longitudinal acceleration which results in movement of the cargo towards one end of the tank and thereby limiting lateral motion of the cargo, as described in Figure 4.9. Figure 4.13 shows the variation in roll moment amplification factor under the entire range of tanks and fill levels considered in the present study, subject to simultaneous acceleration excitations and sprung mass roll motion. Results show an overall decreasing trend of roll moment amplification factor with fill level. The higher

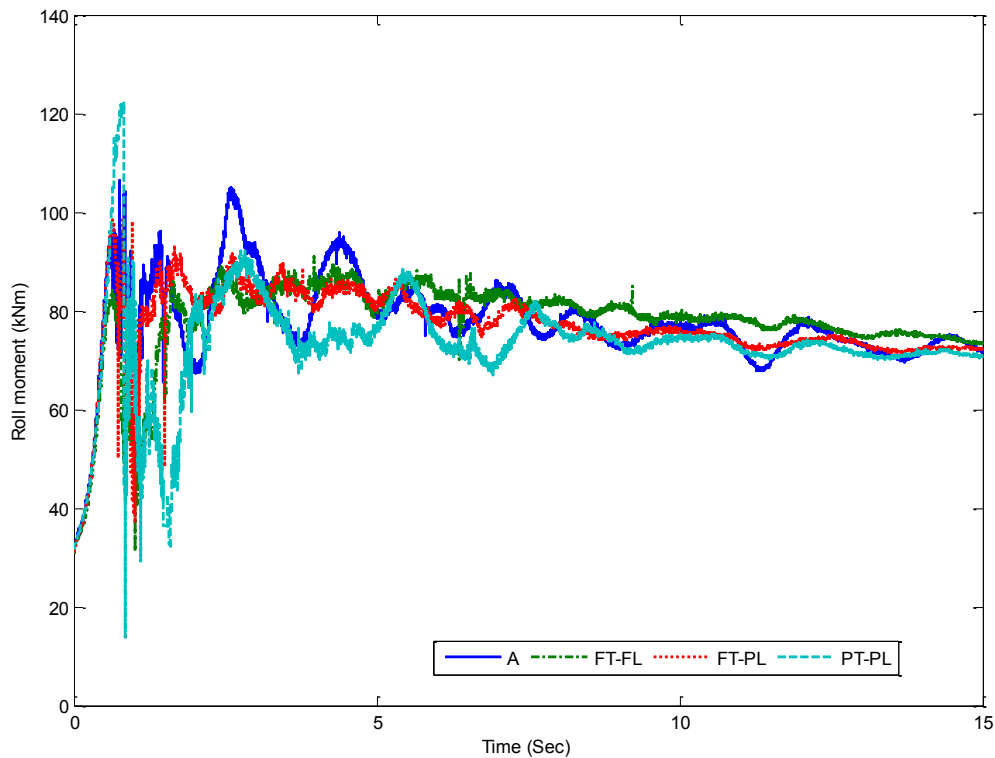


Figure 4.12: Comparisons of roll moment time-histories for all considered tank configurations subject to simultaneous acceleration and 7° sprung mass roll motion at 40% fill level.

peaks in roll moment for tanks A and PT-PL at fill level of 40% also reflected in Figure 4.13 in terms of relatively higher roll moment amplification factor at 40% fill level. However at a higher fill level of 60% all the proposed tank configurations show a reduction of nearly 10% in roll moment amplification factor compared to tank A.

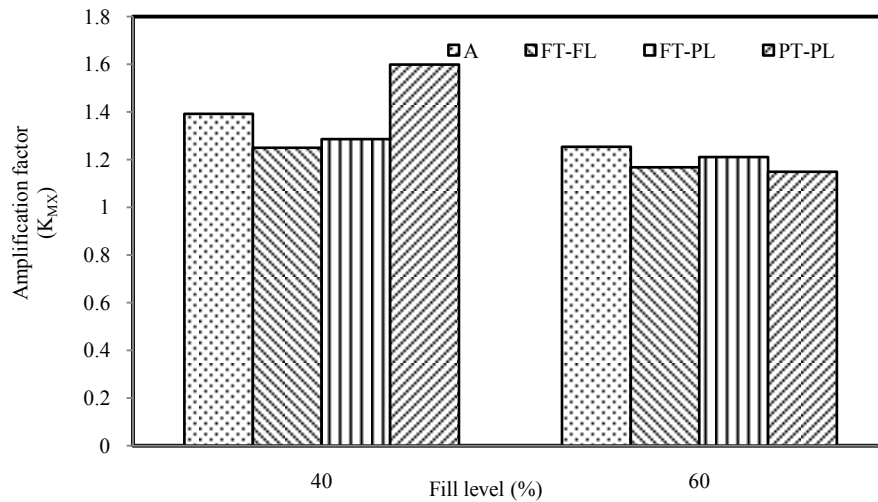


Figure 4.13: Comparisons of roll moment amplification factor under selected accelerations and 7°sprung mass roll motion.

The pitch plane anti slosh effectiveness of the proposed baffle configurations is also evaluated. Figure 4.14 shows the pitch moment time-histories for all tank configurations considered in the present study under 40% fill condition subject to idealized break-in-turn maneuver. Results show considerably higher peak and mean dynamic pitch moment for tank PT-PL compared to the rest of the configurations. This is attributed to greater available space for cargo movement in the pitch plane at low fill level of 40%. However, pitch moment time-histories for FT-FL and FT-PL are comparable with slight differences, which might be associated to the presence of longitudinal baffle structure in tanks FT-FL and FT-PL. Furthermore, the magnitude of

peak pitch moment is observed to be significantly higher than that of the roll moment under similar fill level.

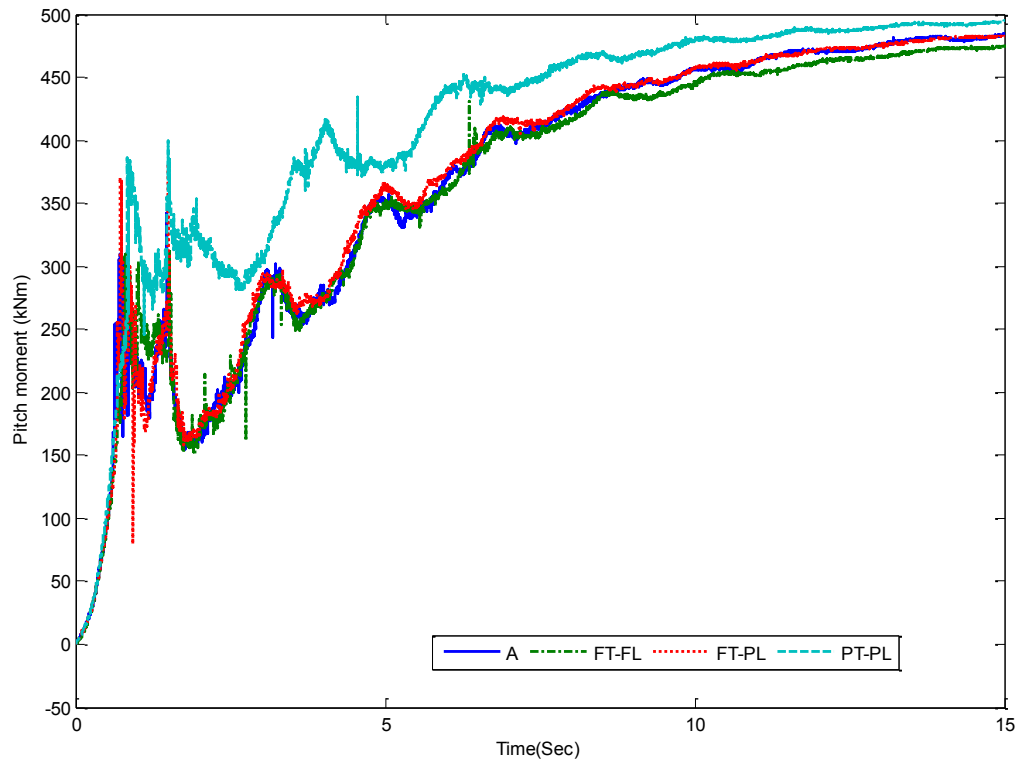


Figure 4.14: Comparisons of pitch moment time-histories for all considered tank configurations subjected to simultaneous acceleration and 7° sprung mass roll motion at 40% fill level.

Figure 4.15 illustrates the variation in pitch moment amplification factor for all the tank configurations under the considered simultaneous acceleration excitations and sprung mass roll motion at 40 and 60% fill levels. Results show similar amplification factors for A, FT-FL and FT-PL tanks while that for tank PT-PL is slightly higher than other configurations. This is due to relatively lower boundary constraints offered by the partial transverse baffles within tank PT-PL.

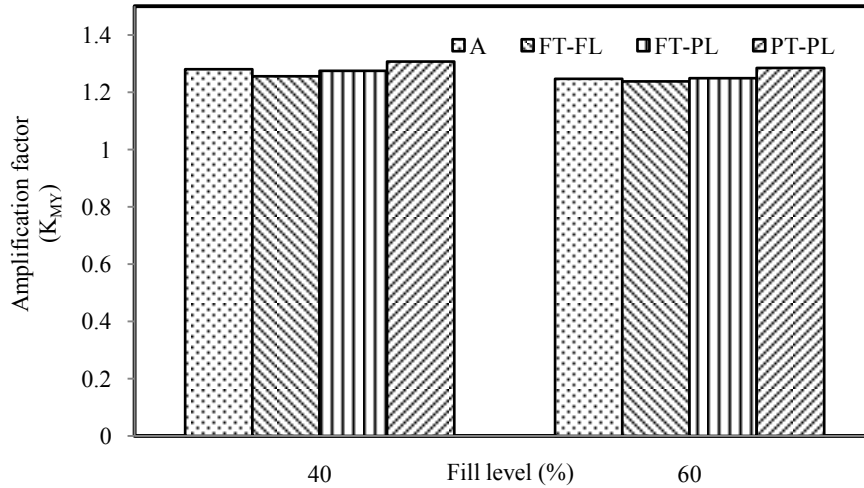


Figure 4.15: Comparisons of pitch moment amplification factor for all considered tank configurations subjected to simultaneous acceleration and 7° sprung mass roll motion.

4.5 Summary

Inclusion of a lateral baffle within the tank can be thought of as introduction of a damper in an analogous system. The baffle dampens the cargo movement by primarily absorbing the fluid flow energy. The same concept is used in the present study to attenuate sloshing of cargo in the roll plane with an ultimate objective of improving roll stability of partly-filled tank vehicles. Effectiveness of the proposed lateral and longitudinal baffle configurations are evaluated in terms of dynamic slosh measures, described in chapter 3, Tanks FT-FL and FT-PL performs well under both simultaneous and lateral excitations. Proposed configurations effectively attenuate lateral slosh movement with a maximum reduction in peak roll moment of nearly 21% compared to tank A at 40% fill level under lateral acceleration alone. Thus, proposed configurations could be considered by tank vehicle industry to improve roll stability of partly-filled road tankers. Although configuration FT-FL yields better results interns of roll plane slosh suppressing under

both selected excitations, configuration FT-PL could also be considered due to relatively lower baffle weight.

CHAPTER 5

CONCLUSIONS AND RECOMMENDATIONS

5.1 Major Contributions of the Dissertation Research

The primary objectives of this research were to investigate: (i) the effect of tank cross-sections on the maneuver-induced dynamic fluid slosh in partly-filled road tankers; and (ii) anti slosh characteristics of different transverse-longitudinal baffles arrangements. Following are considered to be the major contributions of the study:

- a. CFD models are applied for a systematic analysis of the effect of tank cross-section on the steady-state as well as transient slosh responses, which are characterized by cargo load shifts, slosh forces and moments under idealized turning and braking excitations as a function of fill level.
- b. Three different transverse longitudinal baffle arrangements are proposed and their relative effectiveness in suppressing fluid slosh in the roll and pitch planes are evaluated under simultaneous longitudinal and lateral acceleration fields.
- c. Transient and steady-state slosh responses are also investigated under vehicle sprung mass roll motion attributed to tire and suspension compliances and load shift.
- d. Effect of tank cross-section on the fundamental frequency of fluid slosh is investigated as a function of the tank cross-section and the fill level.
- e. The sensitivity of three-dimensional dynamic slosh simulations to changes in the processors are systematically evaluated in terms of computational time.

5.2 Major Conclusions

- a. Dynamic cargo slosh in partly-filled road tanks is strongly affected by the tank cross-section. Wider modified-oval tanks (MC-406) yield greater load shift in the roll plane and thus larger overturning moment under low and moderate fill levels compared to the circular cross-section tanks. A 40% filled modified-oval tank subject to $0.25g$ lateral acceleration and 7° tank roll yields steady-state roll moment that is 16% greater than that for the circular cross-section tanks of identical volume. This is despite the fact that wider cross-section yield relatively lower mass center height. The wider tanks therefore yield relatively lower load shift and roll moment under higher fill levels.
- b. The vehicle sprung mass roll motion encountered in a turning maneuver causes additional lateral shift of the cargo mass center and thus the roll moment. A 7° sprung mass roll causes the lateral cg shift of 0.35m and roll moment of 858kNm for a 40% filled modified-oval tank with total cargo load of 200kN. Wide cross-section tanks yield relatively higher lateral load shift as in case of lateral acceleration excitation.
- c. The peak load shift and slosh forces observed during transient fluid slosh are substantially higher than those estimated from the kineto-static model. The peak responses are further dependent upon tank cross-section. A 40% filled modified-oval tank yields nearly 10% higher peak normalized roll moment compared to the circular tank. The steady-state dynamic response, however, are identical to those deduced from the kineto-static model. A kineto-static model of fluid slosh would thus be appropriate for steady-state directional analysis of partly-filled tanker. The

kineto-static model, however, cannot be applied for slosh analysis of baffled tanks.

- d. Fluid slosh responses exhibit oscillations with minimal damping. The directional responses of a partly-filled road tanker would thus be oscillatory, which cannot be predicted from the kineto-static model.
- e. Fundamental frequency of fluid slosh is affected by both the tank cross-section and baffle configurations. Wider tanks exhibit lower roll plane fundamental slosh frequency compared to the less wide tank cross-section, while presence of baffle yields higher frequency in both roll and pitch planes. The fundamental roll plane slosh frequency of a 40% filled modified-oval tank was observed near 0.48Hz, while that of the circular tank with same fill level was 0.56Hz.
- f. The presence of a longitudinal acceleration arising from braking in addition to lateral acceleration excitation increases the longitudinal load shift considerably but lessens the steady-state lateral load shift. This is attributed to accumulation of cargo in corner of the tank under such excitations.
- g. Conventional transverse baffles help suppress the transient and steady-state slosh in the pitch plane but offer negligible resistance in the roll plane. Addition of a longitudinal baffle could considerably reduce the roll plane slosh. The proposed transverse-longitudinal baffles arrangements yields considerable reduction in the roll plane slosh. The peak roll moment of a 40% filled tank could be reduced by nearly 21% by adding a longitudinal baffle. The proposed transverse-longitudinal baffle arrangements increase the roll plane stability limits by incorporating higher damping ratio in the system compared to that of conventional baffled tanks.

Installation of a longitudinal baffle could increase the damping ration of the system by nearly three times that of conventional baffled tanks.

- h. Complex tank geometry coupled with lateral and longitudinal baffle configurations makes the computation extremely demanding. Parallel computation with just two processors resulted in reduction in the computation time by nearly 56%.

5.3 Recommendations for Future Work

The present study is an attempt to evaluate the effect of tank cross-sections and transverse-longitudinal baffle configurations on the dynamic slosh characteristics of liquid cargo in partly-filled tanks subjected to lateral, longitudinal, and simultaneous lateral and longitudinal acceleration excitations coupled with sprung-mass roll motion. In particular, the present study is an initial effort towards investigating viability of longitudinal baffle configuration with an objective to enhance roll plane stability of the tank trucks. It is clearly evident from the results that the tank cross-section has a strong effect on the dynamic slosh behavior and that a longitudinal baffle offer considerable potential to improve roll plane stability of partly-filled road tankers. The methodology from the present study can be taken forward to optimize longitudinal baffle shape, configuration and positioning. Consequently, more efforts are required to further augment the results of the present study, some of those are mentioned below:

- a. Integration of a dynamic fluid slosh model with a comprehensive vehicle model either within Fluent platform or through co-simulation approach could yield much

desired knowledge on the role of transient fluid slosh and baffles design in view of the directional dynamic analysis of tank vehicles.

- b. Experimental analysis of slosh characteristics within partly-filled tanks of various cross-sections with and without baffles would serve better understanding of slosh phenomenon and also in validation of semi-analytical and numerical slosh models.
- c. Transient roll motion of the sprung-mass could be incorporated in a three-dimensional fluid slosh model using dynamic mesh technique available within FLUENT. This approach would permit simulation of the changes in shape of the fluid domain due to dynamic roll motion of the tank structure.
- d. This study has shown considerable reduction in slosh characteristics with proposed transverse-longitudinal baffle configurations. Improved longitudinal baffle design and configurations could be developed through a well defined optimization function coupled with constraints related to baffle weight and positioning with an objective to minimize lateral slosh within partly-filled tank under lateral, longitudinal, and combined lateral and longitudinal excitations.
- e. Assumption of homogenous lateral acceleration field is acceptable due the large difference in turn radius and tank length. However, application of non-homogenous longitudinal acceleration field could yield improved results under straight-line acceleration/braking.
- f. A linear fluid slosh model may be developed and integrated with a vehicle model to achieve greater computational efficiency and to facilitate design optimizations.

REFERENCES

- 1 Rakheja, S., Sankar, S. and Ranganathan, R. (1988) “Roll plane analysis of articulated tank vehicles during steady-turning”, *Vehicle System Dynamics*, 17: 1, pp. 81-104
- 2 Ranganathan, R., Rakheja, S., and Sankar, S. (1990) “Influence of liquid load shift on the dynamic response of articulated tank vehicles”, *Vehicle System Dynamics*, 19: 4, pp. 177 -200
- 3 Pape, D. B., Barnes, M., and Brock, J.(2007) “Cargo tank roll over study”, Final report by Battelle for department of transportation USA
- 4 http://bulktransporter.com/management/tanktruck/dot_nttc_confrences_issues_0201/1Feb2008.
- 5 Ranganathan, R. (1990) “Stability analysis and directional response characteristic of heavy vehicles carrying liquid cargo”, Ph.D thesis, Concordia University Montreal, Canada.
- 6 Kang, X., Rakheja, S. and Stiharu, .I. (1999) “Optimal tank geometry to enhance static roll stability of partly-filled tank vehicle”, SAE Technical paper series, SP-1486.
- 7 Kandasamy, T., (2008) “Analysis of baffle design for limiting fluid slosh in partly-filled vehicle tanks”, MAsc. thesis, Concordia University Montreal, Canada
- 8 Miralbes, R., Castejon, L., Carrera, M. and Valladares, D. (2010) “Response analyses of a two-phase cryogenic tank to longitudinal and lateral accelerations”, *Int. J. Heavy Vehicle Systems*, vol. 17, nos. 3/4, pp. 237-255.
- 9 Abramson, H.N., (1966) “Dynamic behaviors of liquid in moving containers”, Report, NASA SP-106.
- 10 Modaressi-Tehrani, K., Rakheja, S. and Stiharu, I. (2007) “Three-dimensional analysis of transient slosh within a partly-filled tank equipped with baffles”, *Vehicle System Dynamics*, vol.45, No.6, pp.525-548.
- 11 Budiansky, B. (1960) “Sloshing of liquids in circular canals and spherical tanks”, *Journal of aerospace science.*, vol. 27, no. 3.

- 12 Yan, G.R., Siddiqui, K., Rakheja, S. and Modaressi-Tehrani, K. (2005) "Transient fluid slosh and its effect on the rollover-threshold analysis of partly-filled conical and circular tank trucks", *International journal of heavy vehicle Systems.*, vol. 12, no. 4, pp 323-343
- 13 Modaressi-Tehrani, K., (2004) "Analysis of transient liquid slosh inside partly-filled tank subjected to lateral and longitudinal acceleration fields", MAsc. thesis, Concordia University, Montreal, Canada;
- 14 Yan, G.R., Rakheja, S. and Siddiqui, K. (2010) "Analysis of transient fluid slosh in partly-filled tanks with and without baffles: Part 2 – role of baffles", *Int. J. Heavy Vehicle Systems*, Vol. 17, Nos. 3/4, pp.380–406;
- 15 Bauer, F. (1964) "Fluid oscillations in the containers of a space vehicle and their influence upon stability", NASA TR -187
- 16 Romero, J.A., Ramirez, O., Fortanell, J.M., Martinez, M. and Lozano, A.,(2006) "Analysis of lateral sloshing forces within road containers with high fill levels", *Journal of automobile engineering* vol. 220 part d.
- 17 Xiaodi, K.,(2001) "Optimal tank design and directional dynamic analysis of liquid cargo vehicles under steering and braking", Ph.D thesis, Concordia University Montreal, Canada
- 18 Ziarani, M.M., Richard, M.J., and Rakheja, S., (2004) "Optimization of liquid tank geometry for enhancement of static roll stability of partially-filled tank vehicles", *International Journal. of vehicle design*, vol. 11, No. 2, 2004
- 19 Yan., G.R., (2008) "Liquid slosh and its influence on braking and roll responses of partly-filled tanks vehicles", Ph.D thesis, Concordia University Montreal, Canada
- 20 Abramson, H.N., (1969) "Slosh suppression", Report from NASA, NASA-SP 8031
- 21 Strandberg, L., (1978) "Lateral stability of road containers", Report No. 138A, VTI The Swedish National Road and Traffic Research Institute, Sweden.
- 22 Yan, G.R., Rakheja, S. and Siddiqui, K. (2010) "Analysis of transient fluid slosh in partly-filled tanks with and without baffles: Part 1 - model validation", *International. journal of heavy vehicle systems*, vol. 17, nos. 3/4, pp.359–379
- 23 Salem, M.I., (2000). "Rollover stability of partly-filled heavy-duty elliptical tankers using trammel pendulums to simulate fluid sloshing", PhD thesis, West

Virginia University, USA

- 24 Ibrahim. I.M., (1999) “Anti slosh damper design for improving the roll dynamic behavior of cylindrical tank trucks”, SAE technical paper series, SAE 1999 013729
- 25 Popov, G. (1991) “Dynamics of liquid sloshing in road containers”, Ph.D thesis, Concordia University Montreal, Canada
- 26 Sheu, T. W. H. and Lee, S.-M.(1998) “Large-amplitude sloshing in an oil tanker with baffle-plate/drilled holes”, International journal of computational fluid dynamics, vol. 10, nos. 1, pp 45 - 60
- 27 Lee, D. H., Kim, M.H., Kwon, S.H., Kim, J.W. and Lee, Y.B. (2007) “A parametric sensitivity study on LPG tank sloshing loads by numerical simulations”, International journal of ocean engineering .,vol., 34, pp 3- 9
- 28 Rhee, S.H. (2005) “Unstructured grid based RANS method for liquid tank sloshing”, ASME, vol. 127., pp. 572 - 582
- 29 Fleissner, Florian , Lehnart, Alexandra and Eberhard, P. (2010) “Dynamic simulation of sloshing fluid and granular cargo in transport vehicles”, Vehicle System Dynamics, 48: 1, 3-15
- 30 Winkler, C. Ervin, R. (1999) “Rollover of heavy commercial vehicles”, University of Michigan Transportation Research Institute report, UMTRI-99-19
- 31 Ervin, R. (1983) “The influence of size and weight variables on the roll stability of heavy duty trucks”, SAE Technical Paper Series. SAE-831163.
- 32 Zhanqi, W., Rakheja, S., Cunzhen, S. (1995) “Influence of partition location on the braking performance of a partly-filled tank vehicle”, SAE technical paper series SAE 952639
- 33 Rakheja, S. Sankar, S. and Ranganathan, R., (1987) “Study on liquid tanker stability: steady-turning stability of partly-filled tank vehicle”, CONCAVE Research Report No 13-87.
- 34 Nichols, B. D., and Hirt, C. W , (1971) “Improved free surface boundary condition for numerical incompressible-flow calculations”, Journal of computational physics, vol. 8, No. 3, pp 434-448
- 35 Fluent 6.3 user’s guide, (2006) “Section 25.1.1”, published by Fluent Inc.
- 36 Gambit user’s guide, (1999) “Chapter 3 – The gambit graphical user interface

(GUI)", published by Fluent Inc.

- 37 Billing, J. R. (1998) "An assessment of tank truck roll stability", National Research Council Canada;
- 38 Ervin, R (1986) "The Influence of weights and dimensions on the stability and control of heavy duty trucks in Canada", University of Michigan Transportation Research Institute report, UMTRI-86-35
- 39 "A technical publication from the co-ordination and information center", Dangerous Goods and Rail Safety Government of Alberta Transportation (2010)
- 40 Fluent News Letter (2001) "Fluent 6.0 : tuned to your goals", Published by Fluent Inc. vol. 10, issue 2
- 41 Khan, R. (2008) "Application of CFD technique for modeling NATCO's process equipments", Engineering Simulation Energy Conference, Texas USA
- 42 Code of Federal Regulations, "Specifications for packaging", 49 CFR part - 178.
- 43 Romero, J.A (2005) "Natural sloshing frequencies of liquid cargo in road tankers", Heavy Vehicle Systems, vol. 12, no. 2 pp. 121 - 138
- 44 Romero. J.A., Lozano. A., Ortiz. W (2007) "Modeling of liquid cargo – vehicle interaction during turning maneuvers", 12th IFToMM World Congress, Besancon (France)
- 45 Lloyd, N., Vaiciurgis, E., and Langrish, T.A.G (2002) "The effect of baffle design on longitudinal liquid movement in road tankers: an experimental investigation", Process Safety and Environmental Protection, Transactions of Institution of Chemical Engineers, vol 80, Part B, pp. 181-185
- 46 M. Serdar Celebi , Hakan Akyildiz (2002) "Nonlinear modeling of liquid sloshing in a moving rectangular tank", Journal of Ocean Engineering, vol. 29 1527-1553
- 47 Khezzar, L., Seibi, A.C. and Goharzadeh, A., (2008) "Water sloshing in rectangular tanks- an experimental investigation and numerical simulation", International journal of engineering, vol. 3 issue. 2, pp. 174-184
- 48 Fleissner, F., D'Alessandro, V., Schiehlen, W. and Eberhard, P., (2009) "Sloshing cargo in silo vehicles", Journal of mechanical science and technology, vol. 23, pp. 968 - 973
- 49 Fluent 6.1 UDF Manual, (2003) "Chapter 9-Parallel UDF usage", published by

Fluent Inc.

- 50 Winkler, C. (1987) “Experimental determination of the rollover threshold of four tractor-semitrailer combination vehicles”, University of Michigan Transportation Research Institute report, UMTRI-87-31
- 51 Rakheja, S., Sankar, S., and Ranganathan, R.,(1989) “Influence of tank design factors on the rollover threshold of partly-filled tank vehicles”, SAE technical paper 892480
- 52 Rakheja, S, Ranganathan, R., Billing, J.R., and Mercer., W., (1991) “Field testing of a tank truck and study of fluid slosh”, SAE technical paper 912679
- 53 Nichols, B.D., Hirtz, C. W., and Hotchkiss, R. S., “Fractional volume of fluid method for boundary dynamics”, Los Alamos Scientific Laboratory , University of California
- 54 Ervin, R, Barnes, M., and Wolfe, A., (1985) “Liquid cargo shifting and the stability of cargo tank trucks”, Final Report., University of Michigan Transportation Research Institute report, UMTRI-85-35.